

PRP4K IS A NOVEL HER2-REGULATED MODIFIER OF ANOIKIS AND TAXANE
RESISTANCE

by

Dale Corkery

Submitted in partial fulfilment of the requirements
for the degree of Doctor of Philosophy

at

Dalhousie University
Halifax, Nova Scotia
August 2015

© Copyright by Dale Corkery, 2015

Table of Contents

List of Figures	viii
Abstract	x
List of Abbreviations Used	xi
Acknowledgements	xvi
Chapter 1 Introduction	1
1.1 Preface	1
1.2 PRP4K as a Regulator of Splicing.....	1
1.2.1 Identification of prp4 in <i>Schizosaccharomyces pombe</i>	1
1.2.2 Cloning and Characterization of Mammalian PRP4K.....	2
1.2.3 PRP4K and Spliceosomal Assembly	5
1.3 PRP4K and the Spindle Assembly Checkpoint.....	10
1.4 PRP4K and Viral Infection.....	13
1.5 PRP4K and Cellular Responses to Anti-Cancer Therapies.....	14
1.6 Overview of Thesis Chapters	16
1.7 Author Contributions.....	17
Chapter 2 PRP4K is a HER2-Regulated Modifier of Taxane Sensitivity	18
2.1 Introduction	18
2.1.1 Taxanes: Mechanism of Action	18

2.1.2 The Spindle Assembly Checkpoint and Its Role in Taxane Response	20
2.1.3 Taxanes: Mechanisms of Resistance	21
2.1.3.1 P-gp Overexpression	21
2.1.3.2 β -Tubulin Mutations	22
2.1.3.3 Altered β -Tubulin Isotype Expression	22
2.1.3.4 Altered Expression of Microtubule-Associated Proteins.....	23
2.1.3.5 Alterations in the Apoptotic Pathway.....	24
2.1.3.6 Disruption of the Spindle Assembly Checkpoint.....	25
2.1.4 HER2 Amplification in Breast and Ovarian Cancer	25
2.2 Materials and Methods	31
2.2.1 Patients and Tissue Specimens	31
2.2.2 Tissue Microarray and Immunohistochemistry	31
2.2.3 Staining Quantification	32
2.2.4 Cell Culture	33
2.2.5 Western Blot Analysis	33
2.2.6 shRNA Lentiviral Transduction.....	36
2.2.7 GFP-H2B Cell Line Generation.....	36
2.2.8 Immunofluorescence.....	37
2.2.9 HER2 Inhibition.....	38

2.2.10 <i>In Vitro</i> Cell Viability Assay	38
2.2.11 Statistical Analysis.....	39
2.3 Results	39
2.3.1 High PRP4K Protein Level Correlates with HER2 Amplification in Human Breast and Ovarian Tumours	39
2.3.2 HER2 Signalling Positively Regulates PRP4K	42
2.3.3 Knockdown of PRP4K Decreases the Sensitivity of Cancer Cells to Paclitaxel.....	44
2.3.4 Reduced PRP4K Expression is Associated with Both <i>In Vitro</i> - Derived and Patient-Acquired Resistance to Taxanes	49
2.3.5 PRP4K Expression Correlates with Better Overall Survival in Ovarian Cancer Patients Treated with Taxanes with Low HER2- Expressing Tumours	51
2.4 Discussion.....	55
Chapter 3 Development of a Zebrafish Xenotransplant Model to Study <i>In Vivo</i> Drug Response.....	59
3.1 Introduction	59
3.1.1 Zebrafish as a Model to Study Human Cancers.....	59
3.1.1.1 Mutant Models of Cancer	60
3.1.1.2 Transgenic Models of Cancer	62
3.1.1.3 Xenotransplantation Models	63

3.1.2	Limitations to Using Zebrafish to Study Human Cancer.....	65
3.2	Materials and Methods	67
3.2.1	Zebrafish Maintenance.....	67
3.2.2	Tissue Culture and Cell Labelling	68
3.2.3	Zebrafish Handling, Xenotransplantation and Drug Treatment	68
3.2.4	Embryo Dissociation.....	69
3.2.5	Imaging of the Dissociated Material.....	70
3.2.6	<i>Ex Vivo</i> Proliferation Assay	72
3.2.7	MDA-MB-231 PRP4K Knockdown.....	73
3.3	Results	73
3.3.1	Human Leukemia Proof-of-Principle Studies.....	73
3.3.2	Using the Zebrafish XT Model to Study Taxane Response in Breast Cancer	83
3.3.3	Knockdown of PRP4K Enhances MDA-MB-231 Cell Proliferation in Zebrafish.....	85
3.4	Discussion.....	87
Chapter 4	PRP4K is a Novel Regulator of Anoikis Resistance	90
4.1	Introduction	90
4.1.1	Anoikis.....	90
4.1.2	Anoikis Resistance in Cancer	95

4.1.3 Mechanisms of Anoikis Resistance	95
4.1.3.1 Epithelial to Mesenchymal Transition	96
4.1.3.2 Integrin Expression	97
4.1.3.3 Increased Collagen Expression	98
4.1.3.4 Modulation of Membrane Microdomains	99
4.1.3.5 Autophagy	100
4.2 Materials and Methods	102
4.2.1 Cell Lines and Culture	103
4.2.2 Western Blot Analysis	103
4.2.3 Quantification of <i>In Vitro</i> Proliferation Rates	104
4.2.4 Zebrafish Xenotransplantation	104
4.2.5 Spheroid Cell Growth Assay	105
4.2.6 Soft Agar Colony Formation Assay	105
4.2.7 Immunofluorescence	106
4.2.8 Anoikis Assay Using PolyHEMA Coated Plates	106
4.3 Results	107
4.3.1 Knockdown of PRP4K Accelerates the Growth of ID8 Cells in Zebrafish Embryos	107
4.3.2 Knockdown of PRP4K Enhances Cell Growth in 3D Cell Culture Models	110

4.3.3 Loss of PRP4K Affects Caveolin-1 Localization and Prevents its Degradation Following Cell Detachment	114
4.4 Discussion.....	117
Chapter 5 Conclusion	120
5.1 Preface	120
5.2 Comments on the Future of Zebrafish Xenotransplantation	120
5.3 Molecular Mechanisms of PRP4K Functions	123
5.4 Ascites Development and Chemoresistance.....	125
Bibliography	127
Appendix A Copyright Agreements	162
Appendix B ImageJ Macro	171
Appendix C Cell Lines Used	172

List of Figures

Figure 1.1 PRP4K domain structure and cellular localization.....	4
Figure 1.2 The role of PRP4K in spliceosome assembly.....	7
Figure 1.3 Phosphorylation dependent SR protein shuttling	9
Figure 1.4 PRP4K is required for activation of the SAC.....	12
Figure 2.1 HER2 signaling pathways	29
Figure 2.2 PRP4K is present in lysates in different phosphorylated-states	35
Figure 2.3 PRP4K correlates positively with HER2 expression in breast and ovarian tumours	41
Figure 2.4 HER2 signaling regulates PRP4K expression.....	43
Figure 2.5 Decreased PRP4K expression is associated with an increased cellular resistance to paclitaxel	46
Figure 2.6 Knockdown of PRP4K promotes mitotic slippage over mitotic cell death in paclitaxel treated cells.....	48
Figure 2.7 PRP4K expression is decreased in cells that have an acquired resistance to taxanes	50
Figure 2.8 Evaluation of PRP4K as a biomarker of platinum/taxane response in high-grade serous ovarian cancer.....	54
Figure 3.1 Image analysis of dissociated embryos	71
Figure 3.2 Schematic of <i>in vivo</i> cell proliferation assay.....	76
Figure 3.3 Human K562 and NB-4 cells proliferate within zebrafish embryos	77

Figure 3.4 Fluorescent microscopy analysis of dissociated embryos	78
Figure 3.5 IM, ATRA and PAX toxicity curves.....	81
Figure 3.6 Human K562 and NB-4 cell proliferation in zebrafish embryos can be inhibited by treatment with targeted therapy	82
Figure 3.7 Human MDA-MB-231 cell proliferation in zebrafish embryos can be inhibited with paclitaxel.....	84
Figure 3.8 Knockdown of PRP4K increases MDA-MB-231 proliferation in zebrafish.....	86
Figure 4.1 Mechanisms of apoptosis induction following cell detachment from the ECM.....	93
Figure 4.2 Knockdown of PRP4K increases ID8 cell proliferation in zebrafish.....	109
Figure 4.3 Knockdown of PRP4K increases viability of ID8 cells cultured as spheroids	112
Figure 4.4 Knockdown of PRP4K increases MCF-7 growth in soft agar	113
Figure 4.5 Knockdown of PRP4K affects Cav-1 localization	115
Figure 4.6 Knockdown of PRP4K prevents Caveolin-1 degradation following cell detachment	116

Abstract

PRP4K is an essential kinase identified in *Schizosaccharomyces pombe* for its role in regulating pre-mRNA splicing. In addition to its role in splicing, mammalian PRP4K has also been implicated in mitotic checkpoint signaling, host-viral interactions and the cellular response to several anti-cancer therapies. Work presented in this thesis furthers our understanding of the role of PRP4K in cancer treatment and identifies a novel role for PRP4K with implications in cancer progression and relapsed disease.

A positive correlation between PRP4K and expression of the human epidermal growth factor receptor HER2 was identified in breast and ovarian cancer patient tumours, and shown to be a direct result of PRP4K regulation by HER2 signaling. Knock-down of PRP4K expression reduced the sensitivity of breast and ovarian cancer cell lines to the taxane family of anti-cancer agents, while low PRP4K levels correlated with *in vitro*-derived and patient-acquired taxane resistance. Furthermore, high PRP4K expression correlated with better overall survival amongst patients with HER2^{low} high-grade serous ovarian cancer treated with platinum/taxane-based therapy. Therefore, PRP4K functions as a HER2-regulated modifier of taxane sensitivity and may have prognostic value as a marker of better overall survival in taxane-treated ovarian cancer patients.

To aid in the study of tumour-drug interactions, a zebrafish xenotransplant model was developed which can be used to quantify proliferation rates of human cancer cells engrafted into zebrafish embryos. Unexpectedly, knock-down of PRP4K led to an increased proliferation of breast and ovarian cancer cell lines within zebrafish embryos, which was shown to be due to an increased resistance to anoikis. Loss of PRP4K prevents degradation of caveolin-1 in cells grown under conditions of low attachment which prevents detachment-induced apoptosis and promotes cell growth within three-dimensional microenvironments, like that of the zebrafish embryo.

Collectively, these results demonstrate that downregulation of PRP4K is a potential mechanism through which tumours can acquire a resistance to taxanes. Strikingly, our results also indicate that loss of PRP4K protects cells against detachment-induced cell death, which could contribute to metastatic disease post therapy.

List of Abbreviations Used

γ -TuRC	γ -tubulin ring complex
ABL	Abelson
APAF	apoptosis protease activating factor
APC	anaphase promoting complex
APL	acute promyelocytic leukemia
ATRA	all-trans retinoic acid
BCR	breakpoint cluster region
BH3	Bcl-2 homology domain 3
BID	BH3 interacting-domain death agonist
BNIP3	Bcl-2 nineteen-kilodalton interacting protein 3
BRCA1	breast cancer 1, early onset
BTN3A2	butyrophilin, subfamily 3, member A2
BUB1	binding uninhibited by benzimidazoles 1
CAS	crk-associated substrate
Cav-1	caveolin-1
cdk1	cyclin-dependent kinase 1
CEMM	cholesterol-enriched membrane microdomain
CENP-E	centromere-associated protein E
CLK1	CDC-like kinase 1
CML	chronic myeloid leukemia
crb	crash&burn
DAPI	4',6-diamidino-2-phenylindole

DMEM	Dulbecco's modified Eagle's medium
DISC	death-inducing signaling complex
ECM	extracellular matrix
EGFR	epidermal growth factor receptor
EMT	epithelial to mesenchymal transition
ENU	ethylnitrosourea
EOC	epithelia ovarian cancer
FADD	Fas-associated death domain
FAK	focal adhesion kinase
FasL	Fas Ligand
FBS	fetal bovine serum
FERM	protein 4.1, ezrin, radixin and moesin homology
Grb2	Growth factor receptor-bound protein 2
HER	human epidermal growth factor receptor
hpf	hours post-fertilization
hpi	hours post-injection
IAP	inhibitor of apoptosis
IAP-1	inhibitor of apoptosis protein 1
IM	imantinib mesylate
IR	ionizing radiation
ITSN1	intersectin-1
MAD1	mitotic arrest-deficient 1
MAP	microtubule-associated protein

MAPK	mitogen-activated protein kinase
MCD	mitotic cell death
Mcl-1	myeloid cell leukemia 1
MPS1	monopolar spindle 1
MTD	maximum tolerated dose
mTOR	mammalian target of rapamycin
NBD	nucleotide-binding domain
NES	nuclear export signal
NLS	nuclear localization signal
NMD	non-sense mediated decay
OMM	outer mitochondrial membrane
PAX	paclitaxel
PDK1	phosphoinositide-dependent kinase 1
P-gp	p-glycoprotein
PH	Pleckstrin Homology
PI3K	phosphatidylinositol 3-kinase
PIP ₂	phosphatidyl inositol bisphosphate
PKC	protein kinase C
PML	promyleocytic leukemia
PolyHEMA	Poly 2-hydroxyethyl methacrylate
PP	protein phosphatase
Pre-B ALL	precursor-B acute lymphoblastic leukemia
prp	pre-mRNA processing

PRP4K	pre-mRNA processing factor 4 kinase
PTPC	permeability transition pore channel
rag2	recombination activation gene 2
ROS	reactive oxygen species
RPMI	Rosewell Park Memorial Institute
RRE	Rev response element
S6K	p70S6 kinase
SAC	spindle assembly checkpoint
SEM	standard error of the mean
SFSWAP	Suppressor-of-White-Apricot
SGIP1	SH3-domain GRB2-like (endophilin) interacting protein 1
snRNP	small nuclear ribonucleic protein
SOS	son-of-sevenless
SRPK1	serine-arginine protein kinase 1
SR	serine/arginine-rich
SRSF1	serine/arginine-rich splicing factor 1
T-ALL	T-cell acute lymphoblastic leukemia
TMA	tissue microarray
TMD	transmembrane domain
TNF- α	tumour necrosis factor- α
TRN-SR	transportin-SR
ts	temperature sensitive
TSC2	Tuberous Sclerosis Complex 2

TUBB3	class III β -tubulin
UTR	untranslated region
WT	wild type
XT	xenotransplant

Acknowledgements

First and foremost, I would like to thank my supervisor Dr. Graham Dellaire. Your enthusiasm and passion for research made this experience an enjoyable one. You have taught me that it is important to develop informed hypotheses, but more important to not become attached to them. You taught me to celebrate the small victories in research because there is no predicting how long it will be until the next one. These are lessons that will stick with me throughout my career.

Dr. Jason Berman. I could not have asked for a better mentor to guide me through the steep learning curve associated with the zebrafish model. You have always gone out of your way to offer guidance and support, and for this, I am truly grateful.

Dr. Paola Margnani and Dr. David Jakeman. Thank you for the support and constructive criticism offered over the course of this project.

All the past and present members of the Dellaire/Berman lab. This work would not have been possible without such a tremendous group of people to lean on when things got tough.

Thank you to the Beatrice Hunter Cancer Research Institute and the Cancer Research Training Program who have provided financial support for this work from day one.

Chapter 1 Introduction

This chapter contains material (Section 1.2.3, Figure 1.2, Figure 1.3) originally published in:

“Corkery DP, Holly A, Lahsae S, Dellaire G. 2015. Connecting the speckles: Splicing kinases and their role in tumorigenesis and treatment response. *Nucleus*. (In Press)”

1.1 Preface

Understanding the role of pre-mRNA processing factor 4 kinase (PRP4K) in the treatment and progression of cancer is the central focus of this thesis. This chapter provides an introduction to PRP4K beginning with its role in pre-mRNA splicing for which it was discovered. The limited literature surrounding PRP4K is reviewed to highlight additional roles for PRP4K with an emphasis placed on roles with implications in cancer and cancer treatment. The chapters which follow will present experimental evidence which furthers our understanding of the role of PRP4K in cancer treatment and identifies a novel role for PRP4K with implications for cancer progression and relapsed disease.

1.2 PRP4K as a Regulator of Splicing

1.2.1 Identification of prp4 in Schizosaccharomyces pombe

PRP4K (also known as PRPF4B) was first identified in 1991 when a library of temperature sensitive (ts) *Schizosaccharomyces pombe* fission yeast mutants was

screened for splicing defects (1). In this study, cells of a strain of *S. pombe* with a *ura4* gene deletion (2) were treated with the chemical mutagen nitrosoguanidine and allowed to form colonies on solid medium at 25°C. The colonies, each derived from a single mutagenized cell, were replica-plated and shifted to 37°C which resulted in the identification of 150 ts mutants harbouring mutations which prevented growth at the increased temperature. In the budding yeast *Saccharomyces cerevisiae*, defects in pre-mRNA splicing have been shown to account for greater than 5% of all ts mutants isolated due to the presence of introns within genes encoding ribosomal proteins (3,4). At the restrictive temperature, these mutations block the synthesis of ribosomes due to loss of ribosomal intron splicing (5-7). To determine if any of the *S. pombe* mutants displayed similar defects, the 150 ts mutants were transformed with a *ura4* gene containing an artificial intron. By performing S1 nuclease protection experiments with a probe to the intron-containing gene, the group identified 3 mutants which accumulated un-spliced pre-mRNA at the restrictive temperature. Complementation studies with the three pre-mRNA processing (*prp*) mutants previously identified in *S. pombe* (*prp1*, *prp2*, *prp3*) (8) revealed that only one of the mutants defined a new complementation group, and was named *prp4* (1). Subsequent characterization of the *prp4* gene revealed that the splicing factor encoded by the gene contained the characteristic sequence that defines a serine/threonine protein kinase, making *prp4* the first kinase predicted to play a role in splicing (9).

1.2.2 Cloning and Characterization of Mammalian PRP4K

Cloning of the full length cDNA encoding human PRP4K identified a 170kDa-polypeptide consisting of 1007 amino acids (10) (**Figure 1.1A**). The protein has an extended N terminus containing subdomains rich in lysine-histidine (KH) or arginine-serine (RS) dipeptides (11), similar to those found in the serine/arginine-rich (SR) protein family of splicing factors. Mammalian PRP4K also contains a dual-specificity kinase domain which is 53% identical to that of the kinase domain of the *S. pombe* gene product and two conserved sequence motifs, MI (DDMFA) and MII (DNWTDAEGYYRV), which are essential for prp4 function in fission yeast (11,12). Immunofluorescence microscopy using antibodies directed against the N terminus of mammalian PRP4K revealed a nuclear speckle localization (**Figure 1.1B**) which co-localized with the splicing factor SC35, while western blot analysis identified a 152 kDa protein with multiple bands correlating with varying states of phosphorylation (11). In agreement with a conserved role in splicing, mammalian PRP4K was also shown to interact with pre-mRNA splicing factors PRP6 and Suppressor-of-White-Apricot (SFSWAP) and co-purify with the U5 small nuclear ribonucleic protein (snRNP) (11).

While significant evidence supported a role for PRP4K in the regulation of splicing, it was not until 2010 that the molecular mechanism of this regulation was identified. Work out of the lab of Reinhard Lührman revealed that PRP4K played an essential role in spliceosome assembly (13), discussed in the following section.

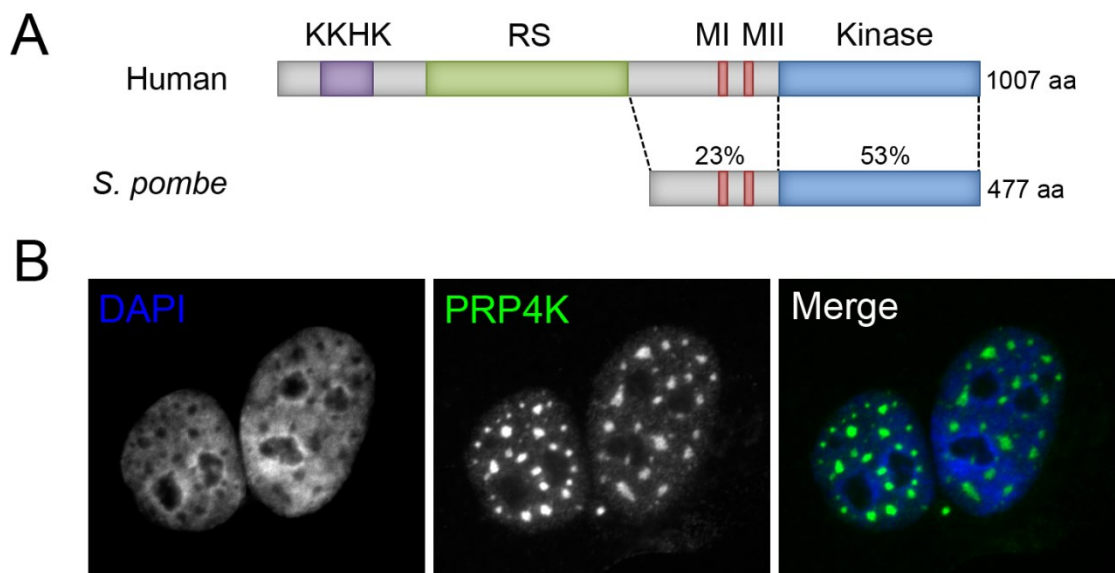


Figure 1.1 PRP4K domain structure and cellular localization. (A) Domain structure of human and *S. pombe* PRP4K. Adapted from (11). Percentage identity to human PRP4K is shown above each domain. (B) Immunofluorescence detection of PRP4K (green) in the SK-BR-3 human breast cancer cell line, counterstained for DNA with DAPI (blue).

1.2.3 PRP4K and Spliceosomal Assembly

Transcribed pre-mRNA must be spliced to remove introns prior to nuclear export and translation. This process is carried out by the spliceosome, a large macromolecular machine composed of five snRNPs and numerous protein cofactors (14). Spliceosome assembly is a complex, multistep process as illustrated in **Figure 1.2**. The first step involves recognition of the 5' and 3' splice sites located on adjacent exons by U1 and U2 snRNP respectively; a process which is mediated by the C-terminal domain of polymerase II. Binding of the U1 snRNP to the 5' splice site is mediated by serine/arginine-rich splicing factor 1 (SRSF1), but only when the RS-domain of SRSF1 is hyper-phosphorylated by the kinases CDC-like kinase 1 (CLK1) and serine-arginine protein kinase 1 (SRPK1) (15,16). Once U1 and U2 snRNP have bound their target splice site, they interact with each other to form the pre-spliceosome (complex A). The next step in assembly involves the binding of pre-assembled U4/U6-U5 tri-snRNP to complex A to form complex B; a reaction catalyzed by several proteins including SNU66, SAD1, and PRP28 (17,18). Complex B next undergoes a series of rearrangements resulting in the release of U1 and U4 snRNPs, creating a catalytically active complex B. Once catalytically active, the complex carries out the first of two splicing reactions to form complex C, containing the free exon from the 5' splice site, and the intron-exon lariat intermediate, from the 3' splice site. Complex C, after a series of rearrangements, carries out the second splicing reaction resulting in a post-spliceosomal complex containing the two spliced exons and the lariat intron. Finally, the remaining U2, U5 and U6 snRNPs are released from the transcript to be re-used in additional rounds of splicing.

In 2010, a study from the lab of Reinhard Lührman identified PRP4K as an essential regulator of spliceosomal assembly (13). Immunoblotting for splicing factors PRP6 and PRP31 in purified tri-snRNPs and B complexes revealed that these two proteins were phosphorylated during spliceosomal assembly, and that this modification was found predominantly within B complexes. With PRP4K having been shown previously to interact with and phosphorylate PRP6 (11), the group wished to determine whether PRP4K was responsible for these specific phosphorylation events. Nuclear extracts were immunodepleted for PRP4K and used for *in vitro* splicing assays which revealed that depletion of PRP4K did not prevent recruitment of PRP6 or PRP31 to the tri-snRNP, but did prevent their subsequent phosphorylation. Furthermore, analysis of spliceosomal complexes, found within the *in vitro* splicing reactions, indicated there was no change in tri-snRNP levels with PRP4K depletion, but there was a significant decrease in complex B formation, accompanied by an increase in complex A. Therefore, the PRP4K-mediated phosphorylation of PRP6 and PRP31 is required for tri-snRNP integration during complex B formation (**Figure 1.2**).

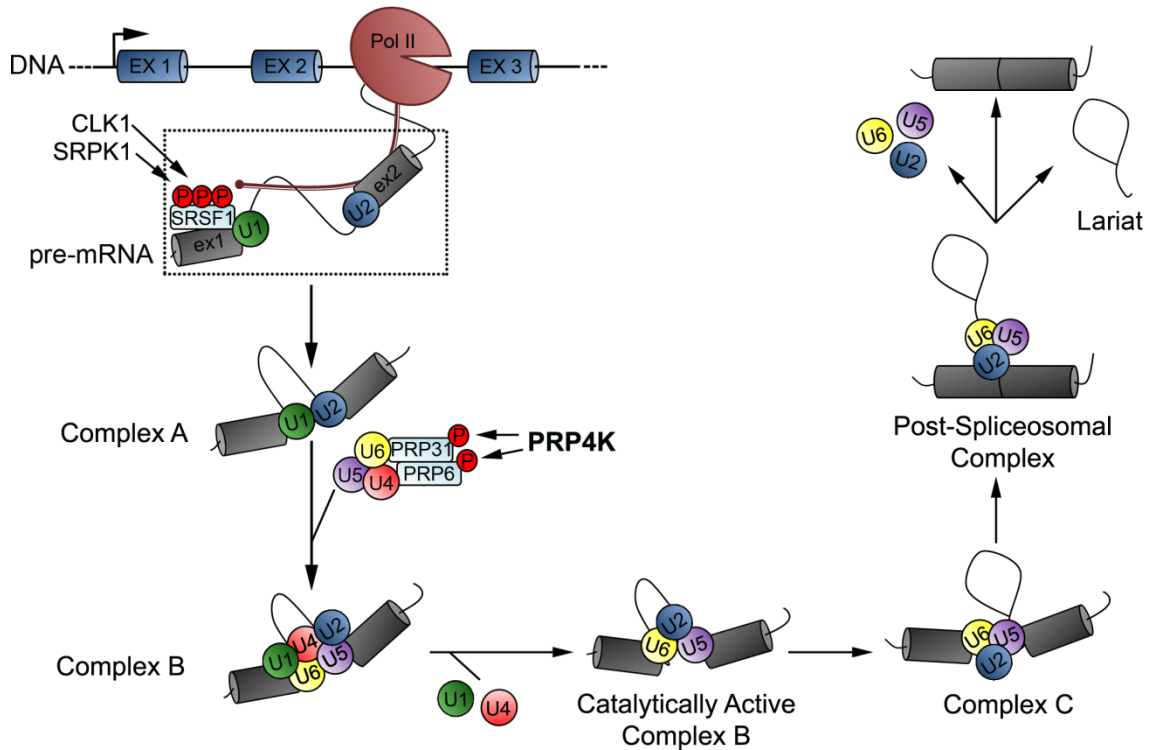


Figure 1.2 The role of PRP4K in spliceosome assembly. Assembly of the spliceosome occurs in a stepwise fashion beginning with the recognition and binding of the 5' and 3' splice site by U1 and U2 snRNP, respectively, to form complex A. This is followed by binding of the U4/U6-U5 tri-snRNP to form complex B; an event which is mediated by the phosphorylation of PRP6 and PRP31 by PRP4K. Complex B undergoes a rearrangement to form catalytically active complex B, which carries out the splicing event in two sequential reactions. The first reaction involves the nucleophilic attack of the first nucleotide of the intron at 5' splice site. This results in the formation of complex C containing a free exon from the 5' splice site and the intron-exon lariat intermediate from the 3' splice site. The second reaction involves the nucleophilic attack of the last nucleotide of the intron at the 3' splice site which releases the lariat intron and allows for ligation of the exons.

In addition to phosphorylating PRP6 and PRP31, PRP4K has also been shown to interact with and phosphorylate the SR protein SRSF1 (also known as SF2/ASF) (10). SRSF1 phosphorylation is essential in mediating 5' splice site selection during constitutive splicing (**Figure 1.2**), and in regulating splice site selection during alternative splicing (19,20). Alternative splicing occurs in an estimated 95% of human gene transcripts enhancing transcriptome complexity and proteome diversity in higher eukaryotes (21). The most frequent alternative splicing event is the choice to include or skip an exon, termed a cassette exon. Other alternative splicing events involve the inclusion of one of two mutually exclusive exons, the use of alternative 3' and 5' splice sites, intron retention and the use of alternative promoters or poly(A) sites (22). Alternative splicing also occurs in the 3' and 5' untranslated regions (UTR) of mRNA which can alter mRNA stability and/or translation efficiency (23). These events are mediated in large part by the SR family of RNA binding proteins and their ability to bind exonic splicing enhancers and influence splice site inclusion or exclusion (24). Phosphorylation of the SR proteins affects both their nuclear localization within nuclear speckle domains and their nucleo-cytoplasmic shuttling (**Figure 1.3**), thereby regulating their ability to bind target transcripts. It is therefore likely that PRP4K plays an additional role in regulating alternative splicing through the phosphorylation of SRSF1 and other SR proteins yet to be identified as substrates.

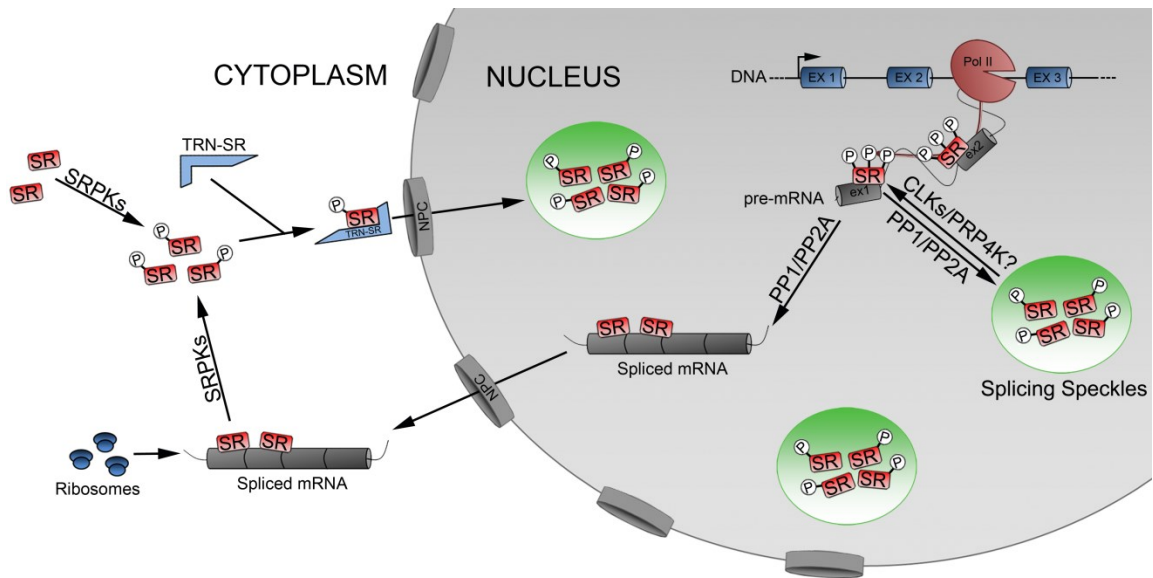


Figure 1.3 Phosphorylation dependent SR protein shuttling. Unphosphorylated SR proteins in the cytoplasm are phosphorylated by SRPK1 and targeted for nuclear import via the SR protein import receptor, transportin-SR (TRN-SR) (25,26). Once in the nucleus, phosphorylated SR proteins become enriched in interchromatin granules called splicing speckle domains. To be recruited from speckles to nascent pre-mRNA, where they act to regulate both constitutive and alternative splicing, SR proteins require additional phosphorylation events (27) which are mediated by the splicing kinase CLK1 (28) and potentially PRP4K. Once splicing is complete, hyper-phosphorylated SR proteins bound to mRNA are dephosphorylated by nuclear phosphatases (protein phosphatase 1 (PP1) and 2A (PP2A)) and are either recycled to the cytoplasm as a chaperone for mRNA export (29,30) where they also play a role in regulating translation of specific transcripts (31) or are re-phosphorylated and returned to speckles to await the next round of splicing.

1.3 PRP4K and the Spindle Assembly Checkpoint

The spindle assembly checkpoint (SAC) acts as an essential regulator of genomic stability by delaying the metaphase-anaphase transition until proper chromosome segregation is guaranteed. The checkpoint becomes activated during metaphase and remains activated until every kinetochore is attached to a microtubule (32) and tension is generated across the kinetochore (33). Activation of the checkpoint begins with recruitment of the checkpoint proteins monopolar spindle 1 (MPS1), binding uninhibited by benzimidazoles 1 (BUB1), BUB3 and centromere-associated protein E (CENP-E) to the unattached kinetochore, which is mediated by the Aurora B/INCENP complex (34). This, in turn, promotes the recruitment of mitotic arrest deficient 1 (MAD1) and MAD2 (35) to create a complex capable of binding and sequestering Cdc20, the activator of the anaphase promoting complex (APC). Once the checkpoint has been satisfied and all kinetochores have bound microtubules, the MAD1-MAD2 complex, along with Cdc20, is ejected from the kinetochore and Cdc20 becomes free to activate APC (36). APC, an E3 ubiquitin ligase, polyubiquitinates two key substrates, cyclin B1 and securin. Cyclin B1 degradation leads to the inactivation of cyclin-dependent kinase 1 (cdk1), initiating exit from mitosis, while degradation of securin activates separase which cleaves the cohesins holding sister chromatids together (**Figure 1.4A**). The cell is then free to progress through the remainder of mitosis leading to the generation of two genetically identical daughter cells.

PRP4K was found to play a role in SAC activation in 2007 when Montembault *et al.* observed PRP4K localized at kinetochores in HeLa cells (37). Knockdown of PRP4K was shown to induce mitotic acceleration and prevent mitotic arrest in cells treated with

nocodazole, a drug which inhibits microtubule dynamics and activates the SAC (37). When the group performed immunofluorescence analysis to determine the localization of SAC checkpoint proteins following PRP4K knockdown, they observed an absence of the checkpoint proteins MPS1, MAD1 and MAD2 at the kinetochores of prometaphase cells. Other checkpoint proteins such as Aurora-B and BubR1 were still present at kinetochores suggesting PRP4K is specifically required for the ordered recruitment/maintenance of MPS1, MAD1 and MAD2 at kinetochores in response to SAC activation (**Figure 1.4B**) (37).

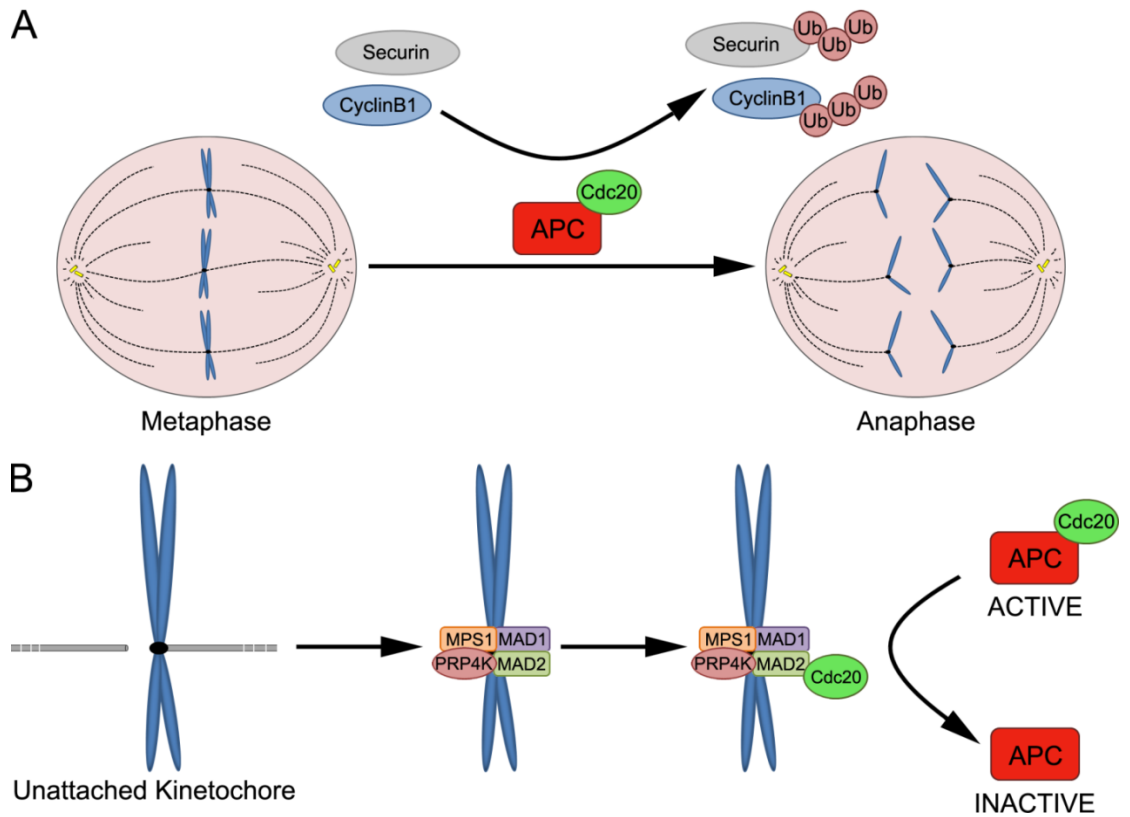


Figure 1.4 PRP4K is required for activation of the SAC. (A) The metaphase to anaphase transition is mediated by the E3 ubiquitin ligase APC. The binding of Cdc20 to APC results in its activation and the subsequent ubiquitination of securin and cyclin B1. Proteasomal degradation of these proteins results in the separation of sister chromatids and the eventual exit from mitosis. (B) Activation of the SAC involves the recruitment of checkpoint proteins PRP4K, MPS1, MAD1 and MAD2 to the unattached kinetochore. This complex sequesters Cdc20 away from APC, holding APC in an inactive state and preventing the metaphase to anaphase transition.

1.4 PRP4K and Viral Infection

Retroviruses are a family of single-stranded RNA viruses characterized by their ability to reverse transcribe genomic RNA into dsDNA upon host cell infection, followed by the subsequent integration into a host chromosome (38). For the majority of retroviruses, transcription of the viral DNA by RNA polymerase II generates a single polycistronic transcript which, through alternative splicing, serves as the precursor for all viral mRNAs. For example, transcription of the HIV-1 genome yields a single transcript which is alternatively spliced to produce greater than 30 mRNAs (39,40) encoding 15 distinct viral proteins (41). Spliced HIV-1 mRNA can be classified into two categories, the fully spliced 1.8-kb size class which encodes the regulatory proteins of HIV expressed early in the viral life-cycle, and the partially-spliced or unspliced 4 and 9-kb size class which encodes the structural, enzymatic and ancillary viral proteins expressed late in the viral life-cycle (42). The temporal expression of the two categories of mRNA is mediated by the splicing of the 9kb transcript. The 1.8-kb size class proteins are expressed early due to the inability to export partially-spliced or unspliced mRNA into the cytoplasm for translation. Included amongst the 1.8-kb regulatory proteins is Rev, a viral adaptor protein which contains an RNA-binding domain specific for the viral Rev response element (RRE), as well as a nuclear localization signal (NLS) and a nuclear export signal (NES) (43). The RRE and the NLS overlap (44) to create a shuttling mechanism whereby Rev proteins accumulate in the cytoplasm and are imported into the nucleus where they bind RREs present in partially-spliced and unspliced viral mRNA. Binding to the RRE masks the NLS which allows for Rev/mRNA export to the cytoplasm via the Crm1/Exportin1 nuclear export pathway (45). The nuclear export of partially or

unspliced mRNA by Rev allows for the transition from early-stage regulatory protein synthesis to late-stage structural/enzymatic synthesis required for new virion production. In addition, Rev has been shown to inhibit spliceosome assembly which promotes the accumulation of partially-spliced and unspliced viral mRNA in the nucleus, further promoting the switch from early- to late-stage protein synthesis (46).

PRP4K was shown to play a potential role in viral infection when it was identified as a binding partner for the HIV-2 Gag polyprotein in a yeast two-hybrid assay (47). HIV Gag proteins are expressed during the late structural/synthetic protein synthesis and play important roles in virion assembly and maturation (48). When bound to PRP4K, HIV-2 Gag inhibits the PRP4K-mediated phosphorylation of SRSF1. Phosphorylation of SRSF1, as described in section 1.2.3, is required to promote U1 snRNP binding to the 5' splice site and initiate spliceosome assembly. Though not yet shown, it is also possible that binding to HIV-2 Gag prevents PRP4K-mediated phosphorylation of PRP6 and PRP31 which would prevent tri-snRNP association with complex A (**Figure 1.2**). Thus, PRP4K binding to HIV-2 Gag inhibits splicing through the prevention of spliceosomal assembly. This data suggests that the synthesis of HIV-2 Gag during the late-stages of the viral life cycle results in the PRP4K-mediated inhibition of splicing which further promotes the accumulation of partially-spliced and unspliced viral mRNA. This would ensure that sufficient late-stage structural/enzymatic transcripts are produced to support virion production and completion of the viral life cycle.

1.5 PRP4K and Cellular Responses to Anti-Cancer Therapies

Two recent studies have provided evidence to suggest that PRP4K plays a role in regulating reactive oxygen species (ROS) production in cells treated with either ionizing radiation (IR) or the phytochemical curcumin (49,50). ROS are a family of highly-reactive molecules and free radicals derived from molecular oxygen. Cellular ROS are generated endogenously with the major sources being hydrogen peroxide and superoxide anions generated as by-products of cellular metabolism (51). Endogenous levels of ROS are scavenged by the cellular antioxidant defense system to prevent cellular damage by these highly reactive molecules. However, if ROS production increases beyond that capable of being scavenged by the defense system, the cell will undergo oxidative stress as a result ROS-mediated damage to DNA, lipids, and proteins (52). If the damage becomes too extensive to repair, the cell will undergo apoptosis through initiation of either the intrinsic or extrinsic apoptotic pathway (53). Many cancer therapies, including both chemotherapeutics and IR, are designed to increase cellular ROS levels beyond the point of repairable damage to induce apoptosis in cancer cells (54). In recent studies, treatment of the human colorectal carcinoma cell line HCT-15, with either the phytochemical curcumin or IR led to an increase in ROS production which corresponded with a decrease in PRP4K expression. Overexpression of PRP4K was shown to prevent ROS production and provide cellular protection from apoptosis in response to both treatments, possibly through the activation of an anti-oxidant enzyme system (49,50). This data suggests that tumours with high PRP4K expression may show increased resistance to radiation therapy or select chemotherapeutics due to increased ROS scavenging.

Finally, two studies have been published which suggest that PRP4K plays a role in the cellular response to the taxane family of anti-cancer agents, although they provide conflicting results as to whether PRP4K promotes taxane-mediated cell death, or protects against it. Taxanes are a family of microtubule-stabilizing agents which bind the β -tubulin subunit of microtubules preventing depolymerization (discussed in detail in Chapter 2). As a result, metaphase cells are unable to generate the tension across their kinetochores required to satisfy the SAC. Taxane-treated cells remain arrested in mitosis and eventually die by apoptosis. In 2007 Swanton *et al.* performed a large-scale RNA interference screen to identify genes which influenced cellular sensitivity to taxanes. Knockdown of PRP4K in HCT-116 colon cancer cells significantly increased cellular resistance to the taxane paclitaxel suggesting PRP4K promotes taxane-mediated cell death (55). A second study performed by Duan *et al.* in 2008 used a similar RNA interference screen to identify genes which could re-sensitize a multidrug-resistant human ovarian cancer cell line to taxanes. In this study, knockdown of PRP4K increased the cellular sensitivity to taxanes suggesting PRP4K prevents taxane-mediated cell death (56). Addressing the controversial role of PRP4K in the cellular response to taxanes is the first aim of this thesis.

1.6 Overview of Thesis Chapters

PRP4K is an essential kinase which, as described above, has frequently been identified in large-scale screens as an important mediator in several cellular processes. However, due to challenges associated with working with the kinase, the literature

surrounding PRP4K is limited. The objective of this thesis was to further our understanding of PRP4K and its role in cancer progression and treatment.

Chapter 2 explores the controversial role of PRP4K in the cellular response to taxanes and evaluates its potential as a predictive biomarker of taxane response in high-grade serous ovarian cancer patients. Chapter 3 describes the development of a novel zebrafish xenotransplantation technique to study *in vivo* drug responses of human cancer cells transplanted in zebrafish embryos. This model was developed to be used as a tool in our study of PRP4K and taxane response but instead, led to the discovery of a novel role for PPR4K in the regulation of anoikis, which is the focus of Chapter 4. Finally, Chapter 5 provides general discussions, conclusions, and future directions based on the completed works presented in this thesis.

1.7 Author Contributions

For sections previously published, DC prepared the manuscripts, JNB and GD provided editorial feedback. Experimental data not performed by DC (**Figures 2.3** and **2.8**) is indicated in the figure legends.

Chapter 2 PRP4K is a HER2-Regulated Modifier of Taxane Sensitivity

This chapter contains material (sections 2.2, 2.3, 2.4, Figures 2.2-2.8) originally published in:

“Corkery DP, Le Page C, Meunier L, Provencher D, Mes-Masson AM, Dellaire G. 2015. PRP4K is a HER2-Regulated Modifier of Taxane Sensitivity. *Cell Cycle*. 14:1059-1069”

2.1 Introduction

2.1.1 Taxanes: Mechanism of Action

Paclitaxel (Taxol), the prototype of the taxane family of cytotoxic agents, was isolated from the bark of the pacific yew tree (*Taxus brevifolia*) in 1971 (57). It was initially approved for use in the treatment of advanced ovarian cancer in 1992 and subsequently endorsed for the treatment of metastatic breast cancer in 1994 and non-small cell lung carcinoma in 1999 (58). Today, paclitaxel and its two semi-synthetic derivatives, docetaxel and cabazitaxel, are amongst the most commonly used chemotherapeutic agents for the treatment of a variety of malignancies, including breast (59) and ovarian (60) cancer.

The taxanes exert their cytotoxic activity through their ability to bind the β -tubulin subunit of microtubules and prevent depolymerization. During prometaphase, after the chromosomes have condensed and the centrosomes have migrated to opposite poles of the cell, γ -tubulin associates with several other proteins to form the γ -tubulin

ring complex (γ -TuRC). The γ -TuRC is recruited to the centrosome and acts as a scaffold for nucleation of the microtubule (61). During nucleation, heterodimers of α - and β -tubulin polymerize head-to-tail to form linear protofilaments. Thirteen protofilaments associate laterally to form the cylindrical microtubule with α -tubulin subunits exposed at one end (the (-) end) and β -tubulin subunits at the other (the (+) end) (62). The (-) end of the microtubule is associated with the γ -TuRC, leaving the (+) end free to bind additional tubulin heterodimers (polymerize) causing the microtubule to extend in length, or remove heterodimers (depolymerize) leading to a decrease in microtubule length. In a process termed “search-and-capture”, centrosome-nucleated microtubules undergo a series of polymerization and depolymerization reactions causing them to probe three-dimensional space until they are captured and stabilized by a sister kinetochore on a condensed chromosome (63). The search-and-capture process continues until every chromosome is bound by two microtubules, one from each centrosome. Once bound by a microtubule, the sister chromatid begins to oscillate back and forth which, combined with depolymerization of the microtubule, generates tension on the kinetochore. Only once appropriate tension is placed on both of the paired kinetochores from opposite poles, is the cell able to proceed from metaphase to anaphase. The checkpoint which regulates the metaphase to anaphase transition is called the SAC, and is discussed in detail in section 1.3. In the absence of drug, the cell will proceed to anaphase, where the cohesins which hold sister chromatids together are cleaved by the cysteine protease separase. Microtubules will then depolymerize, pulling sister chromatids to opposite poles of the cell in preparation for nuclear envelope formation and cytokinesis. Taxanes will reversibly bind the β -tubulin subunits of microtubules at a site which is only present in

assembled tubulin, and not in free α/β heterodimers (64). Binding causes polymerization of lateral protofilaments and enhances microtubule stability which prevents microtubule depolymerization. As a result, proper tension is never achieved across the paired kinetochores and the cell remains arrested in metaphase. The fate of a cell arrested in metaphase is discussed in the following section.

2.1.2 The Spindle Assembly Checkpoint and Its Role in Taxane Response

As discussed in section 2.1.1, taxane treatment stabilizes microtubules preventing tension at the kinetochore and resulting in the prolonged activation of the SAC. For a cell which has undergone prolonged SAC activation, there are four potential outcomes (65): (1) Mitotic cell death (MCD); the arrested cell immediately undergoes apoptosis (66). (2) Exit mitosis without division (Mitotic Slippage) followed by apoptosis. (3) Mitotic slippage followed by indefinite interphase arrest (senescence). (4) Mitotic slippage followed by continued cell division with abnormal genome content. The pathways which regulate the outcome following prolonged SAC activation are unclear, but recent evidence suggests the decision is influenced both by the pathways which regulate cyclin B1 degradation and pathways which induce apoptosis. While SAC activation inhibits the APC-mediated degradation of cyclin B1, it has been shown that, even during SAC activation, cyclin B1 is slowly degraded (67). Eventually, with prolonged SAC activation, the levels of cyclin B1 will fall below the threshold required to maintain mitotic arrest, and the cell will undergo mitotic slippage (67). Therefore, the pathways which govern the rate at which cyclin B1 is degraded will influence how long a cell can remain arrested in mitosis before slippage occurs. If the time is sufficient to

allow apoptotic signals to accumulate, the cell will undergo mitotic cell death (outcome #1), if the time is not sufficient for accumulation of apoptotic signals, or the apoptotic pathways are deficient, the cell will undergo slippage. Determining which factors regulate the rate of cyclin B1 degradation during prolonged SAC activation is important as they could represent a novel mechanism of taxane resistance.

2.1.3 Taxanes: Mechanisms of Resistance

The major limitation in the use of taxanes is the emergence of clinical drug resistance. As a result, much effort has been focused on determining both biological markers for predicting taxane response and the mechanisms underlying intrinsic and acquired resistance to taxane therapy.

2.1.3.1 P-gp Overexpression

The most common mechanism of taxane resistance encountered *in vitro* is the up-regulation of the ATP-binding cassette transporter, P-glycoprotein (P-gp) (68-70). P-gp is a plasma membrane glycoprotein consisting of two nucleotide-binding domains (NBDs) and two transmembrane domains (TMDs), each with six α -helical membrane-spanning segments. The twelve transmembrane segments form an active pore with an affinity for numerous anti-cancer agents including taxanes, anthracyclines, *vinca* alkaloids and epipodophyllotoxins (71-73). Binding of a substrate to the transmembrane region stimulates the ATPase activity of P-gp leading to a conformational change which releases the substrate to the extracellular space (74,75). While there is substantial evidence supporting the role of P-gp in the development of taxane resistance *in vitro*, the value of

P-gp as a marker of taxane response *in vivo* remains unknown due to conflicting clinical reports (76,77).

2.1.3.2 β -Tubulin Mutations

Resistance to taxanes can also result from alterations in tubulin which affect taxane binding and/or microtubule stability. Several point mutations have been identified within β -tubulin which, based on molecular modeling, can directly inhibit taxane binding *in vitro* (78). More commonly, point mutations found within both α - and β -tubulin that lead to increased taxane resistance result in decreased microtubule stability (79,80). These mutations are believed to counteract the stabilizing effect of taxanes. Clinically, the prevalence of tubulin mutations, and the relevance of these mutations in predicting response to taxane-based therapy, is a subject of debate. One study identified β -tubulin mutations in serum DNA isolated from 33% of non-small-cell lung cancer patients, which correlated with poor response to taxane-based therapy (81). This result, however, could not be reproduced in several subsequent studies (82-85). Interestingly, cell lines which have acquired microtubule-destabilizing β -tubulin point mutations *in vitro* often show such an extreme instability of microtubules that they require a constant low dose of taxane to carry out normal cellular functions (80). This observation may help explain the lack of β -tubulin mutations observed *in vivo*.

2.1.3.3 Altered β -Tubulin Isozyme Expression

Altered expression of β -tubulin isoforms has also been shown to influence taxane response. There are six different classes of β -tubulin isoforms (I, II, III, IVa, IVb, and VI)

which differ in only 4-16% of their amino acid residues (86). In mammalian cells, microtubules are comprised of all expressed isotypes, but the ratio of expression has been shown to influence the sensitivity to taxanes. Specifically, increased class III β -tubulin (TUBB3) expression appears to offer the greatest protection against taxane treatment both *in vitro* (87) and *in vivo* (88). The mechanism through which TUBB3 upregulation confers resistance to taxanes is not clear, but may have to do with the altered dynamics of microtubules enriched in TUBB3 (89).

2.1.3.4 Altered Expression of Microtubule-Associated Proteins

Microtubule-associated proteins (MAPs) are a family of proteins which interact with microtubules and regulate their dynamics. Three family members with established roles in taxane sensitivity are stathmin, MAP4 and tau. Stathmin is a soluble cytoplasmic protein which interacts with tubulin dimers and stimulates microtubule catastrophe (90); the switch from microtubule growth to rapid shrinkage (91). Overexpression of stathmin in cancer cells leads to a destabilization of microtubules which can oppose the microtubule stabilizing effects of taxanes and increase the cellular resistance to the drug (92). MAP4, on the other hand, acts as a microtubule stabilizer by promoting the transition from microtubule shortening to elongation (rescue) (93). Loss of MAP4 in cancer cells has been shown to decrease microtubule stability and enhances taxane resistance (94). Tau presents a third scenario for MAP regulation of taxane sensitivity by sharing the same binding site on microtubules as taxanes (95). In this scenario, overexpression of tau would increase cellular resistance to taxanes by preventing taxane binding through direct competition. While pre-clinical studies suggest that tau

overexpression correlates with poor response to taxane-based therapies (96), overexpression of tau *in vitro* does not appear to alter taxane sensitivity (97).

2.1.3.5 Alterations in the Apoptotic Pathway

The induction of apoptosis is a tightly regulated event orchestrated by multiple pathways which contain positive and negative regulatory proteins. Not surprisingly, changes in the expression or activity of many of these proteins can impact taxane sensitivity. One apoptotic protein which has recently emerged as a mediator of taxane sensitivity is Bcl-2. Bcl-2, an anti-apoptotic member of the Bcl-2 family of proteins, functions through the binding and antagonizing of the proapoptotic proteins Bak and Bax. Bak and Bax, upon induction of apoptosis, relocate from the cytosol to the outer mitochondrial membrane where they dimerize and form a pore, releasing cytochrome c into the cytoplasm. Cytochrome c activates downstream caspases which are responsible for cell destruction. Bcl-2 overexpression is common in several types of human cancer (98) yet, paradoxically, its downregulation is associated with increased resistance to taxanes (99). Interestingly, paclitaxel can bind Bcl-2 directly and alter its function, resulting in the opening of a pore in the mitochondrial membrane called the permeability transition pore channel (PTPC) (100). Opening of this pore, much like the dimerization of Bak and Bax, results in the release of cytochrome c, and induction of apoptosis. Therefore, paclitaxel not only functions through the induction of mitotic arrest, but also by regulating the opening of the PTPC through the binding of Bcl-2. This additional function of paclitaxel explains how loss of Bcl-2 can increase resistance to taxanes.

2.1.3.6 Disruption of the Spindle Assembly Checkpoint

As discussed in 2.1.2, a functional spindle assembly checkpoint is essential for taxane-induced cell death. As a result, alterations which disrupt SAC functionality will also impact taxane sensitivity. For example, suppression of checkpoint components MAD2 or BUBR1 abolishes checkpoint function resulting in taxane resistance. In contrast, overexpressing MAD2 in cells with a checkpoint defect resulting from chronically low MAD2 restores checkpoint function and increases sensitivity to taxanes (101,102). Similarly, cell lines expressing a dominant-negative form of BUB1 display reduced checkpoint function and increased taxane resistance (103). Finally, Aurora-A overexpression has been shown to override the SAC resulting in anaphase progression despite defective spindle formation. This is preceded by failed cytokinesis resulting in the generation of a single multinucleated cell. As expected, these cells also display an increased resistance towards taxanes (104).

2.1.4 HER2 Amplification in Breast and Ovarian Cancer

HER2/ErbB2 is a member of the human epidermal growth factor receptor (HER) family of proteins and is overexpressed in a subset of ovarian and breast cancers (105,106). HER2 is a transmembrane receptor protein which consists of a cysteine-rich extracellular ligand-binding domain, a hydrophobic transmembrane domain and an intracellular tyrosine kinase domain. To date, no ligand of the HER2 receptor has been identified. Instead, HER2 signaling is mediated through heterodimerization with ligand-activated members of the HER family (epidermal growth factor receptor (EGFR) or HER3), or in the case of *HER2* amplification, through HER2 homodimerization as well

(107,108). The ability of HER2 to dimerize in the absence of ligand has to do with the unique structure of its extracellular domain. Crystallographic data has revealed that the extracellular domain of HER proteins can exist in either a closed/inhibited conformation or an open/active conformation. Ligand binding induces a conformational switch from the closed to open conformation which promotes dimerization, and subsequent autophosphorylation of the intracellular domain. HER2 is unique in that it is constitutively in the open conformation, allowing dimerization in the absence of ligand (109,110).

Amplification of *HER2* can result in 25-50 copies of the *HER2* gene being expressed leading to a 40-100 fold increase in protein expression (111,112). Because HER2 doesn't require ligand binding for dimerization, amplification leads to hyper activation of signaling pathways downstream of HER2. Upon dimerization, tyrosine residues on the intracellular domain become autophosphorylated by the tyrosine kinase domain and act as docking sites for numerous intracellular signalling molecules. Docking of these signalling molecules results in the activation of a plethora of downstream second messenger pathways which promote cell growth, proliferation, survival, angiogenesis and invasion (113). Of the downstream pathways, the two which seem to be most significantly implicated in tumorigenesis and have been the most extensively studied are the PI3K/Akt pathway and the mitogen-activated protein kinase (MAPK) pathway (**Figure 2.1**).

Heterodimerization of a HER2 with a HER3 receptor results in the phosphorylation of the tyrosine residue within six YXXM PI3K-binding motifs found within the intracellular domain of HER3 (114). Recruitment of PI3K to HER3 serves to

bring PI3K within proximity of its membrane-bound substrate phosphatidyl inositol bisphosphate (PIP₂). PI3K phosphorylates PIP₂ generating PIP₃ which recruits the Pleckstrin Homology (PH) domain-containing enzyme phosphoinositide-dependent kinase 1 (PDK1) to the plasma membrane. Once at the membrane, PDK1 will phosphorylate its substrates including protein kinase C (PKC), p70S6 kinase (S6K) and Akt. Phosphorylation of Akt at Thr308 by PDK1, combined with an independent phosphorylation event at Ser473 mediated by mTORC2, activates Akt. Active Akt can then phosphorylate a variety of kinases and transcription factors which promote tumorigenesis through multiple mechanisms (**Figure 2.1**). For example, Akt can phosphorylate the pro-apoptotic protein BAD, which prevents it from heterodimerizing with Bcl-XL/Bcl-2 to induce apoptosis (115). Akt can also phosphorylate Mdm2, the E3 ubiquitin ligase which targets the p53 tumour suppressor for degradation (116). Mdm2 phosphorylation by Akt targets Mdm2 to the nucleus resulting in the ubiquitination, nuclear export, and degradation of nuclear p53, preventing its transcriptional activity (117,118). As a final example Akt can phosphorylate and activate mammalian target of rapamycin (mTOR) while simultaneously inhibiting mTOR inhibitor proteins PRAS40 (119) and Tuberous Sclerosis Complex 2 (TSC2) (120). Activation of mTOR promotes cell growth and G1 cell cycle progression through S6K signaling and 4EBP1 inhibition (121).

Homodimerization of two HER2 receptors results in the phosphorylation of tyrosine residues within the intracellular domain of HER2 (**Figure 2.1**). Phosphorylation of tyrosine 1139 recruits the adaptor protein Grb2 to the receptor (122). Grb2 acts as a docking protein to recruit, and activate, the Ras guanine nucleotide exchange factor, son

of sevenless (SOS). SOS, in turn, catalyzes the conversion of inactive GDP-bound Ras to the active GTP-bound Ras (123). The activation of Ras by SOS promotes cell proliferation and prevents apoptosis through activation of the Raf/MEK/ERK pathway (124). Briefly, activated Ras functions as an adaptor protein to bind and recruit Raf to the cellular membrane where it is activated through its phosphorylation by membrane-bound kinases such as PAK-1 or other activated Raf kinases (125). Once active, Raf triggers sequential phosphorylation and activation of MEK and ERK. Phosphorylated ERK will translocate to the nucleus where it phosphorylates a variety of transcription factors such as c-Myc, Ets, CREB, c-Jun and FOXO3a culminating in the inhibited transcription of pro-apoptotic genes (Bim, FasL, TRAIL) and genes involved in cell cycle arrest (p27, p21) (124). The PI3K/Akt and Ras/ERK pathways provide an example of how *HER2* amplification can contribute to tumorigenesis through multiple downstream pathways.

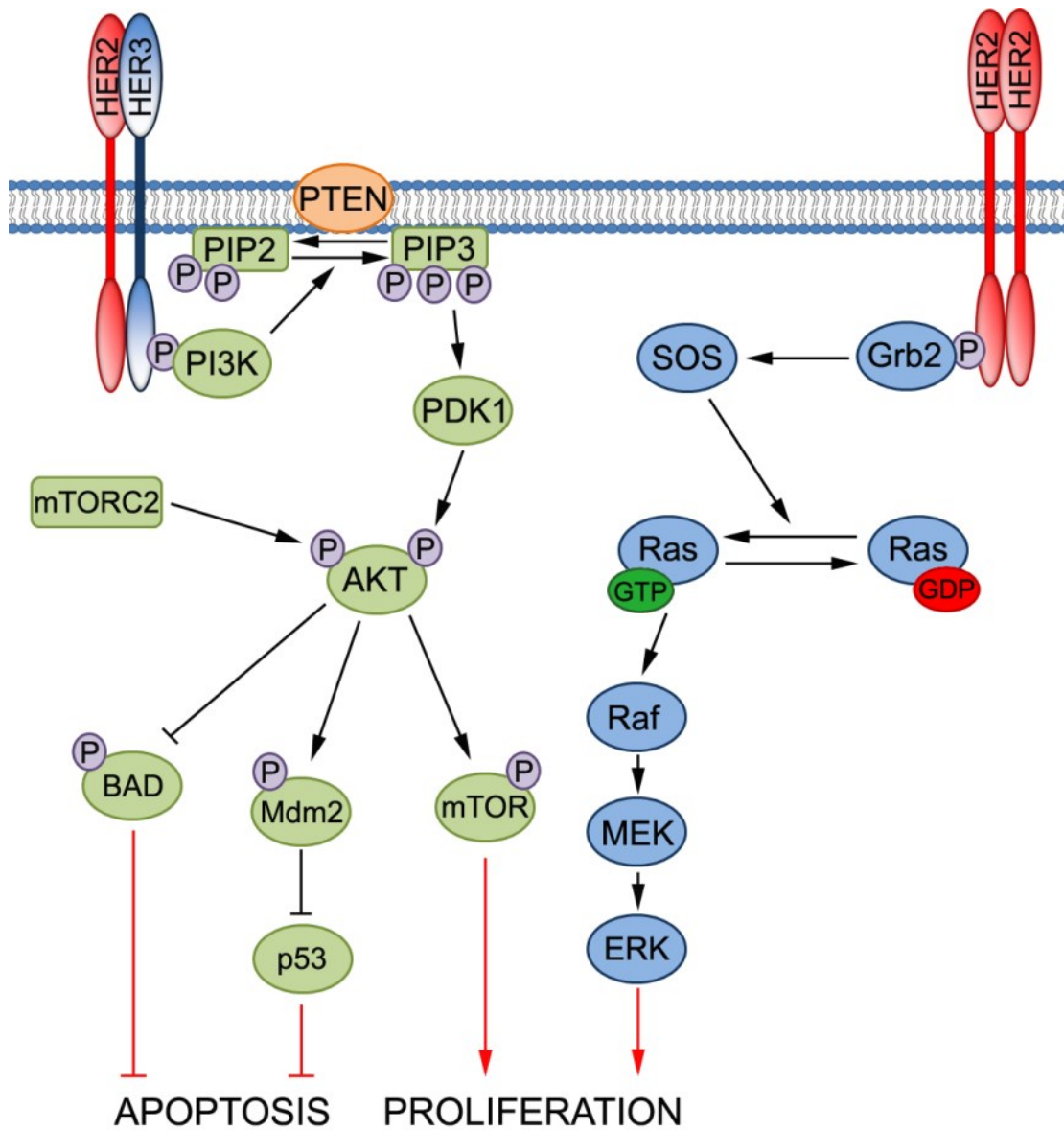


Figure 2.1 HER2 signaling pathways. HER2 homodimerization or HER2/HER3 heterodimerization initiates the activation of various downstream pathways. Included amongst these pathways are the Akt and Ras pathway which inhibit apoptosis and promote cell proliferation. Black arrows indicate intra-pathway signaling events and red arrows indicate the end result of pathway activation.

In addition to the role in tumorigenesis, the amplification/overexpression of the *HER2* gene has also been widely explored for its potential application in predicting taxane response in breast cancer. *In vitro*, *HER2* amplification has been shown to increase cellular resistance to taxanes in breast cancer cells (126), while a number of clinical studies have shown *HER2* amplification to correlate with increased response to taxanes, either as a single agent (127,128), or as part of a combination therapy (129-132). As a result, the use of *HER2* as a biomarker for taxane sensitivity remains controversial, while the mechanism(s) through which *HER2* signaling alters taxane sensitivity remains to be elucidated. A greater understanding of the genes acting downstream of *HER2* with a more direct role in the modulation of taxane sensitivity is essential to improve our ability to predict taxane response.

In this chapter, we identify PRP4K as a novel *HER2*-regulated protein in breast and ovarian cancer. We demonstrate that decreased PRP4K protein level results in reduced sensitivity to paclitaxel in both breast and ovarian cancer cell lines, and that *in vitro*-derived and patient-acquired taxane resistance correlates with reduced PRP4K expression. In addition, high PRP4K protein expression in the biopsies of ovarian cancer patients with tumours expressing low levels of *HER2* correlates with better overall survival to treatment with platinum/taxane-based therapy. Taken together these results implicate PRP4K, through its role in the SAC, as a *HER2*-regulated modulator of taxane sensitivity.

2.2 Materials and Methods

2.2.1 Patients and Tissue Specimens

Ethics approval was obtained by the local institutional ethics board (Comité d'éthique de la recherche du Centre hospitalier de l'Université de Montréal). Tumour samples were collected and banked following appropriate written consent from patients undergoing surgery at the Centre Hospitalier de l'Université de Montréal from 1993 to 2010. An independent pathologist scored tumour grade and stage and a gynecologic oncologist scored tumour residual disease according to criteria from the International Federation of Gynecologists and Obstetricians. Less than 10% of specimens were excluded on quality, and this was not correlated to age of sample. Clinical data on progression-free survival were defined based on imaging and CA125 blood levels. Overall survival was defined as the time from surgery to death from ovarian cancer. Patients known to be alive at the time of analysis were censored to the time of their last follow-up. Patient disease-free survival was calculated from the time of surgery until the first progression. Eligibility criteria for inclusion in the study were as follows: no pre-operative chemotherapeutic treatment for ovarian cancer; platinum-based post-operative chemotherapy treatment, high-grade tumours, serous histopathology subtype and completed informed consent. All patients received a platinum-based chemotherapy as an initial therapy after surgery with the exception of patients who died shortly (<3 months) after surgery. Patients who died from other causes were censored at time of last follow-up.

2.2.2 Tissue Microarray and Immunohistochemistry

The breast and ovarian cancer tissue arrays have previously been described (133,134). Briefly, areas of tumour were selected based on review of a hematoxylin and eosin-stained slide. Formalin-fixed, paraffin-embedded tumor blocks were then biopsied using a 0.6 mm needle and resultant cores were arrayed into a grid in a recipient paraffin block using a Pathology Device Tissue Microarrayer (Pathology Devices Inc.). The breast cancer tissue array contained samples from 141 consented patients who had undergone surgical resectioning with auxiliary lymph node dissection for breast cancer, at the Centre hospitalier de l'Universite de Montreal – Hotel Dieu (CHUM-HD), between 2003 and 2007. The ovarian cancer tissue array contained samples from 260 ovarian cancer patients, with each patient represented by two cores. After review of clinical data, 61 patients were excluded from the final analysis as they did not meet the inclusion criteria. The tissue arrays were then sectioned, stained with hematoxylin-eosin and reviewed by an expert pathologist to confirm tumor content. Tissue arrays were sectioned at 4µm and the slides were stained using the BenchMark XT automated stainer (Ventana Medical System Inc.). Antigen retrieval was carried out with Cell Conditioning 1 (VMSI; #950-123) for 60 min. Prediluted sheep anti-PRP4K (1:100) (H143)(11), or anti-Her2 (DAKO #A0485) antibodies were automatically dispensed, and the slides were incubated at 37°C for 120 min or 30 min, respectively, and antibody binding was detected using the UltraView DAB detection kit (VMSI#760-091). Slides were counterstained with hematoxylin (VMSI#760-2021). All sections were observed by light microscopy at 400x magnification.

2.2.3 Staining Quantification

Tumor sections were scanned and digitally visualized. Epithelial zones were scored according to the antibody staining intensity (value 0 for absent, 1 for weak, 2 for moderate and 3 for high intensity). Each array was independently analyzed in a blind study by two independent observers. Correlation was >80%. The average of all cores with cancer from the same patient was used for the final analysis.

2.2.4 Cell Culture

SK-BR-3, IGROV-1, MCF-7, MDA-MB-231, SKOV-3 and HeLa cell lines (**Appendix C**) were cultured in Dulbecco's modified Eagle's medium (DMEM) (Sigma) supplemented with 10% fetal calf serum, 1% penicillin/streptomycin at 37°C with 5% CO₂. All cell lines were obtained originally from the American Type Culture Collection (ATCC) and validated by STR profiling (DDC Medical) within 6 months of experimentation. MCF-7, MDA-MB-231, SKOV-3 and HeLa cell lines stably expressing shRNAs were cultured as above but using Tetracycline-Free FBS (Invitrogen, 16000-036) and with the addition of 1 µg/mL puromycin. TOV1369 and OV1369(R2) cell lines were cultured in OSE medium (Wisent, 316-030-CL) supplemented with 10% fetal calf serum, 0.5µg/mL amphotericin B (Life Technologies, 15290-018), and 50µg/mL gentamicin (Life Technologies, 15750-078) at 37°C with 5%O₂ and 5%CO₂, as previously described (135).

2.2.5 Western Blot Analysis

Cells were harvested and lysed in ice-cold lysis buffer (20 mM Tris-HCl pH8, 300 mM KCl, 10% Glycerol, 0.25% Nonidet P-40, 0.5 mM EDTA, 0.5 mM EGTA, 1X

protease inhibitors (AEBSF, Aprotinin, Bestatin, E-64, Leupeptin, Pepstatin A)) for 30 minutes on ice. Cell debris was pelleted by centrifugation at 14 800 rpm for 25 minutes at 4°C. Protein concentrations were determined using Bio-Rad Protein Reagent (Bio-Rad, 500-0006). Lysates, with exception of those analyzed in **Figure 2.7A**, were dephosphorylated with calf intestinal phosphatase (Sigma, A2356) as previously described (136). Briefly, 400 µg of protein in 5 mM Tris pH 7.9, 10 mM NaCl, 1 mM MgCl₂, and 0.1 mM DTT were incubated with 100 units of alkaline phosphatase for 30 minutes at 30°C. This allowed for more accurate quantification as PRP4K is present in lysates in several phosphorylated-forms (**Figure 2.2**). Lysates were then mixed 1:1 with 2x sample buffer (4% SDS, 20% glycerol, 10% 2-mercaptoethanol, 0.004% bromphenol blue, 0.125 M Tris HCl ph 6.8) and boiled for 10 minutes prior to separation by SDS-PAGE and western blot analysis with sheep anti-PRP4K antibody (H143) (11), rabbit anti-HER2 antibody (Cell Signaling, #2165), or mouse anti-actin antibody (Sigma, A3853). Protein detection was carried out using chemiluminescence (Thermo Scientific, 34080) and radiographic film (Thermo Scientific, 34091). Quantification of band intensities was performed by densitometry analysis using ImageJ (NIH).

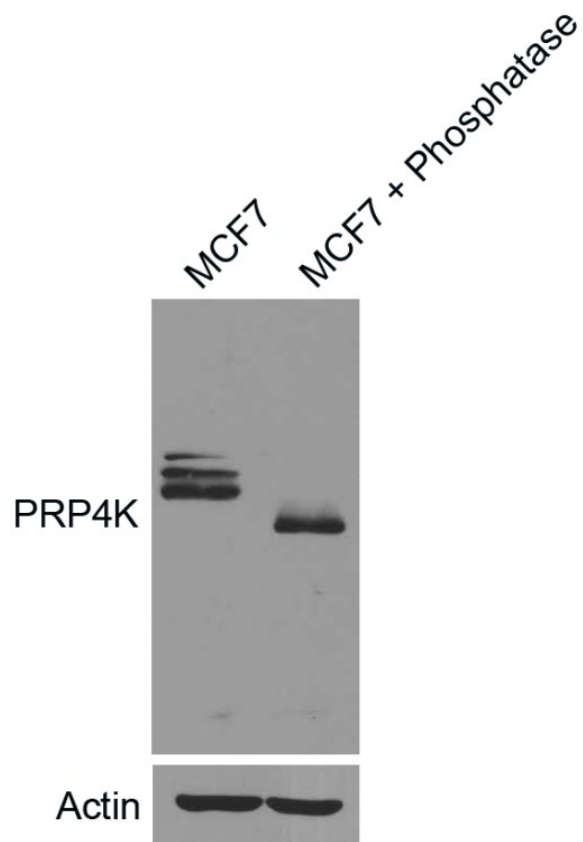


Figure 2.2 PRP4K is present in lysates in different phosphorylated-states. MCF-7 whole cell lysates were treated with calf intestinal phosphatase, or mock treated, and analyzed by western blot analysis using antibodies specific for PRP4K and actin.

2.2.6 shRNA Lentiviral Transduction

To knockdown HER2 in the IGROV-1 and SK-BR-3 cell lines, HER2-targeting GIPZ Lentiviral shRNAs (shHER2-1 = clone: V3LHS_315855, shHER2-2 = clone: V3LHS_315852) were purchased from Thermo Scientific. To create the MCF7, MDA-MB-231, SKOV3, and HeLa-GFP-H2B PRP4K knockdown cell lines, PRP4K-targeting TRIPZ Inducible Lentiviral Human shRNAs (Thermos Scientific) (shPRP4K-1 = clone:V2THS_47787, shPRP4K-2 = clone:V3THS_383960) were purchased. Lentivirus was obtained by co-transfection of a TRIPZ or GIPZ shRNA with vectors expressing proteins required for lentiviral propagation (pMD2.G, pCMV-8.92, and pCMV-8.93 vectors (described previously (137)) into human HEK-293T cells with calcium-phosphate transfection (Promega, E1200), according to manufacturer's directions. After 48 h, media from the transfected cells was filter sterilized using a 0.45 μ filter, and the viral media added to the target cell line for 48 h. To select for viral integration, cells were cultured in the presence of 1 μ g/ml puromycin for at least 48 h. To induce expression of the inducible TRIPZ PRP4K shRNA, 2 μ g/mL doxycycline was added to culture media for 96 h with the drug being replaced every 24 h.

2.2.7 GFP-H2B Cell Line Generation

Cell lines that stably express green fluorescent protein fused to histone H2B (GFP-H2B) were created by transfecting HeLa cells with a GFP-H2B plasmid (Addgene #11680) (138) using the Neon Transfection System (Life Technologies), according to the manufacturer's directions. After 7 days in culture, stably transfected cells were isolated by screening for GFP-positive colonies obtained by limiting dilution.

2.2.8 Immunofluorescence

Cells were plated onto sterile coverslips in a 6-well dish and allowed to adhere overnight. The cells were then transfected with plasmids that would express the protein of interest using Lipofectamine2000 (Life Technologies, 11668027), according to the manufacturer's directions. Plasmids for expressing constitutively active (HER2CA (V659E) (Addgene plasmid # 16259) (139)), and kinase dead (HER2KD (K753M) (Addgene plasmid #16258) (139)) HER2 were obtained from Addgene. Forty-eight hours post-transfection, cells were washed with PBS and fixed in 3% paraformaldehyde for 20 min. Immunolabeling was carried out as previously described (140). Briefly, cells were permeabilized by treating coverslips with 0.5% TritonX-100 (SIGMA-ALDRICH, T8787) for 5 minutes followed by three 5-minute washes with PBS. Cells were blocked in 5% donkey serum (SIGMA-ALDRICH, D9663) in PBS for 20 minutes followed by a 1 hour incubation with antibodies specific for PRP4K (diluted 1:400) and HER2 (diluted 1:200) antibodies in 5% donkey serum in PBS. Following the incubation with the primary antibody, cells were washed 3 times with PBS (5 minutes each wash) and incubated with Alexa Fluor 488-donkey anti-sheep (Life Technologies, A-11015) and Alexa Fluor 555-goat anti-rabbit (Life Technologies, A-21428) secondary antibodies diluted 1:200 in 5% donkey serum in PBS. Cells were washed 3 times with PBS for 5 minutes per wash. DAPI (4',6-diamidino-2-phenylindole) (SIGMA-ALDRICH, D9564) was added to the second of the three washes at a final concentration of 1 µg/ml to visualize nuclei. Coverslips were mounted on frosted glass microscope slides (Fisher Scientific, 12-550-15) using VECTASHIELD antifade mounting medium (Vector Laboratories, H-1000).

Fluorescent images were captured with a Zeiss Cell Observer Microscope under a 63× immersion oil objective lens. Images were processed using only linear adjustments (e.g. brightness/contrast) with Slidebook (Intelligent Imaging Innovations, Boulder, CO) and Adobe Photoshop CS5.

2.2.9 HER2 Inhibition

To inhibit HER2 signaling, SK-BR-3 and IGROV-1 cells were maintained in the presence of 0.1 μM, and 7.5 μM Lapatinib Ditosylate (Selleck, S1028), respectively, for 48 h.

2.2.10 In Vitro Cell Viability Assay

Paclitaxel (Sigma, T7402) was reconstituted in dimethyl sulfoxide (DMSO) and diluted in growth media so that the DMSO concentration was 0.05% or less. To evaluate paclitaxel response *in vitro*, 7 000 cells were plated in individual wells of a 96 well plate, and allowed to adhere for 24 h prior to incubation with the indicated concentration of paclitaxel for 90 min. Following acute 90 minute paclitaxel treatment, the drug was removed and cells were allowed to recover in fresh medium for 72 h, at which point cell viability was measured using the alamarBlue® cell viability assay (Life Technologies, DAL1100) according to the manufacture's protocol. Fluorescence was measured using an Infinite M200 Pro plate reader (Tecan Group Ltd) 4 h after the addition of alamarBlue® reagent. To determine the effect of PRP4K knockdown on paclitaxel response, cell lines stably expressing an shRNA were incubated with 2 μg/ml doxycycline for 92 h to induce

hairpin expression prior to plating in the 96 well plate, and maintained in doxycycline for the remainder of the experiment.

2.2.11 Statistical Analysis

Survival curves were plotted using the Kaplan-Meier curve analysis and the log-rank test was used to test for significance. Univariate Cox proportional hazard models were used to estimate the hazard ratio for PRP4K expression. For the *in vitro* viability assays a Student's t-test was used to compare viability between cell lines. A Spearman correlation test was applied to compare biomarker staining. All statistical analyses were done using the Statistical Package for the Social Sciences software version 11.0 (SPSS, Inc.), and statistical significance was set at $p \leq 0.05$.

2.3 Results

2.3.1 High PRP4K Protein Level Correlates with HER2 Amplification in Human Breast and Ovarian Tumours

Despite PRP4K being an essential pre-mRNA splicing kinase, a number of studies have variously claimed that PRP4K may be oncogenic and a possible molecular target in cancer (56,141) or may be a predictive biomarker of treatment response to chemotherapy. In particular, PRP4K has been shown to play a role in the cellular response to taxanes, although published studies are contradictory as to whether PRP4K increases or decreases sensitivity to taxanes (55,56). Therefore, the role of PRP4K as a biomarker or anti-cancer drug target remains controversial. To better evaluate the possible role of PRP4K in cancer, we performed immunohistochemistry analysis of PRP4K expression in breast and

ovarian tumours using tissue microarrays (TMAs) composed of pre-chemotherapy surgical samples. We scored the intensity of immunohistological staining for PRP4K using a relative scale from 0 to 3, and looked for correlation with a number of commonly used prognostic and therapeutic markers of breast and ovarian cancer (**Figure 2.3A**). A positive correlation was observed between PRP4K and the proliferation marker Ki-67, the recently identified prognostic marker butyrophilin, subfamily 3, member A2 (BTF4/BTN3A2) (142), and the immunological cell markers CD3 and CD68 within the high-grade serous ovarian TMA, while a positive correlation between PRP4K and HER2 was observed within both the ovarian and breast TMA (**Figure 2.3B**).

A

Breast Cancer Correlations

	Stage	Grade	Lymph Node +	Tumour Size	Triple Negative	ER	PR	HER2
Corr. Coeff.†	0.104	0.027	-0.095	0.163	-0.061	-0.042	-0.062	*0.204
p	0.207	0.771	0.33	0.081	0.502	0.637	0.513	0.021
N	114	115	106	115	123	115	112	128

Ovarian Cancer Correlations

	Stage	p53	BTF4	Ki67 Total	CA-125 Pre-Dx	HER2	CD3	CD8	CD68	RD
Corr. Coeff.†	-0.010	0.108	*0.293	*0.298	-0.087	*0.225	*0.171	0.065	*0.170	-0.080
p	0.893	0.184	>0.001	>0.001	0.254	0.007	0.026	0.402	0.024	0.356
N	180	152	179	177	169	0.143	169	167	176	134

B

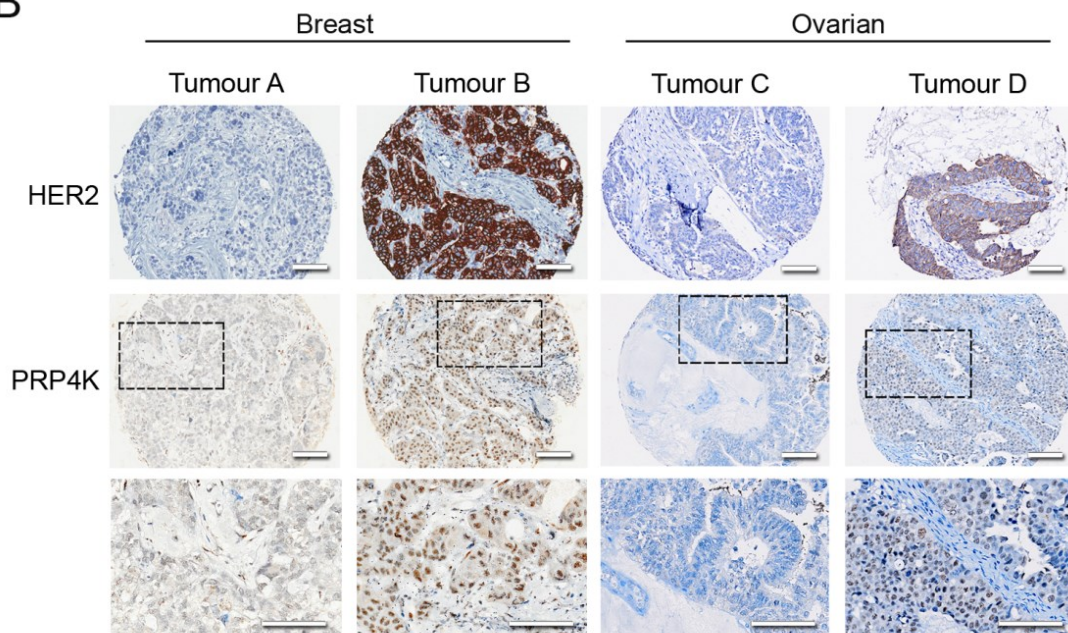


Figure 2.3 PRP4K correlates positively with HER2 expression in breast and ovarian tumours. (A) Breast and ovarian cancer tissue microarrays were used to correlate PRP4K protein levels with commonly used diagnostic and prognostic markers. Results are summarized in table format. † Spearman’s Correlation coefficient (non-parametric); * = Significant; N= number of patients, ER = Estrogen Receptor, PR = Progesterone Receptor, RD = Residual Disease (B) Representative immunostaining of low (tumour A and C) and high (tumour B and D) PRP4K/HER2 (indicated by brown stain) in the breast and high-grade serous ovarian TMA. Dashed black boxes outline a region of the tumour in each TMA stained for PRP4K shown at higher magnification below each panel. Scale bars = 100 microns. *Data presented in this figure was collected by the Mes-Masson lab.*

2.3.2 HER2 Signalling Positively Regulates PRP4K

Since PRP4K levels measured by immunohistochemistry correlated with HER2 expression in breast and ovarian tumours, we next sought to determine if the positive correlation between PRP4K and HER2 was a result of direct regulation of PRP4K protein levels by HER2. To this end, HER2 expression was knocked down in two respective ovarian and breast cancer cell lines, IGROV-1 and SK-BR-3. As shown in **Figure 2.4A**, when cells were transduced with a HER2-targeting shRNA lentiviral vector, there is a significant reduction in both HER2 and PRP4K protein level. To determine if this regulation of PRP4K expression was mediated by active signaling through the HER2 receptor, IGROV-1 and SK-BR-3 cells were treated with the kinase inhibitor lapatinib for 48 h. In both cell lines, inhibition of HER2 signaling led to a decrease in PRP4K protein level (**Figure 2.4B**). Conversely, when the HER2 negative breast cancer cell line MCF-7 was transfected with constitutively active HER2 (139), PRP4K expression increased (**Figure 2.4C**), while the transfection of kinase dead HER2 (139) had no effect. Taken together, these data indicate that PRP4K protein expression is regulated by signaling through the HER2 receptor.

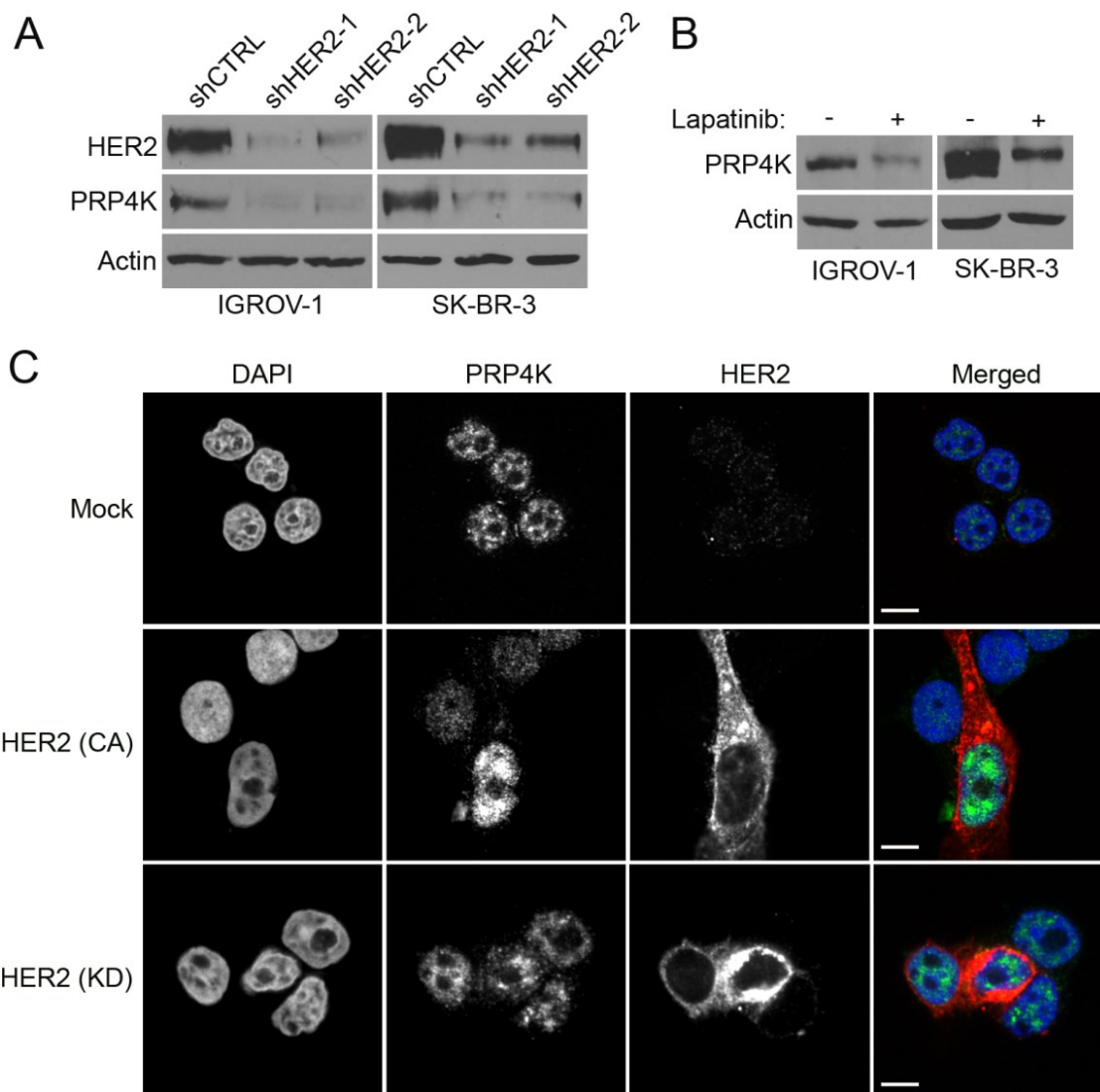


Figure 2.4 HER2 signaling regulates PRP4K expression. (A) IGROV-1 and SK-BR-3 cell lines were transduced with control or a HER2-targeting shRNA lentiviral vector and cultured for 48 h. Total cell lysates were prepared and subjected to western blot analysis for HER2 and PRP4K expression. (B) IGROV-1 and SK-BR-3 cell lines were treated with 0.1 μ M lapatinib for 48 h to inhibit HER2 signaling. Total cell lysates were subjected to western blot analysis for PRP4K expression. (C) MCF-7 cells were transfected with constitutively active (CA) or kinase dead (KD) HER2 and analysed by immunofluorescence confocal microscopy using an anti-HER2 (Red) and anti-PRP4K (Green) antibody. Nuclei were stained with DAPI. Scale bars = 10 microns.

2.3.3 Knockdown of PRP4K Decreases the Sensitivity of Cancer Cells to Paclitaxel

HER2 amplification has received a lot of attention for its potential application in predicting taxane response, although its use as predictive biomarker for taxane treatment remains controversial and the mechanism(s) that might govern the impact of HER2 over expression on the efficacy of taxane response, which might be used to guide therapy, remain to be elucidated. Since PRP4K is regulated by HER2 signalling, we next sought to explore the relationship between PRP4K and taxane response to determine if it could be playing a mechanistic role in the clinical link between HER2 amplification and a positive response to taxane treatment. Since PRP4K is an essential kinase, complete loss of kinase expression is lethal (11). Therefore, to explore the role of PRP4K in the cellular response to paclitaxel we employed an inducible knock-down system that could be used to titrate PRP4K levels without killing the cell or impairing cell division; events that would confound interpretation of taxane sensitivity assays, and may be a factor in previously conflicting studies of taxane drug response in relation to this kinase (55,56). To this end, we generated several breast (MCF-7, MDA-MB-231) and ovarian (SK-OV-3) cell lines stably expressing either a control hairpin (shCTRL), or one of two hairpins targeting PRP4K (shPRP4K-1 and shPRP4K-2) under the control of a doxycycline-inducible promoter. We found that the addition of 2 μ g/ml doxycycline to the culture medium for 96 h led to significant knockdown of PRP4K in all three cell lines without impacting cell viability (**Figure 2.5A**). Acute dosing (90 min) was chosen for the taxane response experiments, as described by Nguyen *et al.* (143), as opposed to the commonly used chronic dosing (48 h), to more closely mimic the type of exposure a cell would experience in a clinical setting where patients are treated intravenously. Intravenous

administration of paclitaxel results in a brief spike in serum taxane levels, followed by rapid drug clearance (144), meaning cells would only be exposed to drug for a short period of time (65). Knockdown of PRP4K expression over 96 h in each cell line resulted in significantly decreased sensitivity to paclitaxel, as measured by an alamarBlue cell viability assay following a 90 minute acute, low dose drug treatment and 72 hour recovery period in drug-free medium (**Figure 2.5B**). Similarly, when PRP4K expression was decreased in SK-BR-3 cells by pre-treating for 48 h with 0.1 μ M lapatinib (**Figure 2.5B**), cells showed decreased sensitivity to paclitaxel, as compared to the untreated control (**Figure 2.5C**).

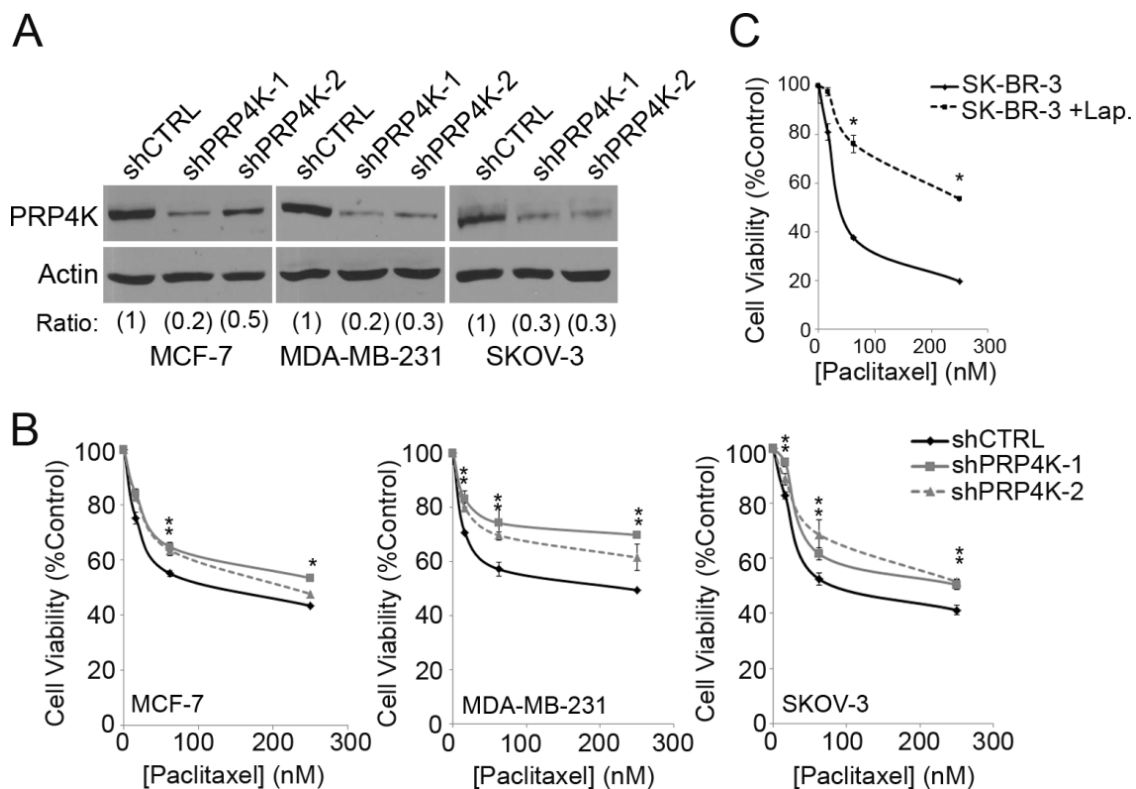


Figure 2.5 Decreased PRP4K expression is associated with an increased cellular resistance to paclitaxel. (A) Cell lines stably expressing a tetracycline-inducible shRNA targeting PRP4K were established using a lentiviral-based system. Hairpin expression was induced for 96 h with 2 μ g/mL doxycycline and PRP4K levels analyzed by western blot analysis. Band intensity was quantified by densitometry, normalized to the actin loading control, and represented as ratios with shCTRL normalized to 1. (B) PRP4K knock down was induced with doxycycline for 96 h followed by paclitaxel treatment at the indicated concentrations for 90 min. Cell viability was measured via an alamarBlue assay after a 72 h recovery in drug-free medium. Data is presented as the mean of triplicates \pm SEM, * p <0.05. (C) SK-BR-3 cells were treated with 0.1 μ M lapatinib for 48 h to decrease PRP4K expression. The cells were then exposed to paclitaxel at the indicated concentration for 90 min. Cell viability was measured via an alamarBlue assay after a 72 h recovery in drug-free media. Data is presented as the mean of triplicates \pm SEM, * p <0.05.

To try to determine the mechanism by which PRP4K regulates taxane sensitivity, PRP4K-knockdown cells stably expressing a GFP-tagged histone H2B were treated with paclitaxel for 90 min and then monitored via live-cell microscopy. Under normal conditions, cells treated with taxane arrest in mitosis via activation of the SAC (59). After prolonged activation (approximately 6 h), the cell typically undergoes apoptosis, or mitotic cell death as shown by the apoptotic nuclear condensation in HeLa GFP-H2B shCTRL cells treated with paclitaxel (**Figure 2.6**). Following the knockdown of PRP4K, taxane-treated cells arrested in mitosis, but instead of undergoing apoptosis, underwent mitotic slippage, and re-entered the cell cycle as indicated by the decondensation of chromatin (**Figure 2.6**). This is consistent with the previously published role of PRP4K in mitotic checkpoint control, where it was shown to recruit MPS1 kinase, MAD1 and MAD2 to the kinetochore in order to establish a functional SAC (37). Thus, the decreased sensitivity of PRP4K knock-down cells to paclitaxel may arise from impaired SAC activity and enhanced mitotic slippage.

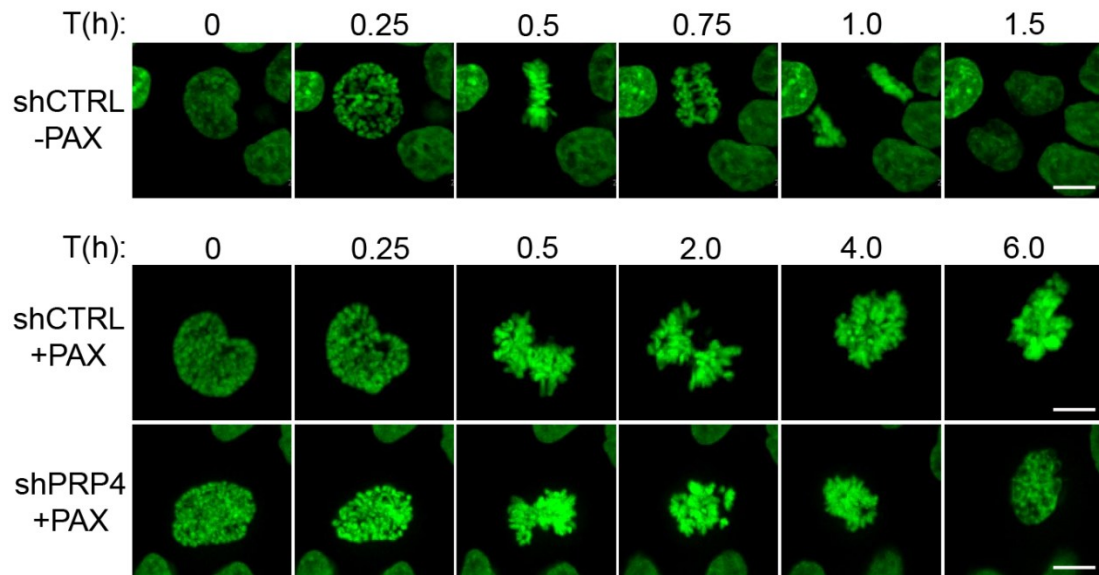


Figure 2.6 Knockdown of PRP4K promotes mitotic slippage over mitotic cell death in paclitaxel treated cells. HeLa GFP-H2B cells were stably transduced with a control hairpin (shCTRL) or a hairpin targeting PRP4K (shPRP4) under control of a doxycycline inducible promoter. Doxycycline (2 μ g/ml) was added to the culture medium to induce hairpin expression for 96 h. Cells were then treated with 20nM paclitaxel, or vehicle control for 90 min. After the treatment, the drug was washed off and cells were imaged using confocal live cell microscopy to monitor cellular response. Scale bars = 10 μ m.

2.3.4 Reduced PRP4K Expression is Associated with Both *In Vitro*-Derived and Patient-Acquired Resistance to Taxanes

Breast and ovarian cancers can acquire resistance to taxanes, resulting in treatment failure in relapsed patients who have previously received taxane-containing chemotherapy regimens. To explore the role of PRP4K in acquired cellular resistance to paclitaxel, MCF-7 cells were maintained in several independent pools of cells cultured in increasing concentrations of paclitaxel for 15 weeks, which resulted in separate populations of cells with increased resistance to chronic exposure to 10 nM paclitaxel (**Figure 2.7A**). Six independent clones were isolated from these resistant pools and analyzed via western blotting for PRP4K protein level. As shown in **Figure 2.7A**, all of the paclitaxel-resistant clones (PAXR1-PAXR6) express reduced levels of PRP4K, as compared to the starting, non-resistant population. In addition, we analyzed PRP4K levels in matched cell lines isolated from a patient diagnosed with high-grade serous ovarian cancer who had received paclitaxel as part of their treatment regimen, and subsequently relapsed and no longer responded to taxane-based therapy (135). The cell line which was isolated prior to paclitaxel treatment (TOV1369) expressed a higher level of PRP4K (**Figure 2.7B**), as compared to the cell line that was isolated post-relapse (OV1369(R2)). Taken together, these results indicate that reduced PRP4K levels are associated with the acquisition of resistance to paclitaxel both *in vitro* and *in vivo*.

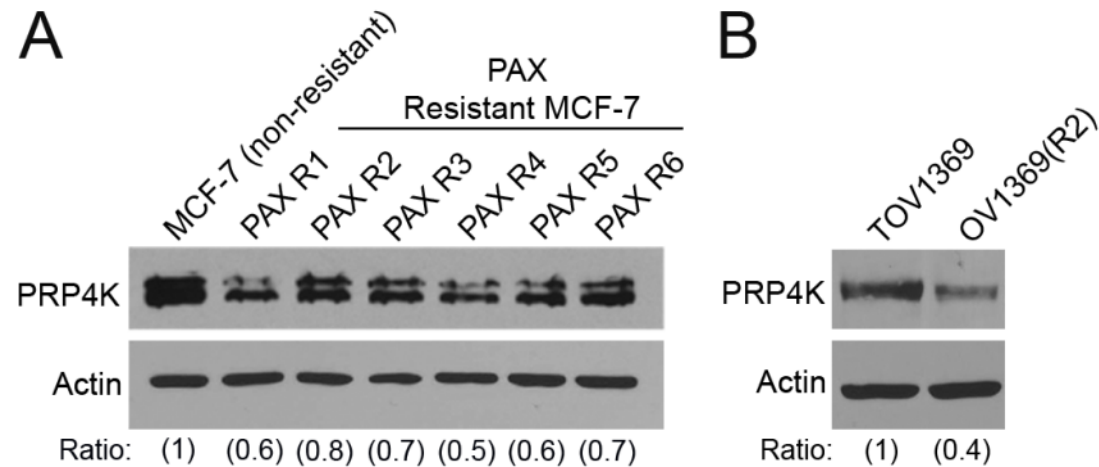


Figure 2.7 PRP4K expression is decreased in cells that have an acquired resistance to taxanes. (A) MCF-7 human breast cancer cells were exposed to a sub-lethal concentration of paclitaxel for 3 weeks. The concentration of paclitaxel in the growth medium was tripled every 3 weeks for 15 weeks to create a resistant population. Individual clones were isolated from the resistant population, and analyzed via western blotting for PRP4K protein level. (B) TOV1369 and OV1369(R2) cell lines were isolated from an ovarian cancer patient pre-taxane treatment, and post-relapse, respectively. Whole cell lysates were prepared from each cell line and PRP4K protein levels were determined via western blotting. Band intensity was quantified by densitometry, normalized to the actin loading control, and represented as ratios.

2.3.5 PRP4K Expression Correlates with Better Overall Survival in Ovarian Cancer Patients Treated with Taxanes with Low HER2-Expressing Tumours

Given that decreased PRP4K expression is associated with reduced sensitivity to paclitaxel *in vitro*, that PRP4K is regulated by HER2 (a controversial predictive biomarker of taxane response), and that acquired taxane resistance is associated with reduced PRP4K levels, we next wanted to determine if PRP4K could serve as a more direct biomarker for taxane response amongst high-grade serous epithelial ovarian cancer patients receiving taxanes as first-line therapy. The taxane-treated cohort of patients from the ovarian tumour TMA from **Figure 2.3** were divided into two categories according to PRP4K status; PRP4K OFF (TMA score of 0) or PRP4K ON (TMA score of 0.5 to 3). The PRP4K ON subclass of patients appear to have a better progression-free and overall survival (**Figure 2.8A**), although this was not statistically significant. In breast and ovarian cancer, *HER2/ERBB2* gene amplification is generally associated with poor survival. While HER2 protein expression by immunohistochemistry has less prognostic power than direct detection of *HER2* gene amplification (145), previous studies have demonstrated that typically only the highest scoring tumours for HER2 expression by immunohistology are found to harbour *HER2* gene amplification (146). Therefore, we rationalized that perhaps the patients with the highest expression of HER2 in our TMA analysis (i.e. score of 2 or 3 out of 3) were likely to progress early irrespective of PRP4K status because of greater *HER2* gene amplification. Indeed, when we compared HER2-high (2-3) versus HER2-low (0-1) patients within our cohort of high-grade serous epithelial ovarian cancer patients, the HER2-high patients display a significantly worse overall survival, as compared to the HER2 low cohort (**Figure 2.8B**). Therefore, we

repeated our analysis removing patients with the high HER2 staining from the cohort. Under these criteria, a significant increase in both time to progression (HR = 0.53 [95% CI 0.27-1.01]; p = 0.05) and overall survival (HR = 0.37 [95% CI 0.15-0.88]; p = 0.03) was observed amongst PRP4K-ON patients, as compared to PRP4K-OFF (**Figure 2.8C**). Thus, in the context of low HER2 expression, PRP4K is a positive prognostic biomarker for high-grade serous ovarian cancer patients treated with platinum/taxane-based therapies. The same analysis could not be done for the breast cancer TMA as those patients did not receive taxanes as part of their treatment regimen.

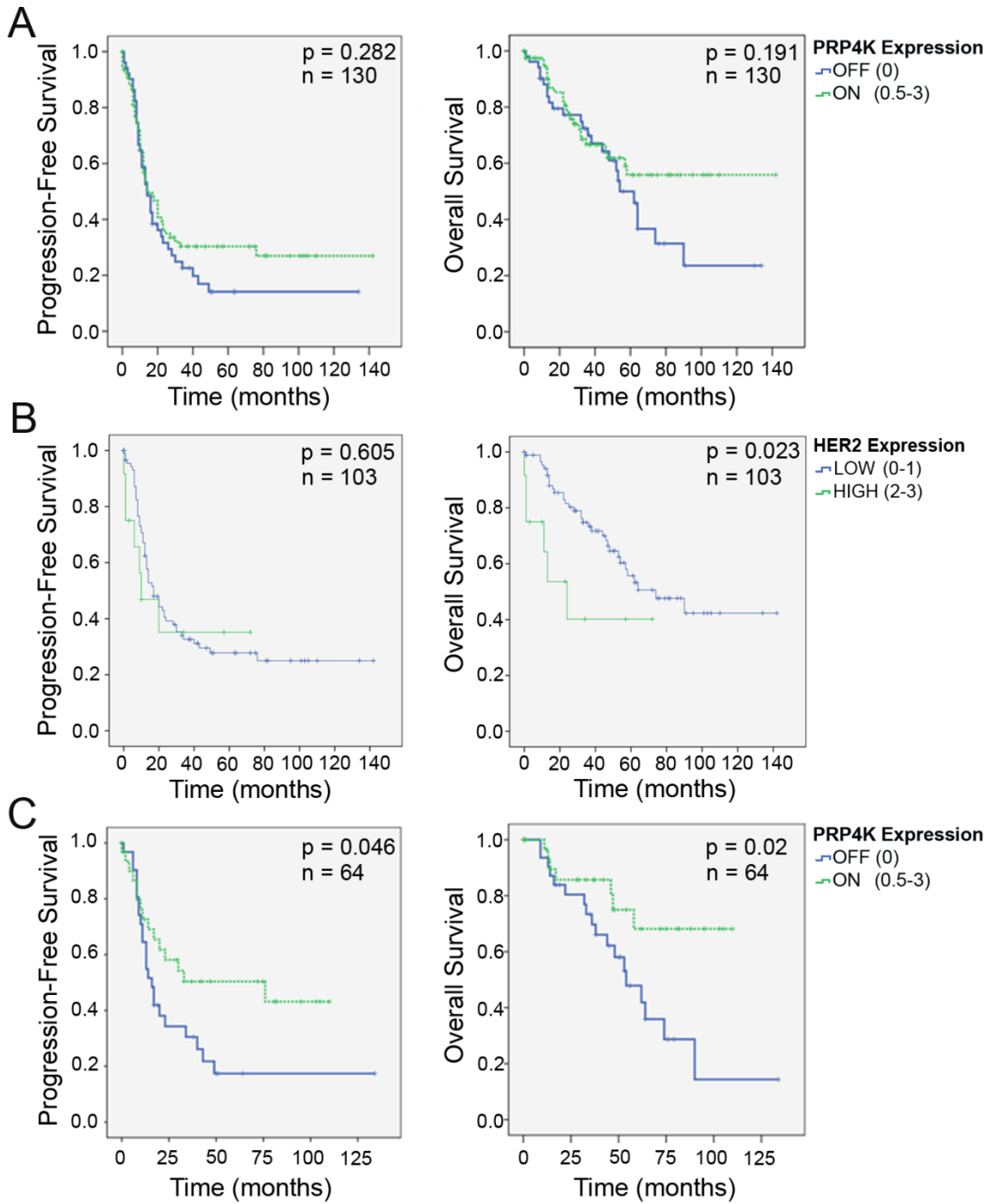


Figure 2.8 Evaluation of PRP4K as a biomarker of platinum/taxane response in high-grade serous ovarian cancer. (A) Kaplan Meier curves of progression-free survival (left) and overall survival (right) in a cohort of 130 ovarian cancer patients treated with platinum/taxane chemotherapy. (B) Kaplan Meier curves of progression-free survival (left) and overall survival (right) in 103 platinum/taxane-treated ovarian cancer patients with either low (0-1), or high (2-3), expression of HER2. Significance (p) is indicated by Log Rank. (C) Kaplan Meier curves of disease free survival (left) and overall survival (right) in 64 patients (i.e. a subset of the 130 in A) with no to moderate (0-1) expression of HER2. Significance (p) is indicated by Log Rank. *Data presented in this figure was collected by the Mes-Masson lab.*

2.4 Discussion

Despite the challenges associated with the development of resistance, taxanes remain one of the most widely used therapies for a range of human malignancies, including breast, lung and ovarian cancer. Biomarkers which can accurately predict taxane response are needed to identify those patients that will benefit from the inclusion of taxanes in their treatment regimen, and those who will not. Numerous biomarkers have been identified that correlate with *in vitro* taxane resistance, however their use clinically to stratify patients according to predicted taxane response has been limited.

In this study we have identified PRP4K as a novel HER2-regulated gene, and investigated its role in the cellular response to taxanes. Immunostaining for PRP4K in human breast and ovarian cancer TMAs revealed a significant correlation between PRP4K and HER2 (**Figure 2.3**), which we confirmed was a result of PRP4K expression being regulated by HER2 signaling (**Figure 2.4**). While the role of HER2 in the cellular response to taxanes *in vitro* remains controversial, the clinical data seems to support a link between HER2 expression and positive response to taxanes in breast cancer (127-132). However, due to the discrepancies between *in vitro* and *in vivo* data, the mechanism(s) linking HER2 signaling to taxane sensitivity remain unknown. To determine if PRP4K was contributing to the observed HER2-mediated taxane sensitivity, we generated breast and ovarian cancer cell lines stably expressing a doxycycline inducible hairpin targeting PRP4K. Across all three cell lines generated, knockdown of PRP4K led to a decrease in cellular sensitivity to paclitaxel. Furthermore, when PRP4K expression was decreased through inhibition of HER2 signaling, cellular sensitivity to paclitaxel also decreased. Together, these data support the hypothesis that HER2

signalling may contribute to taxane response in part by modulating PRP4K gene expression.

In breast cancer, HER2-based therapies target this receptor tyrosine kinase either by antibody (i.e. trastuzumab) or small molecule (i.e. lapatinib) inhibition, and the combination of HER2 pathway inhibition with taxane-based chemotherapy has shown improved outcomes in patients with HER2-positive tumours (147,148). In our experiments, it is important to note that chemical inhibition of HER2 was used as a tool to manipulate PRP4K expression, and reduced taxane effectiveness when given sequentially. This is in contrast to how these drugs are administered in recent clinical trials showing efficacy of combined trastuzumab or lapatinib treatment with taxanes; where treatment consists of trastuzumab or lapatinib being given concurrently with taxane treatments (149,150). It should also be noted that patient outcome is statistically better and patients exhibit fewer side-effects when treated periodically with trastuzumab (given concurrently with taxane) rather than with chronic dosing of lapatinib, which is taken daily with periodic taxane treatment (149). Given our results, it is tempting to speculate that when lapatinib is given daily the chronic exposure to drug may reduce PRP4K expression and as a consequence reduce taxane sensitivity over time; which, could provide a potential explanation for the increased efficacy of trastuzumab periodic treatment over chronic lapatinib treatment regimes.

How PRP4K contributes to taxane sensitivity may be multifactorial considering its critical role in pre-mRNA splicing (11,13), and as a consequence we are actively pursuing how changes in PRP4K expression affect alternative pre-mRNA splicing. However, to date there has been little evidence for splicing factors playing a role in

taxane resistance; whereas paclitaxel-induced apoptosis has been clearly demonstrated to be dependent on the prolonged activation of the SAC (104,151), and disruption of checkpoint function has been shown to increase resistance to taxanes *in vitro* (55,101). With PRP4K playing an important role in SAC function in response to microtubule poisons like nocodazole (37), it is most likely that loss of PRP4K leads to taxane resistance through mitotic checkpoint failure.

Given our *in vitro* data indicating that low PRP4K expression, induced either by inhibition of HER2 signalling or by knock-down of PRP4K, reduces the sensitivity of breast and ovarian cancers to taxanes, we also evaluated PRP4K as a potential prognostic biomarker for outcome in ovarian cancer patients treated with taxane-containing therapies. Although we had PRP4K immunohistochemistry data on both breast and ovarian tumours, none of the patients in the breast cohort were treated first-line with taxane-based chemotherapy. Thus, we focused on 130 tumours in the ovarian cohort from patients that received taxanes as part of their treatment regime and found that again PRP4K (i.e. PRP4K ON) correlated with positive prognosis markers such as BTF4/BTN3A2 (142) ($r = 0.24$, $p = 0.005$, Spearman correlation) and that although not significant, a trend of better survival and increased time to progression was seen in patients with tumours expressing PRP4K (**Figure 2.8A**). In interpreting these results, we noted that although breast cancer patients with tumours harboring a HER2 amplification have better overall survival when their treatment regimen includes taxanes (131), overall, HER2 amplification is associated with poor prognosis in breast (152) and ovarian cancer (145,153). Given the strong correlation between HER2 expression and PRP4K within this cohort, we would expect to preferentially select for HER2-amplified tumours within the

PRP4K ON group. We would thus select for patients with an overall poorer prognosis (**Fig. 2.8B**), irrespective of treatment, as compared to the majority of patients that do not have amplified HER2. Using this rationale, we decided to remove the highest HER2-expressing tumours from the cohort and to evaluate the prognostic power of PRP4K in patients with tumours exhibiting low HER2 levels. In this cohort, PRP4K ON tumours exhibited significant increases in both time to progression (HR = 0.53 [95% CI 0.27-1.01]; p = 0.05) and overall survival (HR = 0.37 [95% CI 0.15-0.88]; p = 0.03), as compared to patients with tumours that exhibited no detectable PRP4K expression by immunohistochemistry (PRP4K OFF).

In summary, this chapter identifies PRP4K as a HER2-regulated modifier of taxane sensitivity, and as a potential prognostic marker for better survival in ovarian cancer patients treated with taxanes that harbour low HER2-expressing tumours. Our data also indicates that reduced PRP4K expression correlates with acquired taxane resistance post-treatment (**Figure 2.7**). Thus, in addition to being a positive prognostic marker for survival in ovarian cancer patients with low or HER2-negative tumours at diagnosis, PRP4K expression could be of value in determining which patients might receive additional benefit (or not) from continued taxane treatment following relapse from previous taxane-based therapy.

Chapter 3 Development of a Zebrafish Xenotransplant Model to Study *In Vivo* Drug Response

This chapter contains material (sections 3.2, 3.3.1, 3.4, Figures 3.1-3.6) originally published in:

“Corkery DP, Dellaire G, Berman JN. 2011. Leukemia Xenotransplantation in Zebrafish—Chemotherapy Response Assay *In Vivo*. British Journal of Haematology. 153:786-789”

3.1 Introduction

3.1.1 Zebrafish as a Model to Study Human Cancers

The zebrafish (*Danio rerio*), a small tropical freshwater fish native to the southeastern Himalayan region, emerged as a model to study vertebrate developmental biology in the 1960's (154,155). There are numerous advantages to using zebrafish as a model organism including the rapid external development and optical clarity during embryogenesis which allows for the visualization of developmental processes. Zebrafish produce large clutch sizes (200-300 embryos per mating pair per week) with short generation times which facilitates genetic analyses while a striking genetic conservation between zebrafish and mammals (approximately 70%) leads to conserved biochemical pathways (156). The potential for zebrafish to be used as a cancer model was first realized in 1982 when zebrafish exposed to carcinogens were shown to develop tumours (157), later shown to share many histological (158) and molecular (159) similarities to human tumours. Since then, numerous strategies have been developed which take

advantage of the strengths of the zebrafish model to study human cancers. These strategies include mutant zebrafish lines with a predisposition to various types of cancer, transgenic zebrafish which express human oncogenes, and the xenotransplantation of human cancer cells into zebrafish embryos.

3.1.1.1 Mutant Models of Cancer

The ability to perform large-scale genetic screens in zebrafish is facilitated by the large clutch size and speed at which embryos develop. Traditionally, random point mutations are induced in male spermatogonia by treating adult zebrafish with a chemical mutagen like ethylnitrosourea (ENU). The male fish (F_0) carrying mutations are crossed with wild type (WT) females to produce a clutch of embryos (F_1), in which the males are expected to be heterozygous for the mutant allele. These progeny males are again crossed to WT females to generate the F_2 family of fish, half of which are expected to be homozygous for the WT allele, and the other half heterozygous for the mutant allele. Crossing of the F_2 siblings will generate the F_3 family of fish in which one-fourth of the F_2 crosses are expected to produce an F_3 progeny which are 50% heterozygous and 25% homozygous for the mutant allele (160). The goal of the screen would be to identify F_3 families of fish which have increased rates of spontaneous neoplasia and work backwards to identify the causative mutation. While large-scale chemical mutagenesis screens have proven useful for identifying mutations within zebrafish which lead to both developmental defects (161,162) and heritable predispositions to cancer (163,164), the genetic mapping required to identify the causative mutation is laborious and time-consuming.

An alternative approach to chemical mutagenesis which allows for the rapid identification of the causative mutation is insertional mutagenesis. Injection of a retrovirus into blastula-stage embryos (1000-2000 cells) results in the integration of viral sequences randomly into the genome. Passing these mutations through the germline, as described above for the chemical mutagenesis, results in an F₃ population of fish which can be screened for increased rates of spontaneous neoplasia. In this case, the viral sequence which was inserted into the genome serves as a molecular tag which can be used to clone the disrupted loci and identify the causative gene (165). These two approaches have led to the establishment of several mutant zebrafish lines with increased predisposition for a defined set of cancer types (163,164,166,167). As an example, the *crash&burn* (*crb*) zebrafish mutant, identified from a large-scale chemical mutagen-based genetic screen, was shown to have a predisposition to vascular and testicular cancers. Genetic mapping of the mutant genome identified a loss-of-function mutation within *bmyb*, a transcriptional regulator of cyclin B (164). The mutant was then employed in a secondary screen in which 16,320 compounds were screened for their ability to suppress the *bmyb*-dependent mitotic defects in *crb* embryos. One compound, persynthamide, was identified for its ability to prevent mitotic defects (168) and may represent a novel compound for the treatment cancers with loss-of-function *bmyb* mutations. This example illustrates how large genetic screens in zebrafish can be used to identify novel cancer initiating genes. Furthermore, the mutant embryo in which the mutation was identified can subsequently be used to screen large libraries of compounds for drugs that target the defined mutation.

3.1.1.2 Transgenic Models of Cancer

A major stepping stone for zebrafish as a cancer model was the emergence of rapid transgenic technology. The first transgenic cancer model in zebrafish was created by Langenau *et al.* who demonstrated that expression of the mouse oncogene *Myc*, under control of the zebrafish *rag2* (recombination activation gene 2) promoter resulted in the rapid onset of T-cell acute lymphoblastic leukemia (T-ALL) in adult zebrafish (169). Wild-type zebrafish embryos were injected with the *Rag2-mMyc* transgene at the one-cell stage of development to create an F₀ population of fish which were mosaic for expression of the transgene. After approximately 44 days, F₀ zebrafish developed leukemia which arose from the thymus and quickly spread into skeletal muscle and abdominal organs (169). A limitation to this model was that transgenic fish were severely diseased by the time they reach sexual maturity (10-12 weeks), making the line difficult to breed and maintain. To address this issue *Myc* was conditionally expressed using both Cre/lox (170) and heat shock (171) promoter systems creating a system amenable to forward genetic and small molecule suppressor screens. The molecular pathways that were activated in response to *Myc* overexpression in these fish closely resembled those found in human T-ALL, proving the zebrafish to be a valid model to study human disease.

A number of transgenic zebrafish cancer models have subsequently been created though the overexpression of various oncogenes including a precursor-B acute lymphoblastic leukemia (pre-B ALL) model created by expressing the oncogenic TEL-AML1 fusion protein (172), a pancreatic neuroendocrine tumour model created by expressing *MYCN* under control of the *myoD* promoter (173), a melanoma model created by expressing activated human *BRAF*^{V600E} under control of the melanocyte-specific *mitfa*

promoter in a *p53* deficient background (174), and an embryonic rhabdomyosarcoma model created by expressing activated Kras^{G12D} under control of the *rag2* promoter (175). These oncogene-driven models are useful for investigating downstream biochemical pathways contributing to cancer progression *in vivo*. In addition, much like the mutant zebrafish lines with an increased predisposition to cancer, the transgenic models can also be used in high-throughput drug screens for the identification of novel compounds which target the expressed oncogene.

3.1.1.3 Xenotransplantation Models

Mouse xenograft models have been used for decades to study the *in vivo* behaviour of human cancer cell lines. More recently, zebrafish have begun to emerge as an alternative xenograft animal model due to their superior imaging quality, amenability to high-throughput drug screening and cost effectiveness, as compared to traditional rodent models.

Xenotransplantation of human cancer cells into zebrafish embryos was initiated in 2005 using a melanoma xenograft model (176). In this study, Lee *et al.* found that human melanoma cells transplanted into zebrafish embryos were highly invasive and migrated randomly throughout the embryonic tissue. In contrast, primary melanocytes integrated normally within the developing skin. The authors concluded that aggressive melanoma cells remain in a dedifferentiated state expressing both mesenchymal and epithelial markers, preventing proper integration into developing organs. In a follow-up study, the same group found that the transplanted melanoma cells secrete Nodal, a potent embryonic morphogen which alters normal embryonic development. Further studies

show that Nodal expression correlates with human melanoma progression and that inhibition of Nodal signaling impairs tumour formation in nude mice (177).

Subsequent studies by Haldi *et al.* determined an incubation temperature of 35°C enabled normal growth of injected human cell lines (usually cultured at 37°C) without compromising zebrafish embryogenesis (usually maintained at 27°C) and established the yolk sac and 48 hours post-fertilization (hpf) as the ideal anatomic location and developmental stage for injection (178). At this stage, adaptive immune responses are not yet established in the embryo, permitting injection of human cells without need for immunosuppression (178-180). Melanoma cells labeled with a fluorescent cell tracking dye were shown to proliferate within embryos as evaluated by manual enumeration of fluorescent cells within a dissociated embryo suspension using a hemocytometer (178). Importantly, it was also shown that zebrafish endothelial cells associate with tumour cell masses and form vessel-like structures, demonstrating for the first time that human tumour cells can communicate with the host microenvironment to induce an angiogenic response. This concept was explored further by Nicoli and Presta, who demonstrated that knockdown of zebrafish VE-cadherin using antisense morpholino oligonucleotides inhibited neovascularization of xenografted tumours (180). This result is consistent with mouse studies which have identified VE-cadherin as a component of the adherens junction shown to play an essential role in angiogenesis (181). These studies highlight how the ease of genetic manipulation in zebrafish can be exploited to study tumour-microenvironment interactions.

While these reports created a critical foundation and demonstrated the suitability of the zebrafish embryo as a host organism, they lack in their ability to reliably quantify

proliferation of the engrafted human cancer cells. A major advantage in using the zebrafish over traditional rodent models is the limited number of cells required for transplant. However, as a result of the small numbers of cells, tumour volume measurements are not possible as would commonly be done in rodent models. Therefore, there is a need for a sensitive cell proliferation assay that can be applied to the zebrafish xenograft model in order to quantify human cancer cell growth within the embryo, and allow for use of the model in studying cellular response to drugs.

3.1.2 Limitations to Using Zebrafish to Study Human Cancer

While the use of zebrafish as a cancer model offers many advantages over traditional tissue culture and rodent models, it is not without its limitations. Comparison of human and zebrafish genomes has identified an obvious zebrafish orthologue for approximately 70% of human genes (156). While this number is strikingly high for a lower vertebrate, several human cancer-associated genes are amongst the 30% which lack a zebrafish orthologue. For example, zebrafish lack orthologues for leukemia inhibitory factor (*LIF*), oncostatin M (*OSM*), interleukin 6 (*IL6*) and breast cancer 1, early onset (*BRC1*) (156), all of which play known roles in cancer development or progression (182-185). This will present a challenge when studying cancers or pathways in which these missing genes play a role. To complicate matters further, the zebrafish underwent a whole genome duplication event during evolution (186) resulting in often multiple paralogues for a given orthologous gene. This genetic redundancy has been shown to influence the role of oncogenes and tumour suppressors in carcinogenesis. For example, the second most mutated tumour suppressor in human cancers, *PTEN*, is expressed as two

paralogs, *ptena* and *ptenb*, within zebrafish (187). These paralogs have been shown to play redundant roles in embryonic development, but not in tumour formation as *ptena* is unable to compensate for the lack of *ptenb* within tumours developing in *ptenb*^{-/-} fish (187). A subtle difference in the functions of paralogs raises concerns over the translatability of research surrounding this prominent tumour suppressor.

Limitations associated with the zebrafish genome can be overcome through the xenotransplantation of human cancer cells into zebrafish embryos, although this model is not without limitations of its own. The lack of an adaptive immune system in zebrafish embryos allows for the engraftment of human cells without fear of host rejection but may also become a limitation to the translation of findings. Adaptive immune cells play essential roles in regulating both cancer progression and the response to treatment (188,189). As a result, there is much debate regarding the translatability of results obtained using immunocompromised xenograft models. The xenotransplant model is also limited by a lack of research to date investigating the zebrafish microenvironment, as it compares to the human tumour microenvironment. Beyond immune cells, the tumour microenvironment is composed of resident fibroblasts, endothelial cells and numerous molecules such as those of the extracellular matrix, proteases, chemokines, cytokines, growth factors, and various metabolites. Interactions between the tumour and various components of the microenvironment influence tumour progression and metastasis (190) supporting the use of *in vivo* model systems for the validation of *in vitro* results. The ability of engrafted cancer cells to induce an angiogenic response within zebrafish embryos (178,180) suggests that there is cross-talk between the cancer xenograft and the host, but the extent of this communication remains unknown. Finally, as described in

section 3.1.1.3, the xenotransplantation model has been limited by an inability to accurately quantify tumour growth. Rodent xenograft models rely predominantly on tumour volume measurements to determine the effect of drug treatments on tumour cell growth, while tissue culture models can directly assess changes in cell viability or cell number. The small size of zebrafish prohibits accurate tumour volume measurements and no methods to accurately quantify changes in cancer cell number within the embryo currently exist.

In this chapter I present a robust cell proliferation assay developed for use with the zebrafish xenotransplant (XT) model. I transplant K562 and NB-4 human leukemia cell lines characterized by distinct cytogenetic abnormalities into transparent *casper* embryos, a combinatorial zebrafish pigment mutant (191), and apply the developed proliferation assay to quantify cell growth within the embryo. I then conduct proof-of-principle studies in which transplanted embryos are treated with targeted therapeutics and the effect on proliferation quantified. Finally, I apply the model to our study of PRP4K and taxane sensitivity.

3.2 Materials and Methods

3.2.1 Zebrafish Maintenance

Adult *casper* zebrafish were maintained in the Aquatics Laboratory at the IWK Health Centre (Halifax, NS) as described by Westerfield (192). The use of zebrafish in these studies was approved by the Dalhousie University Animal Care Committee.

3.2.2 Tissue Culture and Cell Labelling

Human K562 (gift of Drs. Donald Small and Robert Arceci (Johns Hopkins School of Medicine)) and NB-4 (gift of Dr. David Waisman (Dalhousie University)) cells were cultured in Rosewell Park Memorial Institute (RPMI) 1640 medium containing 10% fetal bovine serum (FBS) with the addition of 1% penicillin/streptomycin. MDA-MB-231 shCTRL/shPRP4 cells (described in 2.2.6) were cultured in DMEM containing 10% Tetracycline-Free FBS (Invitrogen) with the addition of penicillin/streptomycin. For labelling, 5 million cells were pelleted by centrifugation for 5 minutes at 400 x g. The cell pellet was re-suspended in PBS containing the lipophilic cell tracking dye CM-DiI (Invitrogen, 5µg/mL final concentration) and incubated for 5 min at 37°C followed by an additional 20 min at 4°C. The suspension was centrifuged for 5 min at 400 x g and the pellet washed twice with PBS to remove excess dye. After the final wash the pellet was re-suspended in 500µl of media to produce a final cell concentration of 10⁶cells/mL.

3.2.3 Zebrafish Handling, Xenotransplantation and Drug Treatment

Prior to injecting cancer cells at 48 hpf, zebrafish embryos were dechorionated using a 10 mg/ml stock solution of pronase (Roche Applied Science). Embryos were anaesthetized with tricaine (Ethyl 3-aminobenzoate methanesulfonate salt, MS-222, Sigma-Aldrich) at a final concentration of 200 µg/ml, and placed in a Petri dish on their sides on a ramp comprised of 1% agarose. CM-DiI-labeled cells were loaded into a glass micropipette pulled by a P-97 Flaming/Brown micropipette puller (Sutter Instrument Co., Novato, CA). The needle was placed in a PLI-100 Pressure Injector (Harvard Apparatus,

Holliston, MA) and 25-50 cells were delivered, as a single injection, into the yolk sac of each embryo (Injection conditions: 40ms pulse time, 4.6 psi positive pressure) using a Leica MZ6 modular stereomicroscope (Leica, Germany). Visual inspection of a test injection onto a glass coverslip was used to estimate the presence of 25-50 cells prior to injection into the animal. Following injection, embryos were allowed to recover at 28°C for 1 hour and then transferred to 35°C where they remained for the rest of the experiment (178). At 24 h post injection (hpi), embryos were screened for the presence of a fluorescent cell mass at the site of injection, and only embryos with a mass of uniform size were used for proliferation studies. Embryos xenotransplanted with human cancer cells were then maintained in groups of 15-20 within individual Petri dishes prior to drug treatment. Imatinib mesylate (IM), all-trans retinoic acid (ATRA), paclitaxel (PAX), or vehicle control (0.05% DMSO) were added directly to the fish water, at indicated concentrations, for 48 h.

3.2.4 Embryo Dissociation

Populations of embryos were dissociated at 24 hpi and 72 hpi with or without drug treatment. For dissociations, 15-20 embryos were euthanized by tricaine overdose, placed in a 1.5 mL Eppendorf tube and incubated in protease solution (0.25% trypsin, 1mM EDTA, 2.25 mg/mL Collagenase (Sigma) in 1.2mL sterile PBS) for approximately 45 min at 35°C. During the dissociation, the suspension was homogenized every 10 min by passage through a Pasteur pipette and monitored visually for complete dissociation. Once the dissociation was complete, the reaction was stopped by the addition of 200µl of stop solution (30% FBS, 6 mM CaCl₂ in sterile PBS). Cells were then pelleted by

centrifugation for 5 min at 2000rpm at 4°C. The cell pellet was then washed with 1 mL of chilled 0.9x PBS with 5% FBS, and pelleted again prior to resuspension in 0.9x PBS with 5% FBS at a volume of 10µl per embryo.

3.2.5 *Imaging of the Dissociated Material*

To enable the *ex vivo* quantification of xenografted leukemia/breast cancer cells, engrafted embryos dissociated as above at a concentration of 1 embryo/10µl were pipetted as a 10µl bolus on a glass slide as a hanging droplet and imaged by fluorescence microscopy using an inverted Axio Observer Z1 microscope equipped with a Colibri LED light source (Carl Zeiss, Westlar, Germany). Each droplet was imaged as a 5x4 mosaic under a 5x objective using an AxioCam Rev 3.0 CCD camera and Axiovision Rel 4.0 software (Carl Zeiss Microimaging Inc.). The use of a 5x4 image grid creates an internal 3x2 array of 6 fields of view that are uniform in cell distribution and are approximately one tenth of the total droplet area, which equates to 1µl of the 10µl bolus (**Figure 3.1**). To ensure droplets were of a uniform size, only droplets in which the internal 3x2 grid fit within the entire droplet were used for calculating cell numbers. For analysis, at least 4 of the 6 internal fields of view were selected that were free of cellular debris that could affect the accuracy of the cell counts.

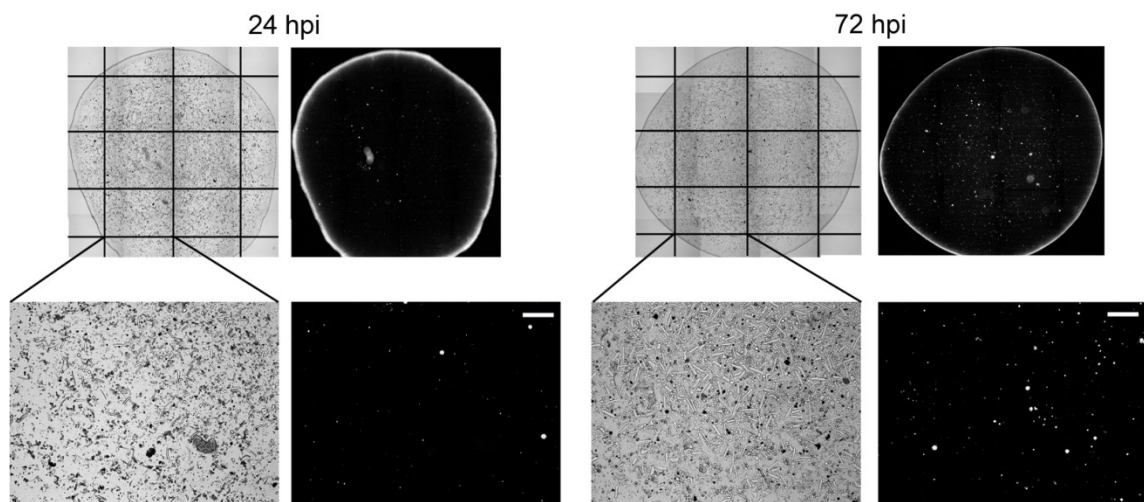


Figure 3.1 Image analysis of dissociated embryos. Representative brightfield and fluorescent images of a hanging bolus from dissociated K562 xenotransplanted embryos at 24 and 72 hpi. Individual 10 μ l boluses mounted on a glass slide were imaged as a 5x4 mosaic under a 5x objective. Higher magnification fields are shown below. Scale bar = 200 μ m.

3.2.6 *Ex Vivo Proliferation Assay*

Cells fluorescently labelled with CmDiI were counted within the micrographs of each of the 4 fields of view using a semi-automated cell quantification macro executed in ImageJ (NIH, Bethesda, MD) (**Appendix B**). This macro converts the images to a single stack and adjusts the fluorescence intensity threshold before counting fluorescent cells in each image using the “Particle Picker” tool set to count particles of a minimum size empirically determined for each cell line. Briefly, the distribution of cell size was determined from micrographs taken of CmDiI-labelled leukemia cells in suspension prior to xenotransplantation, and the minimum size for particle selection was set as the mean cell area minus one standard deviation. In addition, dissociated cells were stained with 10nM DRAQ5 viable nuclear stain (Biostatus Ltd.) for 5 min prior to imaging to confirm that all cells counted contained a nucleus by scoring only cells that are fluorescent when illuminated at both 560 nM (i.e. CmDiI) and 630 nM (i.e. DRAQ5). These measures ensured that whole cells, and not cell particles, were counted. The average number of cells per field of view was then determined from 4 micrographs from a minimum of 5 individual boluses from each sample (i.e. n=20 images encompassing ~50 μ l of the total 100 μ l suspension). Each experiment was then repeated in triplicate. Since each 10 μ l bolus represents 1 embryo, and each field of view is equivalent to 1 μ l of the embryo cell suspension using the 5x objective, I determined the average cell count per embryo by multiplying the cell count per field of view by 10 (e.g. 4 counts per field of view = 40 cells per embryo). In this way, proliferation of leukemia/breast cancer cells can be represented in absolute terms as the number of cells/embryo, or in relative terms as a fold

increase in cell number based solely on the cell count per field of view, at 24 and 72hpi with or without drug treatment.

3.2.7 MDA-MB-231 PRP4K Knockdown

For experiments involving the knockdown of PRP4K, MDA-MB-231 shPRP4/shCTRL cells (described in 2.2.6) were treated with 2 µg/ml doxycycline for 48 hours prior to transplant. Following transplant, 10µg/ml doxycycline was added to the fish water of engrafted embryos to ensure hairpin expression throughout the duration of the experiment.

3.3 Results

3.3.1 Human Leukemia Proof-of-Principle Studies

To validate the use of the zebrafish XT method as a tool to study *in vivo* drug response, I conducted proof-of-principle studies using the K562 and NB-4 human leukemia cell lines which are characterized by cytogenetic abnormalities known to be effectively targeted by small molecule inhibitors. K562 cells harbor the *BCR-ABL* fusion gene that results from the t(9;22)(q34;q11) translocation generating the Philadelphia chromosome found in 90% of patients with chronic myeloid leukemia (CML) (193). Imatinib mesylate specifically targets the Abelson (ABL) receptor tyrosine kinase that is constitutively activated by the breakpoint cluster region (*BCR*)-*ABL* fusion gene, and has revolutionized the management of chronic-phase CML (194). By contrast, all-trans retinoic acid selectively targets the retinoic acid receptor alpha-promyleocytic leukemia (*PML-RARA*) fusion gene product arising from the t(15;17)(q22;q12) translocation found

in the majority of patients with acute promyelocytic leukemia (APL) and present in the NB-4 leukemia cell line (reviewed in (195)). ATRA therapy promotes leukemic cell differentiation by alleviating the aberrant transcriptional repression induced by the PML-RAR α fusion protein, and its efficacy has converted a previously devastating disease into the most treatable subtype of AML (196,197).

To study the ability of K562 or NB-4 human leukemia cells to engraft within zebrafish embryos, I injected 25-50 fluorescently-labeled cells into the yolk sac of 48 hour-old *casper* zebrafish embryos. Injected embryos were screened for the presence of a fluorescent mass at the site of injection and the behaviour of leukemia cells was monitored by live-cell microscopy. Cell proliferation was quantified by counting the number of fluorescent cells present in cell suspensions generated from the enzymatic dissociation embryos at 24 and 72 hpi, as outlined in **Figure 3.2**. Injected embryos tolerated the presence of human leukemia cells for up to 7 days, during which time the engrafted leukemia cells proliferated and circulated within the embryonic vasculature (**Figure 3.3A**). Fifteen to twenty embryos were dissociated at each time point and the cell suspension was mounted on a glass slide as a hanging drop for imaging (**Figure 3.1**). The number of leukemia cells was determined from fluorescent micrographs of the dissociated cells using a semi-automated cell quantification macro executed in ImageJ (NIH, Bethesda, MD) (**Appendix B**). Using this proliferation assay, I observed a reproducible increase in K562 cell number from 90 to 230 cells per embryo (i.e. 2.6-fold) and NB-4 cell number from 50 to 170 cells per embryo (i.e. 3.4-fold) over the 48 hour time period (**Figure 3.3B**). I confirmed that I was enumerating only intact leukemia cells after dissociation by staining with the cell permeable viable DNA-binding dye, DRAQ5,

which stained the nuclei of all CmDil labelled cells counted in our experiments (**Figure 3.4**). This proliferation assay is both robust and reproducible, allowing for the rapid *in silico* quantification of cell proliferation, without observer bias, and represents a substantial improvement over prior crude approaches associated with large confidence intervals (178).

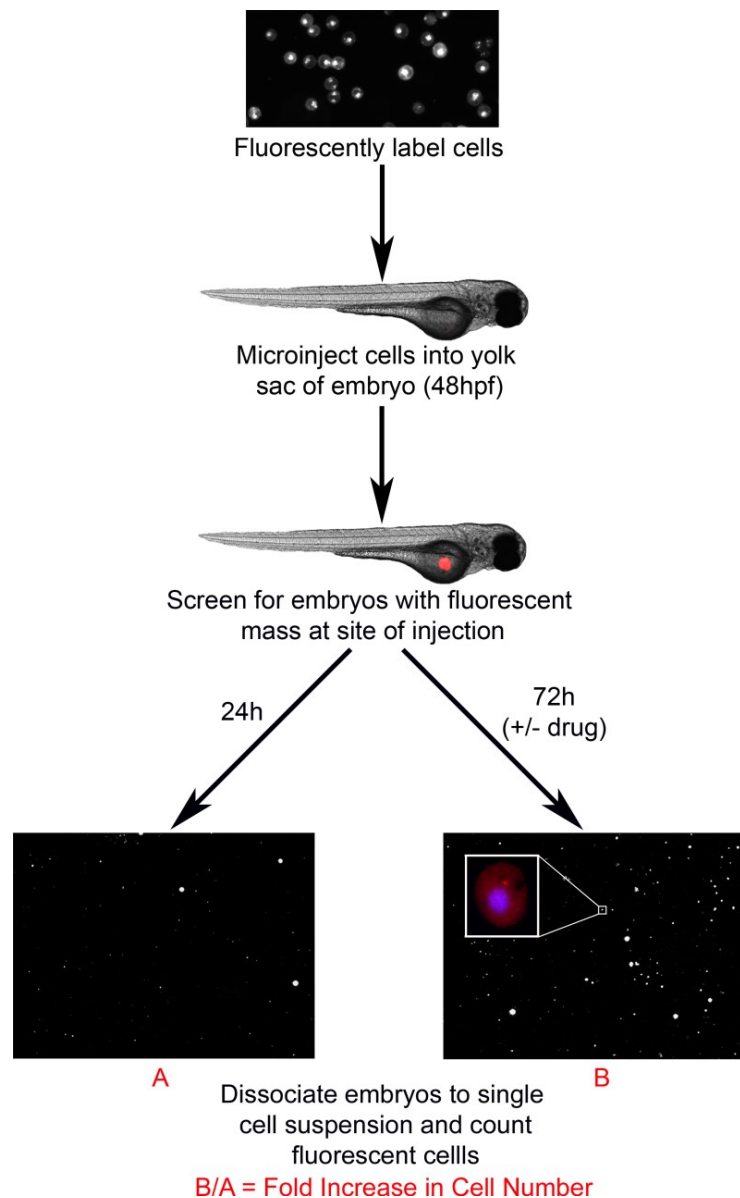


Figure 3.2 Schematic of in vivo cell proliferation assay. Human cancer cells are fluorescently labeled with a cell tracking dye. Approximately 25-50 fluorescently labeled cells are microinjected into the yolk sac of 48 hpf *casper* embryos. Embryos are screened using fluorescent microscopy for the presence of a fluorescent mass at the site of injection. Positive embryos are divided into two groups; one of which is maintained at 35°C for 24 h, and the other group is maintained at 35°C for 72 h with or without drug. At the end of each time point embryos are enzymatically dissociated to a single cell suspension and the number of fluorescent cells in the suspension are counted. The number of fluorescent cells present at 72 h divided by the number of fluorescent cells present at 24 h represents the fold increase in cell number. Insert in image B shows a single cell stained with CM-DiI (red) and DRAQ5 (blue).

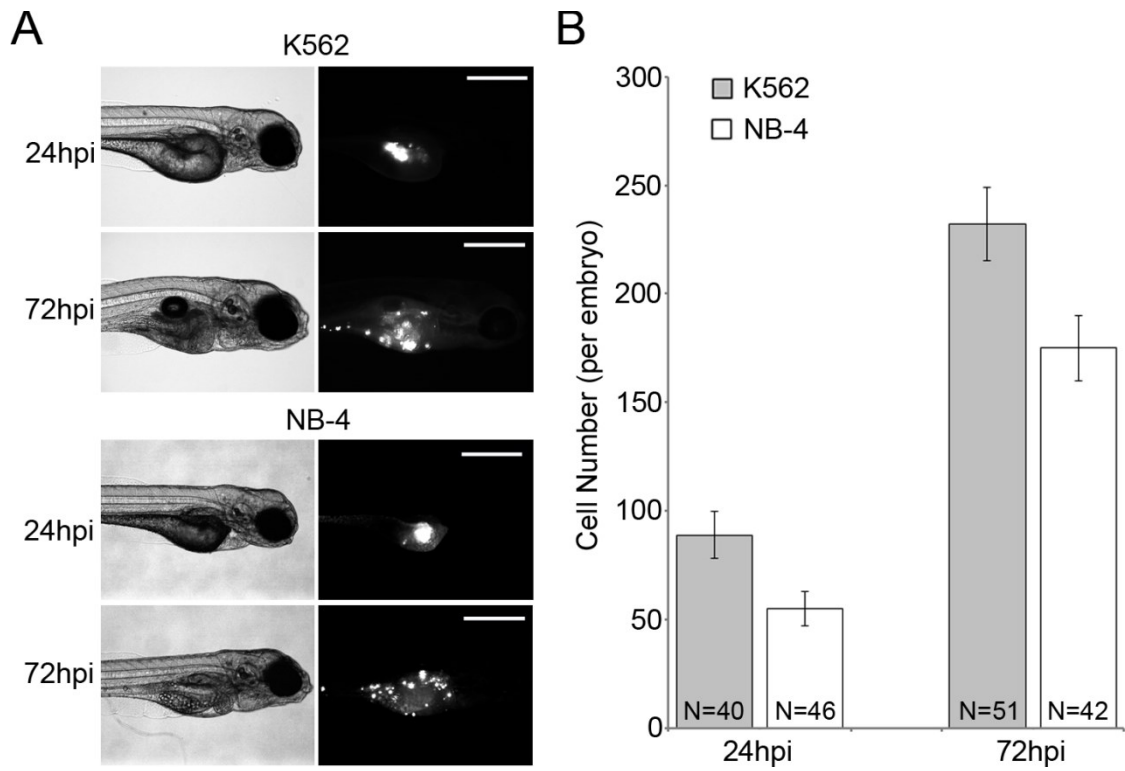


Figure 3.3 Human K562 and NB-4 cells proliferate within zebrafish embryos. (A) Representative brightfield and fluorescent images are shown of zebrafish embryos transplanted with either human K562 or NB-4 cells at 24 and 72 hpi. Scale bars, 500µm. (B) Embryos at 24 and 72 hpi were dissociated and the number of fluorescent cells counted. The average number of cells per embryo was determined at each time point in both NB-4 and K562 transplanted animals and is depicted as a bar graph. N = the total number of embryos analyzed in 3 independent experiments. Error bars = SEM.

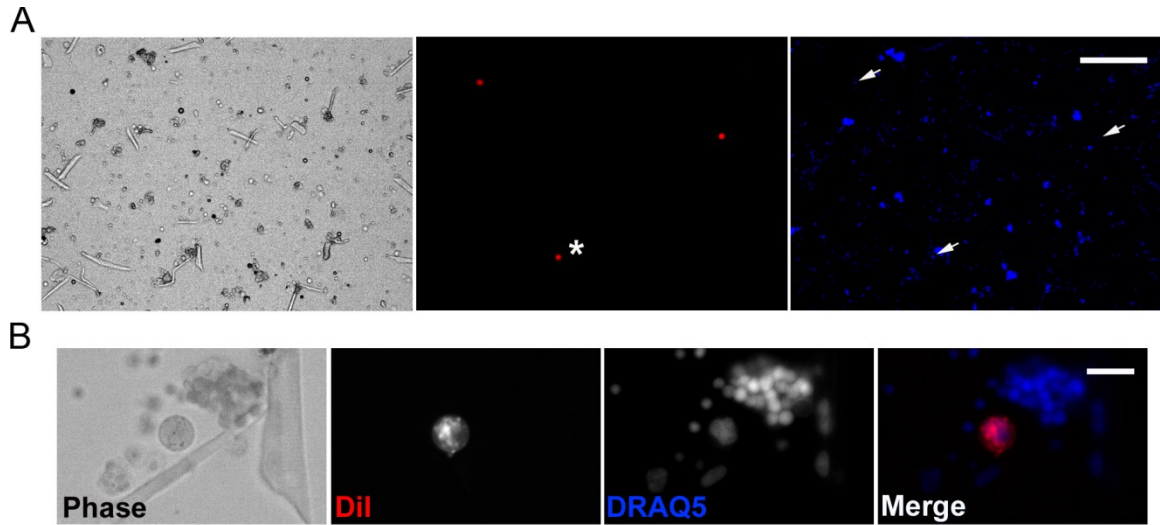


Figure 3.4 Fluorescent microscopy analysis of dissociated embryos. NB-4 xenotransplanted embryos were dissociated at 48 hpi and the resulting cell suspension analyzed by fluorescent microscopy. **(A)** Representative images taken under a 5x objective are shown. The three cells in the field of view that stain positive for CmDiI colocalize with individual nuclei (white arrows) stained with DRAQ-5. Scale Bar, 200 μ m **(B)** A higher magnification field of view taken with a 40X objective is shown below. This image clearly indicates that the NB-4 cells being enumerated contain intact nuclei (*). Scale bar = 20 μ m.

To determine whether this xenotransplantation assay could be used to evaluate specific tumor-drug interactions *in vivo*, I exploited the known responses to targeted therapies of the molecular alterations in each leukemia cell line. Specifically, I used IM to target the BCR-ABL fusion protein in K562 cells and ATRA to target the PML-RAR α fusion protein in NB-4 cells. To establish a dose of each drug which could be used to treat embryos without inhibiting survival, toxicity curves were generated by exposing 48 hour old zebrafish embryos (2 embryos per well in a 96-well plate) to increasing concentrations of IM (0-400 μ M) or ATRA (0-0.8 μ M) and scoring embryo viability after 48 hours of exposure. As our starting dose, I selected 50% of the maximum tolerated dose (MTD) to ensure embryo survival would not be impacted. This dose equated to 20 μ M of IM and 0.2 μ M of ATRA (**Figure 3.5**). To evaluate drug response, K562 and NB-4 engrafted embryos were divided into groups of 15-20 and treated either with vehicle control or the respective targeted therapy for 48 hours. Following 48 hours of exposure to 20 μ M IM, K562 xenotransplanted embryos displayed a significant decrease in the number of engrafted leukemia cells compared to vehicle-treated control embryos, as quantified using the *in silico* proliferation assay outlined above ($p < 0.001$). Similarly, NB-4 xenotransplanted embryos exposed to 0.2 μ M ATRA demonstrated a significant reduction in the number of engrafted leukemia cells as compared to vehicle-treated embryos ($p < 0.001$) (**Figure 3.6**). To confirm that these results were due to specific tumor-drug interaction, the reciprocal experiments were performed whereby K562 xenotransplanted embryos were treated with ATRA and NB-4 xenotransplanted embryos were treated with IM. In contrast to the targeted drug treatment, exposure of K562 cells to 0.2 μ M ATRA or NB-4 cells to 20 μ M IM failed to significantly affect leukemia cell

proliferation (**Figure 3.6**). These studies confirm that the reduction in cell proliferation rates observed is due to targeted tumour-drug interactions rather than non-specific cellular toxicity.

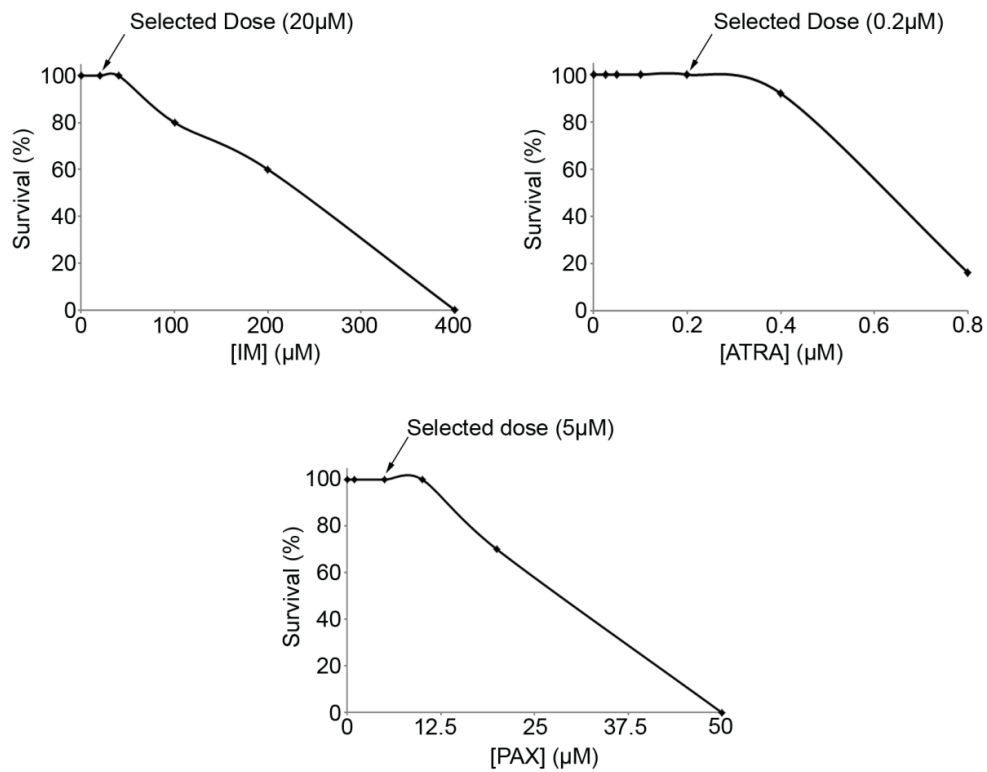


Figure 3.5 IM, ATRA and PAX toxicity curves. 48 hour zebrafish embryos were treated with increasing concentrations of IM (0-400 μ M), ATRA (0-0.8 μ M) and paclitaxel (PAX) (0-50 μ M) for 48 h. Following 48 h treatment, embryos were examined for viability and the percentage viability was plotted versus drug dose. N=12 embryos at each dose.

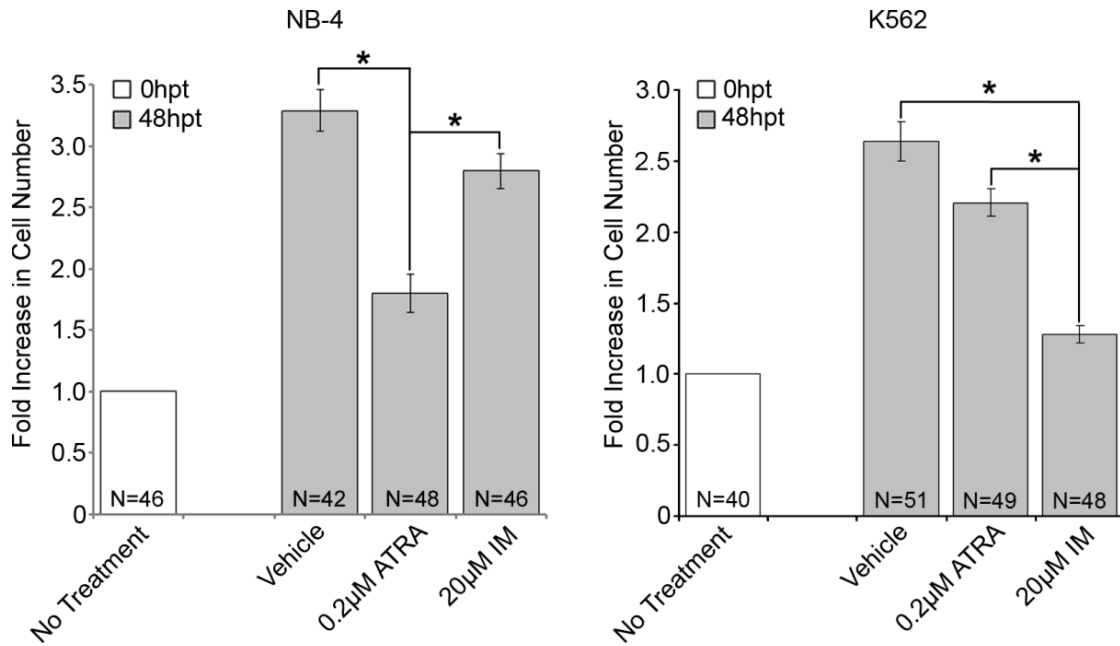


Figure 3.6 Human K562 and NB-4 cell proliferation in zebrafish embryos can be inhibited by treatment with targeted therapy. NB-4 and K562 xenotransplanted embryos were treated with ATRA (0.2µM), IM (20µM) or vehicle (0.05% DMSO) for 48 h. Embryos were dissociated, fluorescent cells counted and are represented as a bar graph. ATRA-treated NB-4 xenotransplanted embryos had significantly fewer NB-4 cells as compared to vehicle-treated and IM-treated embryos. IM treated K562 xenotransplanted embryos had significantly fewer K562 cells as compared to vehicle-treated and ATRA-treated embryos. * p<0.001.

3.3.2 Using the Zebrafish XT Model to Study Taxane Response in Breast Cancer

With proof-of-principal studies validating the use of the zebrafish XT model to study drug response in human leukemia cell lines, I next wished to determine if the model could be applied to study taxane response in breast cancer. MDA-MB-231 human breast cancer cells were labeled with CM-DiI and transplanted into 48 hour old zebrafish embryos. Using the proliferation assay outlined above, I observed a 1.5- and 2-fold increase in MDA-MB-231 cell number at 72 and 96 hpi, respectively (**Figure 3.7B**). Importantly, the addition of 5 μ M paclitaxel (**Figure 3.5**) to the fish water completely inhibited MDA-MB-231 cell proliferation in the embryo (**Figure 3.7C**). These results suggest that the zebrafish XT model can be effectively applied to the study of taxane response using human breast cancer cell lines.

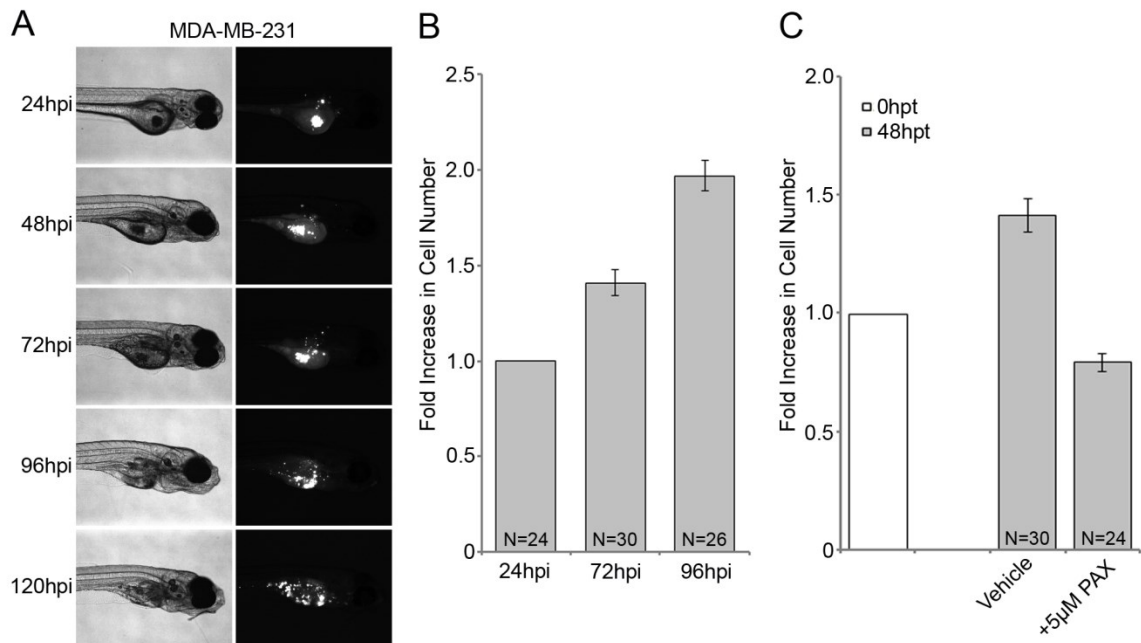


Figure 3.7 Human MDA-MB-231 cell proliferation in zebrafish embryos can be inhibited with paclitaxel. (A) Brightfield and fluorescent images of a zebrafish embryo transplanted with MDA-MB-231 cells imaged every 24 hours for 5 days. (B) MDA-MB-231 engrafted embryos at 24, 72 and 96 hpi were dissociated and the number of fluorescent cells counted. The fold change in cell number was determined and represented as a bar graph. Error bars = SEM. (C) MDA-MB-231 xenotransplanted embryos were treated with vehicle (0.05% DMSO) or 5µM PAX for 48 hours. Groups of embryos were dissociated, fluorescent cells counted and the fold change in cell number represented as a bar graph. N = the total number of embryos analyzed from 2 independent experiments. Error bars = SEM.

3.3.3 Knockdown of PRP4K Enhances MDA-MB-231 Cell Proliferation in Zebrafish

As discussed in Chapter 2, loss of PRP4K expression is associated with increased cellular resistance to taxanes. As a supplement to these studies, I wished to employ the zebrafish XT model to study how knockdown of PRP4K in human breast cancer cells would impact their response to taxanes within the *in vivo* environment of the zebrafish embryo. To accomplish this, I transplanted the MDA-MB-231 doxycycline-inducible shCTRL/shPRP4 cell lines I generated for studying *in vitro* taxane response in section 2.3.3 into zebrafish embryos. Hairpin expression was induced by culturing cells in the presence of 2 $\mu\text{g/ml}$ doxycycline for 48 hours prior to transplant (**Figure 3.8A**), and maintained through the addition of 10 $\mu\text{g/ml}$ doxycycline to the fish water post-transplant. Unexpectedly, the knockdown of PRP4K led to increased proliferation of MDA-MB-231 cells within the zebrafish embryos as compared to cells expressing a control hairpin (**Figure 3.8B**). While this observation raises the interesting question of why PRP4K loss increases proliferation rates *in vivo* and not *in vitro* (see Chapter 4), it prohibits the use of the zebrafish XT model to study taxane response as proliferation rate influences response to drugs which target mitosis.

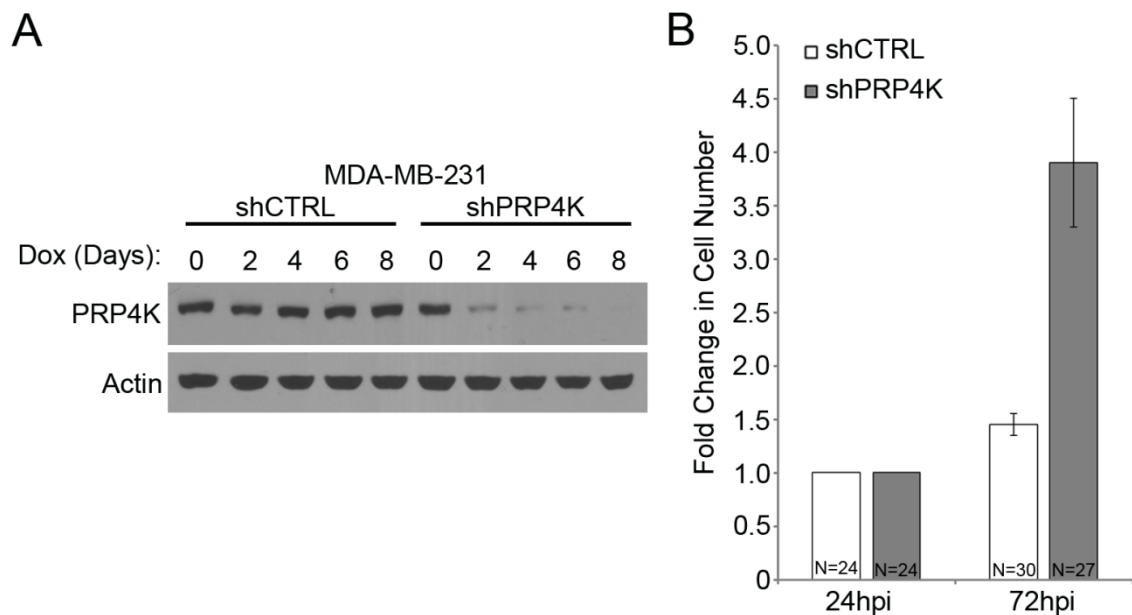


Figure 3.8 Knockdown of PRP4K increases MDA-MB-231 proliferation in zebrafish. (A) Western blot showing PRP4K protein levels in MDA-MB-231 shCTRL/shPRP4K cells treated with 2 μ g/ml doxycycline for up to 8 days. (B) MDA-MB-231 shCTRL and shPRP4K cells were transplanted into zebrafish embryos. Groups of embryos were dissociated at 24 and 72 hpi and the number of fluorescent cells counted to determine the fold change in cell number over the 48 hour period. N = total number of embryos analyzed from 2 independent experiments. Error bars = SEM.

3.4 Discussion

The zebrafish XT model described in this chapter allows for rapid *in silico* quantification of cell proliferation, representing a substantive improvement over previous xenotransplantation models which depend on manual enumeration (178) or the non-quantitative visual evaluation of relative cell number (198) to assess proliferation of engrafted cells. In comparison, our assay provides greater sensitivity and is capable of detecting more subtle and accurate changes in cell number in a shorter time frame. Moreover, since statistically an individual droplet represents a single embryo, this approach provides the opportunity to analyze small numbers of animals that would be technically challenging using flow cytometry. By incorporating this technique together with the unique imaging capabilities of the zebrafish, and its inherent capacity for high throughput chemical screening, we have positioned this model as an innovative system for identifying effective anti-proliferative agents. In fact, following its development, we employed the zebrafish XT system to successfully study a series of modified prodigiosene compounds for their ability to target human leukemia cells transplanted in zebrafish embryos (199).

The small number of cells and embryos required for engraftment and proliferation provides the opportunity for the study of drug-tumour interactions in primary patient samples, which may not be easily expanded in tissue culture or available in sufficient quantity for flow cytometry. We have recently demonstrated that T-ALL cells isolated from the bone marrow of pediatric T-ALL patients could be transplanted into zebrafish embryos, and proliferation quantified using the methods described above (200). In this study, the failure of one patient's engrafted cells to respond to the gamma-secretase

inhibitor compound E led to the discovery of a gain-of-function *NOTCH1* mutation, which was confirmed by Sanger sequencing of the *NOTCH1* gene. The short time-frame required to complete these experiments (less than 2 weeks from bone marrow isolation to drug response data) suggests that the zebrafish XT model could be applied in the clinical setting to help direct treatment decisions in an effort to personalize cancer therapy. Large-scale studies using primary patient samples which compare zebrafish XT drug response data to matched clinical outcomes will be essential in determining whether the zebrafish XT model could be used to inform clinical decision-making.

To date, the majority of zebrafish xenotransplant studies have been carried out using 48 hour old embryos due in large part to the lack of an adaptive immune system at this stage in development. However, recent work out of the Langenau lab describes the development of an immunocompromised homozygous *rag2*^{E450fs} mutant zebrafish (201) which will enable xenotransplant studies to be carried out in adult zebrafish as well. While xenotransplantation into adult zebrafish would not provide the same benefits as embryos (amenability to drug screening, small number of cells required for engraftment, and the ability to rapidly transplant large numbers of embryos), the adult microenvironment with which engrafted cells interact would be more complex and should better recapitulate the human tumour microenvironment. Furthermore, a larger host will permit the growth of larger tumour masses which would have a greater dependence on neovascularization and be subject to an oxygen gradient from the tumour periphery moving towards the hypoxic core of the mass. Given that hypoxia has been shown to be associated with tumour progression and resistance to therapy (202), an adult zebrafish xenotransplant model may prove to be beneficial in evaluating drug response.

Therefore, as we move towards employing the zebrafish XT model in drug screening, the most informative and cost-effective method may be to use zebrafish embryos to conduct the primary large-scale drug screen followed by the testing of prioritized compounds in an adult XT model.

The rationale behind developing the zebrafish XT model was to create an *in vivo* drug response assay that I could use to study the role of PRP4K in the cellular response to taxanes in breast and ovarian cancer. I have demonstrated that the human breast cancer cell line MDA-MB-231 was able to engraft and proliferate in zebrafish embryos, and that this proliferation could be inhibited by treating embryos with paclitaxel. However, when I knocked down PRP4K I observed an unexpected increase in cell proliferation within the zebrafish embryos. While this observation prohibited us from using the zebrafish XT model in our study of taxane resistance, it prompted us to study the mechanism behind the observed increase in proliferation, which is the focus of Chapter 4 of this thesis.

Chapter 4 PRP4K is a Novel Regulator of Anoikis

Resistance

4.1 Introduction

4.1.1 Anoikis

To properly develop and maintain homeostasis, multicellular organisms depend on the ability of cells to grow and differentiate only when in the correct context within a tissue. Interactions between specific integrin receptors on the cell surface and their extracellular matrix (ECM) counterparts indicate that the cell is in the correct location and transduce signals promoting proliferation and survival (203-205). When these interactions are lost, cells undergo a form of programmed cell death termed anoikis, which prevents dysplastic cell growth.

Anoikis was first described in the early 1990s when two studies revealed that epithelial cells deprived of attachment to the ECM underwent classical apoptosis (203,206). Importantly, it was shown that apoptosis could be blocked by culturing cells on non-adherent plates with immobilized integrin $\beta 1$ antibody, but not with antibodies recognizing other cell surface proteins. This suggested that integrin binding and the resulting downstream signaling could suppress anoikis. It was also shown that epithelial cells could be switched from anoikis-sensitive to anoikis-resistant through oncogenic transformation or by treating cells with scatter factor (also known as hepatocyte growth factor (HGF)), a fibroblast-secreted protein which promotes the motility of epithelial cells (207). These results were the first to show that anoikis is mediated by integrin signaling, transformation, and epithelial to mesenchymal transition (EMT).

Induction of apoptosis following detachment from the ECM can follow either the intrinsic mitochondrial-mediated pathway or the extrinsic death receptor-mediated pathway (**Figure 4.1**). In the intrinsic pathway, proteins of the Bcl-2 pro-apoptotic family (Bak and Bax) relocate from the cytosol to the outer mitochondrial membrane (OMM) upon induction of apoptosis. In the OMM Bak and/or Bax assemble into large homo-oligomers forming a pore in the membrane resulting in the release of cytochrome c (208). Cytochrome c interacts with the apoptosis protease-activating factor (APAF) and pro-caspase-9 in the cytoplasm to form the 'apoptosome', which functions to promote the dimerization and subsequent activation of caspase 9 (209). Once activated, the initiator caspase 9 activates the effector caspases, caspase-3 and caspase-7, to induce cell destruction (210). Anoikis has been shown to initiate the intrinsic pathway through the activation of Bim (211). Bim is a pro-apoptotic member of the Bcl-2 homology domain 3 (BH3)-only family of proteins and is found sequestered to the microtubule-associated dynein motor complex (212). Following the loss of integrin engagement to the ECM, Bim is upregulated and translocates from the dynein motor complex to the mitochondria (211) where it promotes Bak and Bax homo-oligomerization either directly through the activation of Bax (213-215), or indirectly through suppression of the pro-survival Bcl-2 members Bcl-xL and Mcl-1 (216,217).

The extrinsic apoptotic pathway is initiated following the binding of extracellular death ligands such as tumour necrosis factor- α (TNF- α) or Fas Ligand (FasL) to their respective transmembrane receptors. Binding stimulates receptor oligomerization which recruits Fas-associated death domain (FADD) and the initiator caspase-8, to form the death-inducing signaling complex (DISC). Formation of the DISC

results in oligomerization of caspase-8, facilitating its autoactivation through self-cleavage (218,219). Active caspase-8, much like in the intrinsic pathway, activates the effector caspases, caspase-3 and caspase-7, to induce cell destruction. Anoikis has been shown to initiate the extrinsic pathway by upregulating the Fas receptor while simultaneously downregulating c-Flip, an endogenous antagonist of caspase-8 (220,221). Furthermore, unliganded integrins have been shown to recruit caspase-8 to the membrane where it can become activated in a death receptor-independent manner (222).

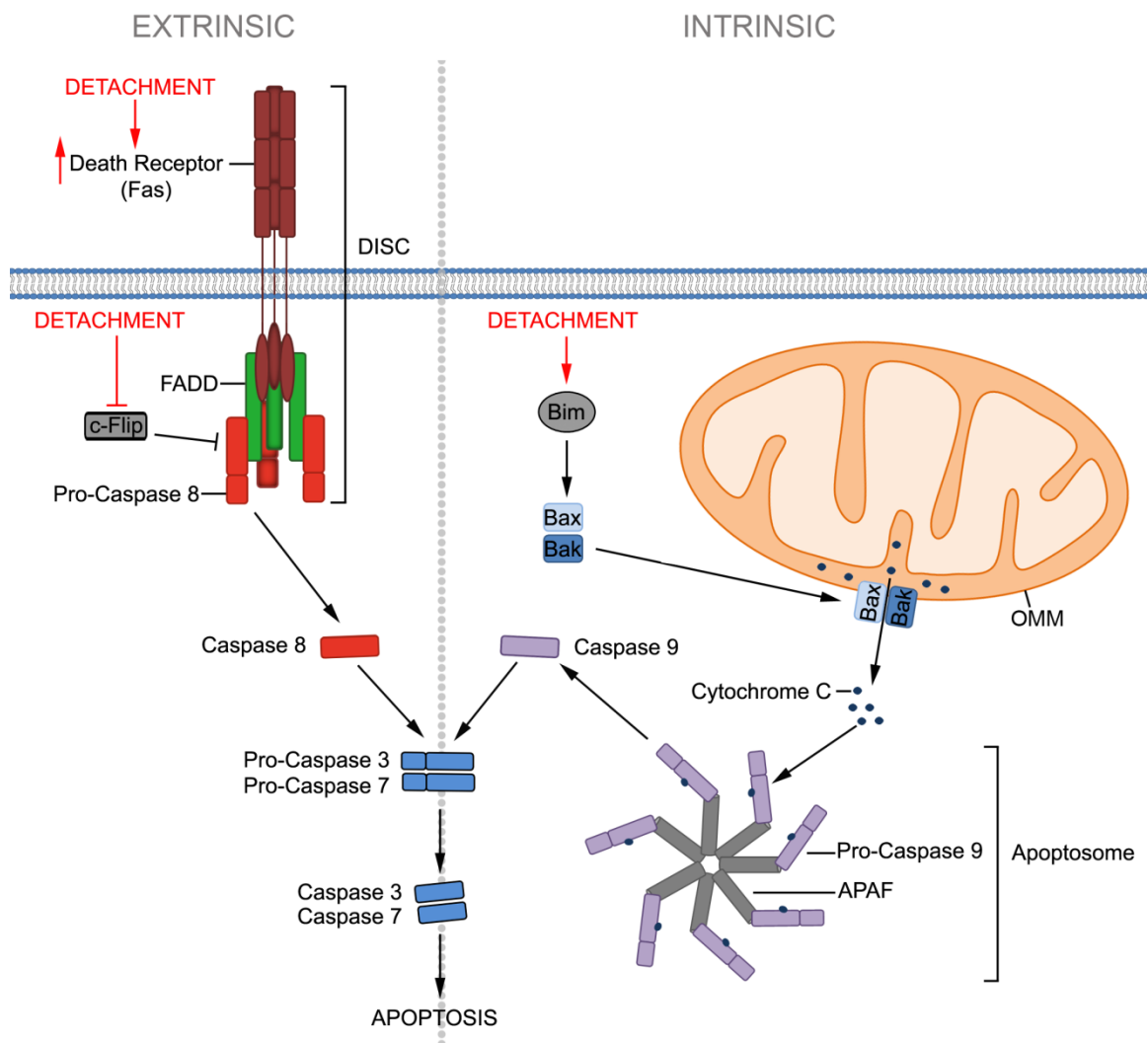


Figure 4.1 Mechanisms of apoptosis induction following cell detachment from the ECM. Anoikis has been shown to induce both the intrinsic and extrinsic apoptotic pathway following cell detachment. The intrinsic pathway is activated through the up-regulation of Bim which promotes Bak and Bax dimerization in the OMM. The extrinsic pathway is activated through the up-regulation of Fas death receptor and the concurrent inhibition of c-Flip.

In addition to activating intrinsic and extrinsic apoptotic pathways, integrin detachment from the ECM shuts off integrin-mediated survival signaling pathways. Integrins bind the ECM in clusters resulting in the formation of focal adhesions; large multi-protein structures which form the mechanical link to the ECM and act as a signaling hub to initiate cellular signaling events promoting cell survival, proliferation, and migration (223). A key mediator of this signaling is the non-receptor tyrosine kinase focal adhesion kinase (FAK). FAK is recruited to focal adhesions and activated through disruption of an intra-molecular auto-inhibitory interaction between the amino-terminal FERM (protein 4.1, ezrin, radixin and moesin homology) domain and its kinase domain (224,225). Displacement of the FERM domain is preceded by autophosphorylation of tyrosine 397, exposing a docking site for phosphatidylinositol 3-kinase (PI3K) (226) and Src family kinases (227). Recruitment of PI3K to FAK (much like its recruitment to HER3, as described in section 2.1.4) serves to bring PI3K within proximity of its membrane-bound substrate PIP_2 . Phosphorylation of PIP_2 by PI3K leads to the activation of Akt and inhibition of apoptosis, as described previously (see 2.1.4). Recruitment of Src to FAK allows Src to phosphorylate FAK at tyrosine 925 which mediates its interaction with growth factor receptor-bound protein 2 (Grb2) (228). Grb2 acts as a docking protein to recruit, and activate, the Ras guanine nucleotide exchange factor, SOS (229). The activation of Ras by SOS promotes cell proliferation and prevents apoptosis through activation of the Raf/MEK/ERK pathway (124), as described in section 2.1.4, and illustrated in **Figure 2.1**. Detachment of integrins from the ECM results in the disruption of focal adhesions and inhibition of the associated Akt and Ras signaling.

The multiple mechanisms through which detachment from the ECM leads to proliferation arrest and induction of apoptosis is a testament to how important anoikis is in the development and maintenance of cellular homeostasis. Accordingly, the deregulation of anoikis is associated with several human diseases like diabetes and cardiovascular disease (230) while the acquisition of resistance to anoikis represents a critical step in tumour progression and metastasis.

4.1.2 Anoikis Resistance in Cancer

Tumour metastasis is a multistep process which includes the invasion of surrounding tissue, intravasation, transport through the circulatory system, extravasation and growth at the secondary site (231). Anoikis acts as barrier to prevent metastasis by inducing cell death following tumour cell detachment at the primary site, or while traveling through the circulatory or lymphatic systems. Therefore, acquisition of anoikis resistance is an essential prerequisite for tumour metastasis. In addition, anoikis resistance is required for the peritoneal dissemination of ovarian and gastric cancer cells. These cancers have a more direct route for metastasis due to their location and to the frequent accumulation of ascites fluid in the peritoneal cavity. In this case, anoikis-resistant tumour cells can detach from the primary tumour directly into the ascites fluid, disseminate throughout the peritoneal cavity and attach at a secondary location. The acquisition of anoikis resistance can be accomplished through multiple mechanisms, discussed below.

4.1.3 Mechanisms of Anoikis Resistance

4.1.3.1 Epithelial to Mesenchymal Transition

EMT is the biological process through which polarized, immotile epithelial cells undergo a phenotypic switch to become migratory mesenchymal cells (232). This process is routinely activated during wound healing, inflammation and embryogenesis and is characterized by the loss of several epithelial proteins including E-Cadherin and β -catenin, accompanied by the increased expression of mesenchymal proteins like N-cadherin, vimentin and fibronectin. Further to its activation during regular biological processes, EMT also provides tumour cells with the invasive properties required for metastasis while serving as a mechanism to suppress anoikis. Anoikis suppression is a result of key players involved in EMT also modulating genes involved in apoptosis and cell survival. For example, transcription factors Twist and Snail are both upregulated during EMT as a means of repressing E-Cadherin transcription (233,234). Upregulation of Twist is also associated with increased expression of the anti-apoptotic Bcl-2 protein (235), while Snail has been shown to transcriptionally repress the pro-apoptotic protein BH3 interacting-domain death agonist (BID) and effector caspase-6 (236). Furthermore, Snail has been shown to transcriptionally repress PTEN leading to Akt pathway activation and suppression of apoptosis through the phosphorylation-mediated inactivation of the pro-apoptotic protein Bad (237).

Another important transcription factor in the induction and maintenance of EMT is NF- κ B (238). NF- κ B, best known for its role in the inflammatory response, has recently been implicated in EMT through multiple mechanisms including the transcriptional upregulation of Twist (239) and the stabilization of Snail (240). In its inactive form, NF- κ B is bound to I κ B and sequestered in the cytoplasm. Phosphorylation

of I κ B releases NF- κ B which translocates to nucleus and induces target gene expression. Constitutive activation of NF- κ B is sufficient to induce EMT *in vitro*, and is observed in many malignant cancers (241-243). NF- κ B signaling directly up regulates Bcl-2, inhibitor of apoptosis protein 1 (IAP-1) and osteoprotegerin, all of which inhibit apoptosis and prevent anoikis following cell detachment (244). These examples illustrate how induction of EMT can protect cells from anoikis by inhibiting the apoptotic pathway at multiple locations.

4.1.3.2 Integrin Expression

Integrins are a class of adhesive cell surface receptors composed of non-covalently associated α and β subunits. In vertebrates, there are 18 α and 8 β subunits that can assemble into 24 unique receptors possessing different binding properties and different tissue distributions (245,246). Oncogenic transformation has long been known to lead to alterations in integrin α/β composition, shown to support cancer initiation and progression (247). In many cases, this is due to a loss of integrins specific for adhesion to the ECM and an increase in the abundance of integrins which stimulate cell survival, migration, proliferation and invasion. An example of integrin switching shown to specifically increase anoikis resistance is the switch from $\alpha\nu\beta 5$ to $\alpha\nu\beta 6$ integrin observed in squamous cell carcinomas (248). Cells expressing $\alpha\nu\beta 5$ induce the intrinsic apoptotic pathway when grown under conditions of low attachment, while cells expressing $\alpha\nu\beta 6$ activate the pro-survival PI3K-Akt pathway under the same conditions. Similarly, $\alpha\nu\beta 3$ integrin expression in carcinoma cells was shown to enhance anchorage-independent cell growth *in vitro* and increase metastasis *in vivo* (249). The $\beta 3$ integrin tail was shown to

recruit and activate c-src which, in turn, phosphorylates crk-associated substrate (CAS), a large adaptor protein which promotes cell invasion and survival (250,251). Importantly, this recruitment was shown to be independent of integrin attachment (249) and provides a potential mechanism behind the aggressive nature of $\alpha v\beta 3$ -expressing tumours (252-254).

4.1.3.3 Increased Collagen Expression

The interactions between integrins on the cell surface and collagen in the ECM inform the cell that it is in the proper location and stimulates FAK-mediated pro-survival signaling. Detachment of the integrins from collagen during the metastatic process arrests cell growth, and induces apoptosis, as described above. An interesting mechanism of anoikis resistance beginning to emerge in the literature involves the overexpression and secretion of collagen by tumour cells as a means of maintaining the integrin-collagen interaction in the absence of attachment. This form of autocrine collagen signaling was first described by Burnier *et al.*, who observed an enhanced liver-metastasizing potential in murine lung carcinoma cells overexpressing type IV collagen (255). These cells demonstrated a sustained activation of the $\alpha 2$ integrin-FAK-PI3K pathway in the absence of ECM attachment, which protected the cells from anoikis and promoted metastasis. In an independent study, overexpression of NOTCH3 in epithelial ovarian cancer cells was shown to promote anoikis resistance through the upregulation of *COL4A2*, the gene encoding the α chain of type IV collagen (256). This, again, led to sustained FAK signaling under detached conditions and protection from anoikis. These studies identify a unique mechanism of anoikis resistance whereby cancer cells overexpress components of

the ECM to coat the surface of the cell and maintain pro-survival integrin signaling in the absence of attachment.

4.1.3.4 Modulation of Membrane Microdomains

Integrin binding to the ECM triggers the relocation of effector proteins, such as FAK and Rac1, to cholesterol-enriched membrane microdomains (CEMMs), which act as platforms to regulate the localization and activation of these effector molecules (257). Following integrin detachment from the ECM, CEMMs are endocytosed as a means of shutting down the associated signaling pathways (258). The process of internalizing integrins following detachment from the ECM is regulated by caveolin-1 (Cav-1), the key structural protein of a specific type of CEMM called caveolae. Loss of Cav-1 has been shown to impair detachment-induced CEMM endocytosis, which correlates with increased signaling through the PI3K pathway and an acquired resistance to anoikis (259). Interestingly, transformation of NIH 3T3 cells by various oncogenes leads to a reduction in Cav-1 levels (260), while targeted down-regulation of Cav-1 was shown to be sufficient to drive NIH 3T3 transformation (261). These results suggest that targeting of Cav-1 could be a commonly used mechanism in tumorigenesis to evade anoikis.

An alternative role for Cav-1 in the acquisition of anoikis resistance involves its interaction with the anti-apoptotic protein myeloid cell leukemia 1 (Mcl-1). Mcl-1 is a member of the Bcl-2 family of proteins which prevents apoptosis by binding to and sequestering pro-apoptotic proteins Bak and Bax, preventing their assembly into homo-oligomers in the OMM and the subsequent release of cytochrome c (217,262). Cell detachment from the ECM has been shown to induce a rapid ubiquitination and

proteasome-dependent degradation of Mcl-1 followed by Bax activation and apoptosis (263). Interestingly, Cav-1 has been shown to interact with Mcl-1 and prevent its degradation by blocking Mcl-1 ubiquitination (264). As mentioned previously, Cav-1 is a major structural component of CEMMs/caveolae which are endocytosed in response to cell detachment. Following endocytosis, Cav-1 within the endosome is ubiquitinated which targets endosomal Cav-1 for degradation via lysosomal fusion (265). As a result, Cav-1 protein levels decrease following cellular detachment from the ECM (264,266,267). Taken together, this data suggests a model in which Mcl-1 is bound to Cav-1 within caveolae preventing its degradation. Following detachment from the ECM, Cav-1 and Mcl-1 are internalized leading to Cav-1 ubiquitination and degradation. Loss of Cav-1 exposes the ubiquitination site within Mcl-1 leading to its degradation and activation of Bak and Bax resulting in the induction of apoptosis. In agreement with this model, treating human lung cancer cells with hydrogen peroxide or nitric oxide has been shown to prevent Cav-1 degradation following cell detachment resulting in sustained pro-survival signaling and anoikis resistance (266,267).

4.1.3.5 Autophagy

Autophagy is an intracellular degradation system through which unnecessary or dysfunctional cellular components are catabolically degraded (268). This process begins with the engulfment of intracellular cargo by an isolation membrane (also known as a phagophore) which sequesters the cargo in a double-membraned autophagosome. The autophagosome fuses with a lysosome promoting the degradation of its contents by lysosomal acidic proteases. Amino acids and other by-products of the degradation are

exported into the cytoplasm by lysosomal permeases and transporters where they can be re-used in protein synthesis and metabolism (268). While autophagy plays a well-defined role in several physiological processes including adaptive responses to starvation (268), antigen presentation (269), elimination of intracellular microbes (270) and quality control of intracellular proteins and organelles (271), its role in cancer progression is complicated by the fact that it performs both tumour-suppressing and –promoting functions. Under conditions of starvation and hypoxia, frequently observed in poorly vascularized tumours, autophagy can provide an alternate energy source and provide protection from metabolic stress (272,273). As a result, inhibition of autophagy has been shown to decrease cell survival in response to metabolic deprivation (272). In contrast, loss-of-function mutations in the autophagy pathway are associated with tumour progression in multiple types of cancer, including both breast and ovarian cancer (274-276). Tumour suppression has been shown to be mediated, at least in part, by the role of autophagy in maintaining genomic integrity. Autophagy clears cells of damaged ROS-producing mitochondria. In autophagy-deficient cells, ROS accumulates leading to DNA damage (277). Furthermore, autophagy can influence the dynamics of DNA repair by regulating the levels of dNTPs (278) and supplying ATP (279) required for DNA synthesis during repair. ROS accumulation has also been shown to promote the degradation of anaphase blockers securin and cyclin B1 leading to a compromised SAC (280). Accordingly, deficiencies in autophagy have been shown to be associated with increased DNA damage, gene amplification and aneuploidy (281) which promotes tumorigenesis.

Autophagy has also been shown to play a role in the cellular response to ECM detachment, as reduced integrin signaling induces autophagy in epithelial cells and

fibroblasts. Importantly, knockdown of autophagy regulators inhibits autophagy induction following ECM detachment and enhances apoptosis, suggesting autophagy plays a protective role against anoikis (282). Accordingly, up-regulation of Bcl-2 nineteen-kilodalton interacting protein 3 (BNIP3), a potent inducer of autophagy, has been recently shown to induce anoikis resistance in hepatocellular carcinoma cells (283). Furthermore, ID8 mouse ovarian cancer cells serially transplanted in mice develop anoikis resistance and display increased rates of autophagy, as compared to the starting anoikis-sensitive cell population (284). While the exact mechanism through which autophagy promotes survival in the absence of ECM attachment is not clear, these results show that anoikis resistance can be acquired through increased rates of autophagy.

In this chapter, I identify increased anoikis resistance as the mechanism behind the increased proliferation rates observed in MDA-MB-231 shPRP4K cells transplanted in zebrafish embryos that was described in Chapter 3. Using an ID8 shPRP4K cell model I confirm increased proliferation in zebrafish embryos following PRP4K knockdown. By recapitulating the three-dimensional microenvironment of the zebrafish yolk sac through *in vitro* spheroid culture, I demonstrate that loss of PRP4K enhances cell viability when cells are grown under non-adherent conditions. The mechanism through which loss of PRP4K induces anoikis resistance may be a consequence of, or relate to, an inability to internalize and degrade Cav-1 following detachment.

4.2 Materials and Methods

4.2.1 Cell Lines and Culture

ID8 cells (a kind gift from Dr. Brent Johnston (Dalhousie University)), a cell line derived from spontaneous *in vitro* transformation of C57BL/6 mouse ovarian surface epithelial cells, were cultured in Dulbecco's modified Eagle's medium (Sigma) supplemented with 10% fetal calf serum, 1% penicillin/streptomycin at 37°C with 5% CO₂. To create the ID8 PRP4K knockdown cell lines PRP4K-targeting GIPZ lentiviral shRNAs (shPRP4K-A = clone: V3LMM_463188, shPRP4K-B = clone: V3LMM_463189, shPRP4K-C = clone: V3LMM_463192, shPRP4K-D = clone: V3LMM_463191, Non-silencing shCTRL = RHS4346) were purchased from Thermo Scientific. Lentivirus was produced by co-transfection of the GIPZ shRNA, pMD2.G, pCMV-8.92, and pCMV-8.93 vectors into human HEK-293T cells as described in section 2.2.6. Viral media was harvested from HEK-293T cells, diluted 1:1 with fresh media, and used to infect ID8 cells. For infection, target cells were incubated with viral media for 24 h followed by the addition of fresh virus and an additional 24 h incubation. After a 48 h recovery in virus-free media, shRNA-expressing cells were selected for by adding 2 µg/ml puromycin to the media. MCF-7 shPRP4K cell line generation was performed as described in section 2.2.6.

4.2.2 Western Blot Analysis

Whole cell lysates were prepared as described in section 2.2.5. For the western blots performed in this chapter, lysates were not treated with calf intestinal phosphatase in order to preserve Akt phosphorylation. Lysates were mixed with 2x sample buffer and boiled prior to separation by SDS-PAGE and western blot analysis. Antibodies used were

sheep anti-PRP4K antibody (H143) (11), rabbit anti-Caveolin-1 antibody (Cell Signaling, #4060), rabbit anti-Akt (pan) antibody (Cell Signaling, #4691), rabbit anti-Phospho-Akt antibody (Ser473) (Cell Signaling, #9271), rabbit anti-E-Cadherin (Cell Signaling, #3195), rabbit anti- β -Catenin (Cell Signaling, #8480), and mouse anti-actin antibody (Sigma, A3853).

4.2.3 Quantification of *In Vitro* Proliferation Rates

To determine the *in vitro* proliferation rates of ID8-shCTRL, ID8-shPRP4K-A and ID8-shPRP4K-B cells, 50 000 cells were plated in individual wells of a 6-well plate. Cells were trypsinized and counted using a haemocytometer at 24 and 48 h after plating to determine the total number of cells present.

4.2.4 Zebrafish Xenotransplantation

Xenotransplantation of ID8-shCTRL and ID8-shPRP4K cells into zebrafish embryos was carried out as described in section 3.2.3. Briefly, cells were labeled with the lipophilic cell tracking dye, CM-DiI, and 25-50 cells were delivered, as a single injection, into the yolk sac of 48 hour old *casper* zebrafish embryos. At 24 hpi, embryos were screened for the presence of a fluorescent mass at the site of injection. Positively screened embryos were imaged at 24 and 72 hpi to observe cell behaviour and proliferation quantified by enzymatically dissociating groups of embryos (at least 15 per group) to a single cell suspension and counting the number of fluorescent cells present, as described in sections 3.2.4, 3.2.5 and 3.2.6.

4.2.5 Spheroid Cell Growth Assay

Spheroids were formed by dropping 2,500 cells in 50 μ l regular DMEM onto the lid of a 10 cm tissue culture dish. The lid was inverted and placed onto the base of the dish containing 10 mL PBS. After 7 days in culture, spheroids were imaged using an Axio Zoom V16 fluorescent microscope (ZEISS) and individual spheroids were harvested by touching a PCR tube (Axygen) filled with medium to the hanging droplet containing the spheroid. Spheroids were allowed to settle to the bottom of the PCR tube and three quarters of the medium was removed. The tube was then filled with PBS to wash the spheroids and dilute the remaining medium. This process was repeated twice more to remove as much medium as possible. Spheroids were then re-suspended in trypsin and incubated at 37°C for 15 minutes to generate a single cell suspension. The cell suspension was plated in an individual well of a 6-well plate and grown for 7-10 days to allow colony formation. Once visible colonies had formed, plates were rinsed with PBS and fixed/stained with a solution of 6% glutaraldehyde (Electron Microscopy Sciences, 16220) and 0.5% crystal violet (SIGMA-ALDRICH (C6158), for 30 minutes at room temperature, as described previously (285). Images of each well were captured with a digital camera and the number of colonies quantified using ImageJ (NIH).

4.2.6 Soft Agar Colony Formation Assay

Six-well plates were coated with a 1 ml base layer of 1% agarose in DMEM (2% NuSieve low melting point agarose in H₂O (Lonza, 50081) mixed 1:1 with 2X DMEM) and allowed to solidify. MCF-7 shCTRL and shPRP4K cells were re-suspended in 0.35% agarose at a concentration of 500 cells/ml and 1 ml of the suspension was layered on top

of the 1% agarose base layer. Plates were incubated at 37°C for 12 days to allow for colony formation. To feed the cells, 1 ml of fresh media was added to the top of the 0.35% agarose layer and replaced every 4 days. At the end of the 12 day incubation, colonies were imaged under a 25X magnification using an Axio Zoom V16 fluorescent microscope (ZEISS) equipped with a Plan NeoFluar Z 1 X/0.25 objective. Colonies were enumerated using ImageJ (NIH).

4.2.7 Immunofluorescence

MCF-7 shCTRL and shPRP4K-1 cells were plated onto sterile coverslips in a 6-well dish and treated with 2 µg/ml doxycycline for 72 hours to induce hairpin expression. Cells were washed once with PBS and fixed in 3% paraformaldehyde for 20 min. Immunolabeling was carried out as described in section 2.2.8 using a Caveolin-1 primary antibody (Cell Signaling) diluted 1:400 and an Alexa Fluor 488-donkey anti-rabbit secondary antibody (Life Technologies, A-21206) diluted 1:200. Fluorescent images were captured with a Zeiss Cell Observer Microscope under a 63× immersion oil objective lens. Images were processed using only linear adjustments (*e.g.* brightness/contrast) with Slidebook (Intelligent Imaging Innovations, Boulder, CO) and Adobe Photoshop CS5.

4.2.8 Anoikis Assay Using PolyHEMA Coated Plates

Poly 2-hydroxyethyl methacrylate (PolyHEMA) (SIGMA-ALDRICH, P3932) was dissolved in 95% ethanol at a concentration of 20 mg/ml by stirring for several hours

at 65°C. Tissue culture plates were coated with PolyHEMA (4 ml per 10 cm plate) and left to dry overnight at 37°C. To determine the changes in protein expression under non-adherent conditions, ID8-shCTRL, ID8-shPRP4K-A and ID8-shPRP4K-B cells were plated on PolyHEMA coated and non-coated tissue culture dishes for 24 h then harvested for western blot analysis.

4.3 Results

4.3.1 Knockdown of PRP4K Accelerates the Growth of ID8 Cells in Zebrafish Embryos

To follow up on the observation that knockdown of PRP4K enhanced MDA-MB-231 cell proliferation in zebrafish embryos (section 3.3.3), I generated ID8 cell lines stably expressing either a control hairpin (shCTRL), or one of four unique hairpins targeting PRP4K (shPRP4K-A through D). The ID8 cell line was derived from mouse ovarian surface epithelial cells which were allowed to spontaneously transform *in vitro* (286), and is routinely transplanted in mice as an orthotopic, syngeneic model of epithelial ovarian cancer (EOC) which replicates the phenotype of the human disease (287). I chose this cell line in anticipation of future mouse studies. As shown in **Figure 4.2A**, expression of each of the four PRP4K-targeted hairpins resulted in a substantial decrease in PRP4K protein levels. To determine the impact of PRP4K knockdown on *in vitro* cell proliferation rates, a defined number of ID8-shCTRL and two of the ID8-shPRP4K cell lines (ID8-shPRP4K-A, ID8-shPRP4K-B) were plated and the number of cells counted every 24 hours to determine the rate of growth. As shown in **Figure 4.2B**, knockdown of PRP4K had no significant impact on the rate of *in vitro* cell proliferation.

To determine if knockdown of PRP4K in ID8 cells altered their ability to proliferate in the zebrafish XT model, as was observed with MDA-MB-231 shPRP4K cells, ID8-shCTRL and ID8-shPRP4K-A cells were transplanted into 48-hour old zebrafish embryos as described in section 3.2.3. At 24 hours post injection embryos were screened for the presence of a fluorescent mass at the site of injection and cell proliferation visualized by imaging individual embryos at 24 and 72 hours post injection (**Figure 4.2C**). Cell growth was quantified using the cell proliferation assay described in Chapter 3 (**Figure 4.2D**). Over the 48 hour time period, ID8-shCTRL cells showed very little growth within embryos while there was approximately a 2-fold increase in ID8-shPRP4K-A cell number over the same time period. These results are in agreement with those presented in Chapter 3; knockdown of PRP4K enhances cell growth in zebrafish embryos.

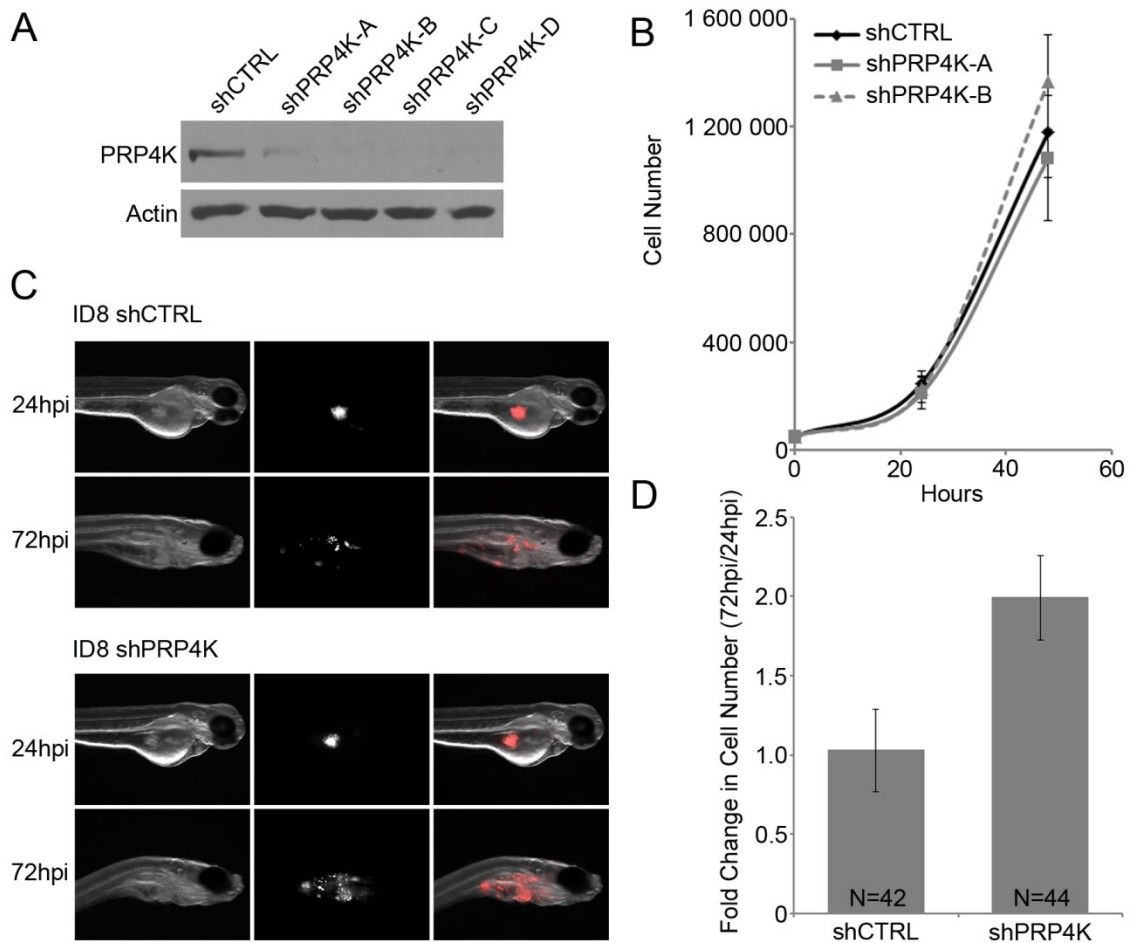


Figure 4.2 Knockdown of PRP4K increases ID8 cell proliferation in zebrafish. (A) ID8 cells were transduced with control or PRP4K-targeting shRNA lentiviral vectors to generate cell lines stably expressing the indicated hairpin. Knockdown of PRP4K was confirmed by western blot analysis. (B) *In vitro* proliferation rates were determined by plating 50 000 cells for each cell line and performing cell counts every 24 hours. Data is presented as mean of four independent experiments (\pm SD). (C) Representative brightfield and fluorescent images are shown of zebrafish embryos transplanted with either ID8-shCTRL or ID8-shPRP4K-A cells at 24 and 72 hours post injection (hpi). (D) Groups of at least 15 embryos at 24 and 72 hpi were dissociated and the number of fluorescent cells counted. The fold change in cell number was calculated from three independent experiments and the mean represented as a bar graph. Error bars = SEM.

4.3.2 Knockdown of PRP4K Enhances Cell Growth in 3D Cell Culture Models

Perhaps the most significant difference between the *in vitro* environment of a tissue culture plate and the *in vivo* environment of a zebrafish embryo is the attached versus suspended conditions under which the cells are forced to grow. In a tissue culture plate cells will adhere to the hydrophilic polystyrene surface and grow as a two-dimensional monolayer. In the zebrafish XT model, cells injected into the yolk sac grow within a three-dimensional environment lacking an adherent hydrophilic surface. To determine if the increased proliferation rates of PRP4K-knockdown cells engrafted in zebrafish embryos was due to an enhanced ability to proliferate under non-adherent conditions, ID8-shCTRL and shPRP4K cells were grown as spheroids using a hanging drop culture. Spheroids were cultured for 7 days (**Figure 4.3A**), after which individual spheroids were harvested, trypsinized and plated in individual wells of a 6-well plate. The cells were allowed to adhere and proliferate until visible colonies had formed (**Figure 4.3B**). Quantifying the number of colonies per well (**Figure 4.3C**) revealed that knockdown of PRP4K increased cell viability in ID8 cells grown as spheroids. Similarly, knockdown of PRP4K in the MCF7 human breast cancer cell line (described in 2.2.6) increased colony formation for cells suspended in soft agar (**Figure 4.4A & B**). Together, this data supports the hypothesis that knockdown of PRP4K enhances the ability of cancer cells to survive and proliferate under non-adherent conditions.

The ability of transformed cells to grow under anchorage-independent conditions provides an indication of tumorigenic potential and is often associated with a transition from an epithelial-to-mesenchymal (EMT) phenotype (288). To determine if PRP4K was enhancing anchorage-independent growth by promoting EMT, MCF-7 shCTRL and

shPRP4K cells were harvested and subjected to western blot analysis to determine the protein levels of 2 canonical EMT marker proteins (**Figure 4.4C**). E-Cadherin is a calcium-dependent cell-cell adhesion molecule which is down-regulated during EMT, while β -catenin is a transcription factor in the Wnt signaling pathway involved in regulating cell adhesion and is also down-regulated during EMT. Knockdown of PRP4K had no effect on either E-Cadherin or β -catenin protein level suggesting the cells have not undergone EMT, and that an alternative mechanism was promoting anchorage-independent growth.

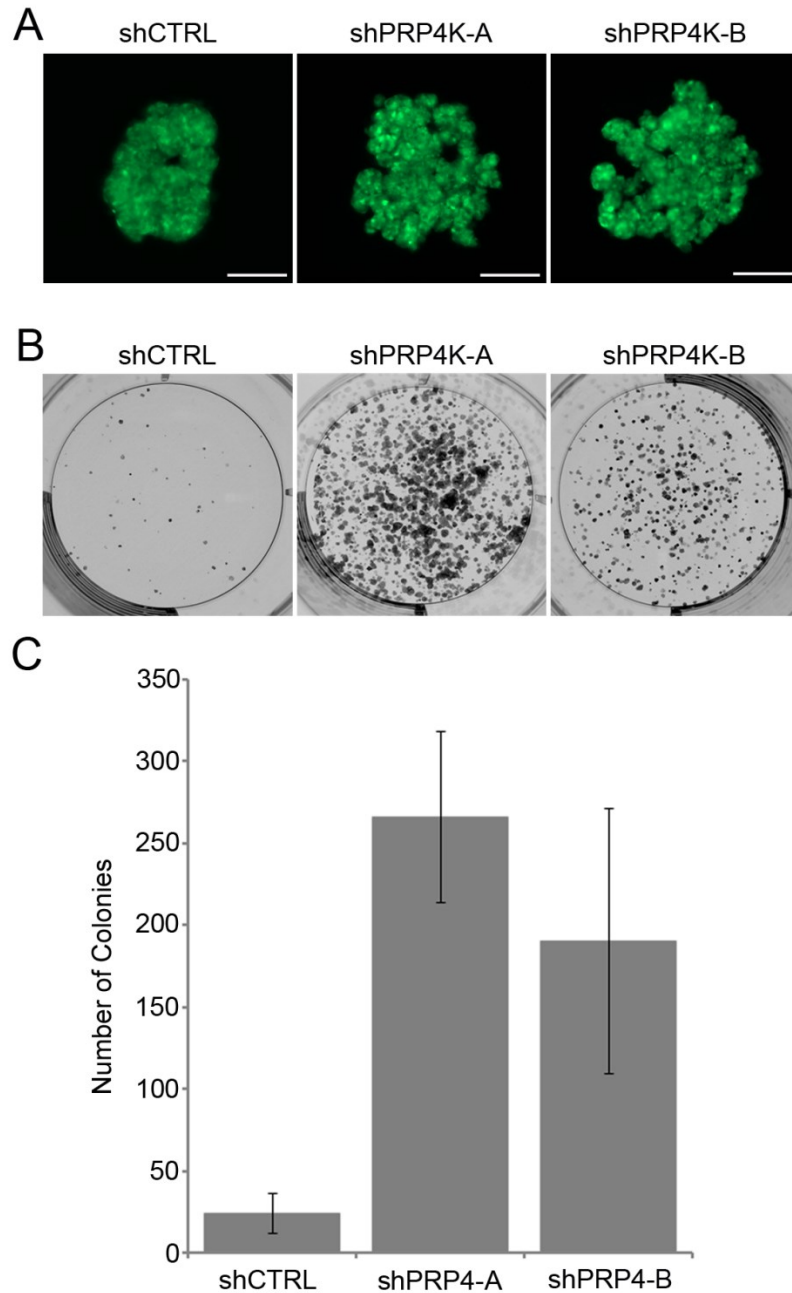


Figure 4.3 Knockdown of PRP4K increases viability of ID8 cells cultured as spheroids. (A) Representative images of ID8 spheroids after 7 days in culture. Scale bars = 250 μ m. (B) Individual spheroids were harvested, trypsinized and plated in individual wells of a 6-well plate. After 5 days in culture colonies were fixed and stained with crystal violet. Representative images show colony growth for each of the three cell lines. (C) Stained colonies from three independent experiments were counted using ImageJ and represented as the mean colony number. Error bars = SEM.

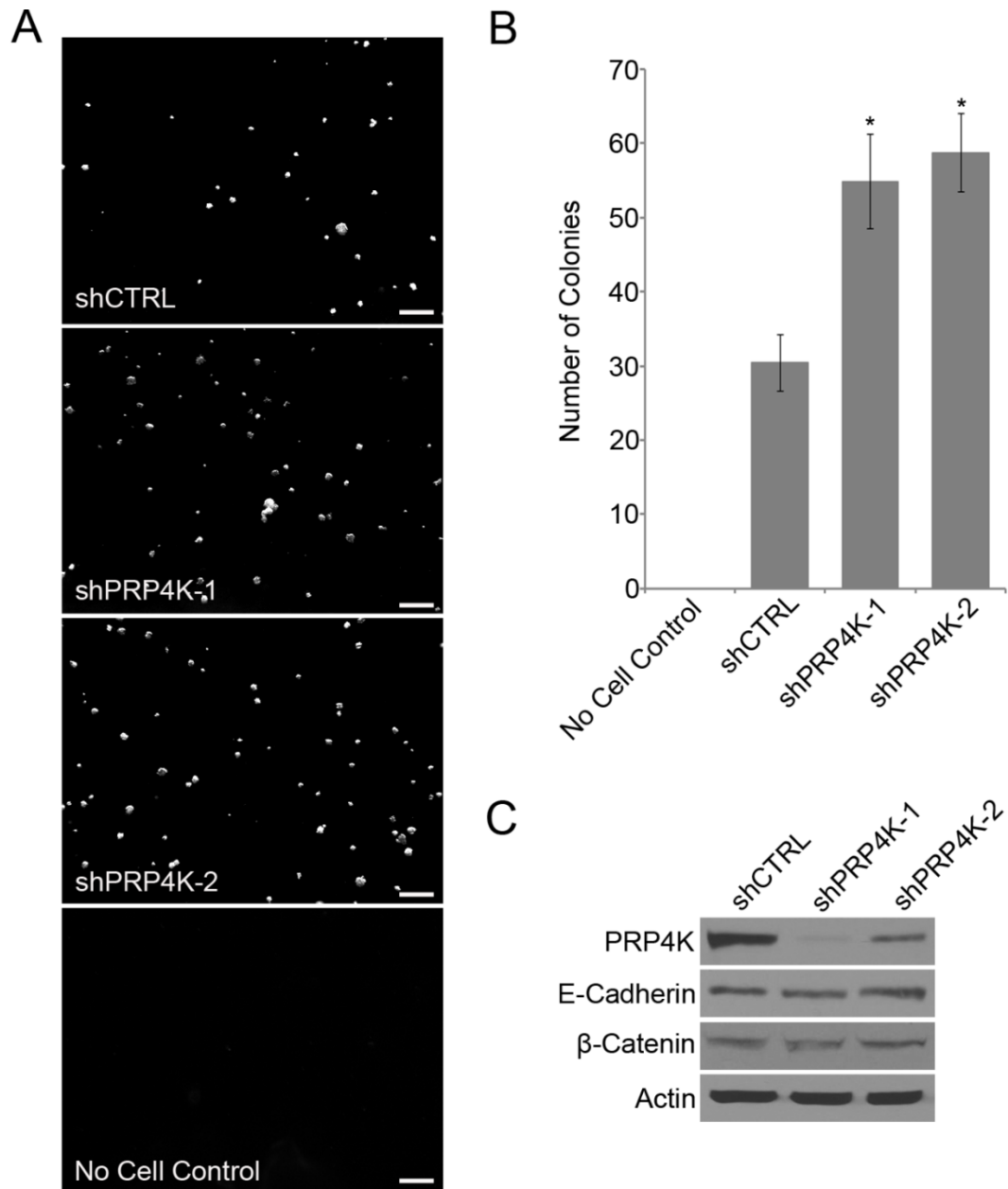


Figure 4.4 Knockdown of PRP4K increases MCF-7 growth in soft agar. (A) Representative images of indicated cell lines growing as colonies in soft agar 12 days after plating. Scale bars = 500 μ m **(B)** Colonies were counted from 4 random fields of view and represented as the mean from 3 independent experiments. Error bars = SD. * $p < 0.005$. **(C)** MCF-7 shCTRL, shPRP4K-1 and shPRP4K-2 cell lines were cultured under adherent conditions and analysed by western blot analysis for PRP4K, E-Cadherin, β -Catenin and actin protein steady-state levels.

4.3.3 Loss of PRP4K Affects Caveolin-1 Localization and Prevents its Degradation Following Cell Detachment

The ability of adherent cells to be grown as anchorage-independent spheroids, or as colonies in soft agar, requires a resistance to anoikis; an apoptotic program induced by loss of cell adhesion (289). One mechanism through which cells trigger apoptosis following detachment is through the internalization and degradation of Cav-1. Cav-1 is an essential protein constituent of the plasma membrane caveolae, and has been shown to interact with the anti-apoptotic protein Mcl-1, preventing its ubiquitin-mediated proteasomal degradation (264). It has been proposed that cell detachment leads to the internalization and degradation of Cav-1 resulting in the release, and subsequent degradation, of Mcl-1. Loss of PRP4K induces an aggregated Cav-1 localization at the cellular membrane of MCF-7 cells suggesting a potential defect in Cav-1 trafficking or function (**Figure 4.5**). To determine if loss of PRP4K was impacting Cav-1 degradation following detachment, ID8-shCTRL, ID8-shPRP4K-A and ID8-shPRP4K-B cells were cultured for 24 hours either as an attached monolayer or as a non-adherent suspension using Poly-HEMA coated plates. After 24 hours in suspension ID8-shCTRL cells had significantly decreased levels of Cav-1 which corresponded with a reduction in Akt serine 473 phosphorylation (**Figure 4.6**) indicating a reduction in Akt signaling. Interestingly, this is also accompanied by a decrease in PRP4K expression. In contrast, PRP4K-knockdown cells failed to degrade Cav-1 and had increased Akt phosphorylation (**Figure 4.6**). This data suggests that loss of PRP4K prevents Cav-1 degradation resulting in activation of Akt and increased resistance to anoikis.

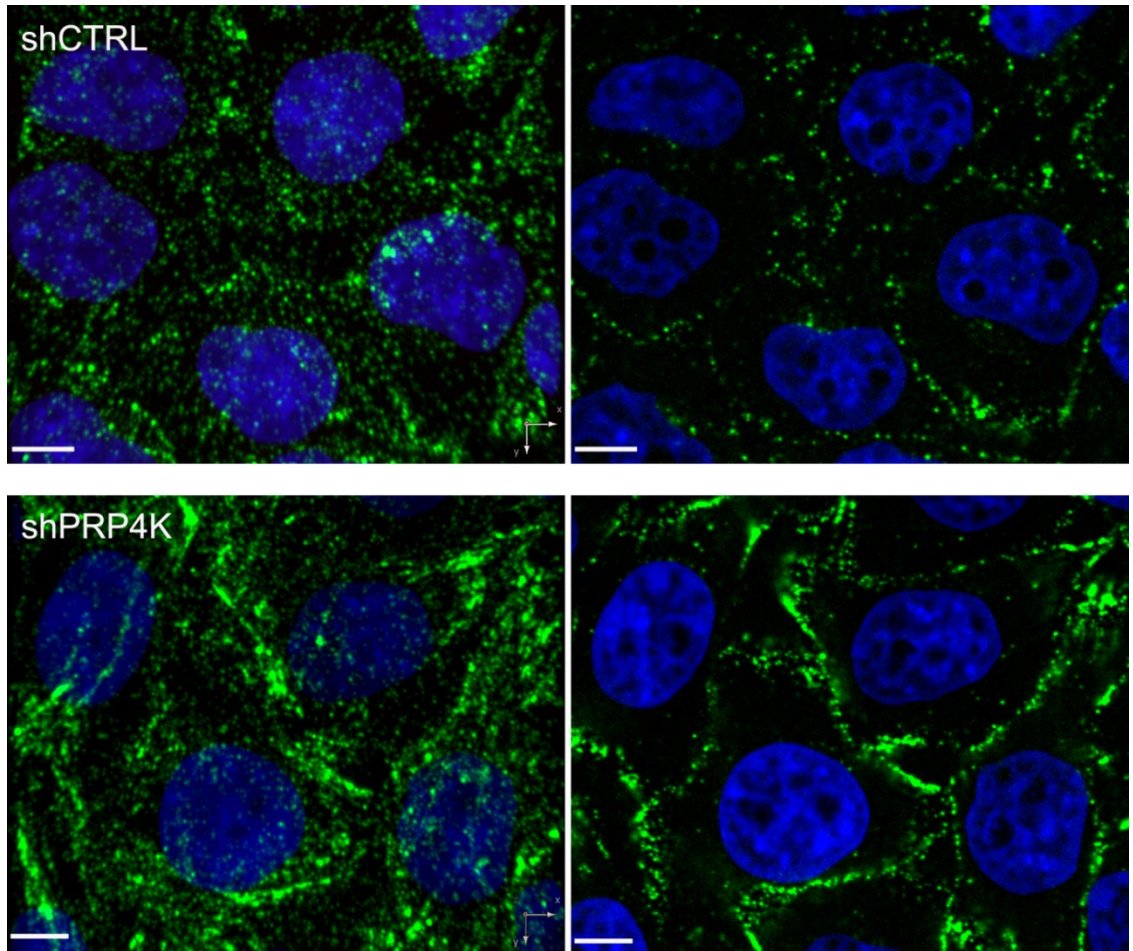


Figure 4.5 Knockdown of PRP4K affects Cav-1 localization. MCF-7 shCTRL and shPRP4K cells were cultured in the presence of doxycycline for 72 hours to induce hairpin expression. Cells were fixed and analysed by immunofluorescence confocal microscopy using an anti-Cav-1 antibody (Green). Nuclei were stained with DAPI (blue). Images on the left are a 3D rendering of 20 z-stacks captured at 0.5 μ m intervals. Images on the right are a single plane from the centre of the z-stack showing membrane localization. Scale bars = 10 μ m.

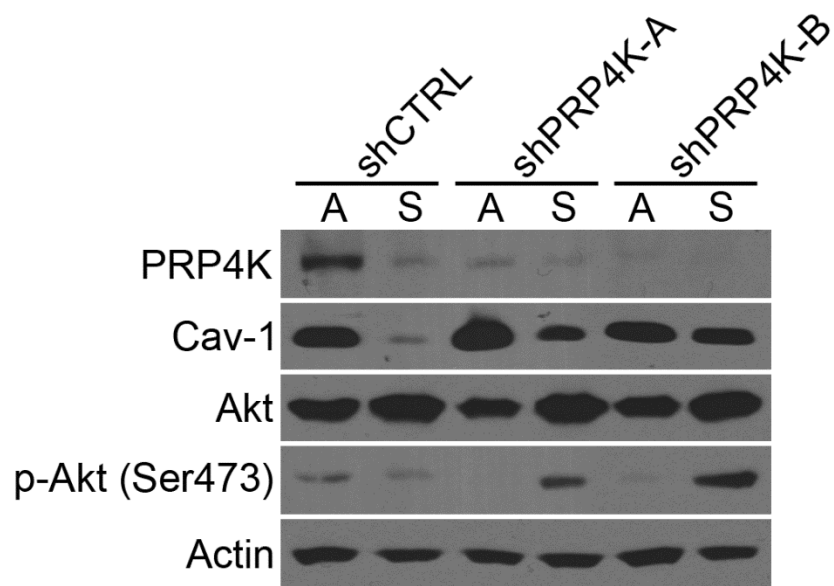


Figure 4.6 Knockdown of PRP4K prevents Caveolin-1 degradation following cell detachment. ID8 shCTRL, shPRP4K-A and shPRP4K-B cells were cultured for 24 hours as an attached monolayer (A) or in suspension (S). Total cell lysates were prepared and subjected to western blot analysis for presence of the indicated proteins.

4.4 Discussion

Anoikis acts as a critical barrier to metastasis by inducing apoptosis in tumour cells which have detached from the primary tumour and entered the circulatory or lymphatic system. As such, the acquisition of anoikis resistance is an essential prerequisite for metastasis. Understanding the molecular mechanisms through which cancer cells evade anoikis under non-adherent conditions is important in understanding the process by which cancer cells disseminate from the primary tumour site to ectopic locations.

In this study I identify loss of PRP4K as a novel mechanism of anoikis resistance. Knockdown of PRP4K expression in human breast (MDA-MB-231) and mouse ovarian (ID8) cancer cell lines resulted in increased proliferation rates when cells were engrafted into 48 hour old zebrafish embryos (**Figure 3.8 and 4.2**), but had no effect on *in vitro* proliferation rates (**Figure 4.2B**). The greatest difference between *in vitro* culture conditions and the conditions within a zebrafish embryo is the three-dimensional environment and lack of ECM contacts within the yolk sac of the embryo, as compared to the two-dimensional adherent conditions of a tissue culture plate. Therefore, I hypothesized that loss of PRP4K was increasing cell proliferation within the embryo by promoting anchorage-independent growth. This hypothesis was confirmed by showing that loss of PRP4K increased viability when cells were grown as spheroids (**Figure 4.3**) or as colonies in soft agar (**Figure 4.4**). These results suggest that the zebrafish XT model could have a novel application in the study of anoikis as cell proliferation within the cell-free three-dimensional microenvironment of the yolk sac requires evasion of the detachment-induced apoptotic pathway. This consideration was originally overlooked

during the development of the zebrafish XT model due to our choice of anoikis-insensitive leukemia cell lines used in proof-of-principal studies. Interestingly, by 72 hours post injection most of the yolk has been consumed by the embryo (**Figure 4.2C**) and the transplanted cells had re-established contact with the developing zebrafish tissue. This process would be similar to a cell traveling through the circulatory system and establishing contact at a secondary location, whereby only cells which can survive detachment from the ECM for a period of time will form a secondary tumour. Therefore, the zebrafish XT model, when applied to solid tumours, may more accurately predict drug response in metastases due to selection for anoikis resistance. To confirm this, additional studies are required to determine if the developing zebrafish tissue offers enough similarities to human tissue to support ECM contacts with engrafted cancer cells and activate integrin-mediated signaling pathways. In addition, the characterization of cell lines serially transplanted in zebrafish embryos will determine what impact the selection process has on the cellular response to anoikis, which can then be compared to similar studies carried out in mice (284).

How PRP4K loss contributes to anoikis resistance appears to be linked to Cav-1 stability following detachment. Degradation of Cav-1 in response to integrin detachment from the ECM has been shown to reduce Akt signaling (259) and induce apoptosis through the ubiquitin-mediated degradation of Mcl-1 (264). I have shown that knockdown of PRP4K prevents degradation of Cav-1 in cells cultured under conditions of low-attachment for 24 hours (**Figure 4.6**). I have also demonstrated that the inability to degrade Cav-1 is accompanied by increased Akt signaling which is known to activate the pro-apoptotic protein Bad (237) and activate mTOR signaling (121) to protect cells from

anoikis. The inhibition of Cav-1 degradation following ECM detachment has been demonstrated previously in lung cancer cells which have been treated with nitric oxide (267) or hydrogen peroxide (266). It would therefore be interesting to determine if either of these treatments has any impact on PRP4K expression. It is also important to determine the mechanism through which PRP4K is regulating Cav-1 degradation. Preliminary immunofluorescence staining for Cav-1 in adherent MCF7 shPRP4K cells reveals a more aggregated Cav-1 localization at the cell membrane, suggesting a potential defect in Cav-1 trafficking (**Figure 4.5**). Immunofluorescence staining for Cav-1 in MCF7 shPRP4K cells grown under conditions of low attachment will determine whether loss of PRP4K is preventing Cav-1 internalization. In addition, Cav-1 immunoprecipitation followed by western blot analysis using an anti-ubiquitin antibody will show whether loss of PRP4K prevents Cav-1 ubiquitination following detachment (266,267).

In summary, this chapter identifies an increased resistance to anoikis as the mechanism behind the increased proliferation rates observed in cells transplanted into zebrafish embryos following the knockdown of PRP4K. My data indicates that loss of PRP4K expression prevents the degradation of Cav-1 following cell detachment which may be the mechanism behind the evasion of anoikis.

Chapter 5 Conclusion

5.1 Preface

PRP4K is emerging as an important regulator of both cancer progression and the response to treatment. The work presented in this thesis expands our understanding of PRP4K as a regulator of taxane response while identifying a novel role for PRP4K in the regulation of anoikis aided by the development of a zebrafish xenotransplantation model. This chapter will discuss the future of zebrafish xenotransplantation and suggest a potential common mechanism through which PRP4K could be regulating multiple cellular processes. Finally, the conclusions drawn from this thesis will be combined to offer a potential mechanism which links relapse from taxanes with metastatic spread.

5.2 Comments on the Future of Zebrafish Xenotransplantation

A significant achievement of this thesis work has been the development of a zebrafish xenotransplantation model which can be used to accurately quantify drug response in human cancer cells engrafted in zebrafish embryos. While this technique has been applied in several studies exploring drug responses in leukemia (199,200,290), several questions remain that need to be addressed before the goal of drug screening or clinical application can be realized. Most importantly: how similar is the zebrafish microenvironment to that of humans? As discussed in Chapter 4, cellular interactions with the microenvironment regulate numerous signaling pathways impacting cell survival. To date, no studies have been done to determine whether or not there is enough conservation between zebrafish and human tissue to support these interactions with

engrafted human cancer cells. This becomes particularly important when engrafting adherent cell lines due to the dependence on these interactions for preventing the induction of anoikis.

Adherent cell lines adapted to *in vitro* growth will experience a degree of cell death when grown under low-attachment conditions due to the induction of anoikis. With the yolk sac as the preferred site of injection and 48 hpf the preferred stage of embryo in which to inject, transplanted cells could remain suspended in yolk for up to 48 hours, at which point the majority of the yolk will have been consumed and the cells will make contact with zebrafish tissue. In moving forward, it will be important to determine if zebrafish collagen can actively engage integrin receptors on engrafted human cancer cells and stimulate integrin-mediated signaling pathways. If yes, then the engraftment of anoikis-sensitive adherent cell lines may result in the selection of an anoikis-resistant population followed by re-activation of integrin signaling and more accurately model metastatic disease. A detailed analysis of the zebrafish microenvironment including differences and similarities to a human tumour microenvironment will be essential in validating the use of the zebrafish as a xenograft model.

A major advantage in using a living vertebrate model to perform drug screening is the ability to pair drug discovery with toxicology studies. In addition to an amenability to high-throughput screening, zebrafish offer several advantages over traditional rodent models of toxicology. First, zebrafish develop from a single-cell to larvae with fully functioning organ systems within 5 days, which greatly reduces the time for various toxicity assays. Furthermore, zebrafish embryos are transparent and develop *ex utero* allowing for visualization of organ development and toxicity phenotypes. As a result, the

zebrafish is rapidly gaining acceptance as an alternative animal model for toxicology (291). A prime example of how the zebrafish XT model can be combined with toxicity studies is the recent publication which identified the compound visnagin as a cardioprotectant against doxorubicin-induced cardiomyopathy (290). Doxorubicin is a DNA binding anti-cancer agent used in the treatment of a wide variety of human cancers including both leukemia and solid tumours. The use of doxorubicin is limited by cardiotoxicity and an increased risk of heart failure associated with use of the drug. In a recent study from the lab of Randall Peterson, zebrafish treated with doxorubicin were shown to develop extensive pericardial edema and cardiac defects which recapitulated several aspects of doxorubicin-induced cardiomyopathy in humans (290). Taking advantage of the amenability of the zebrafish to high-throughput screening, the group screened 3000 compounds for their ability to prevent cardiac toxicity in embryos treated with doxorubicin. One compound, visnagin, was identified for its ability to prevent the overt morphological effects of doxorubicin on the zebrafish heart. To ensure that visnagin would not interfere with the anti-tumour activity of doxorubicin, our lab transplanted human T-ALL cells (Jurkat) into 48-hour old zebrafish embryos. Engrafted embryos were treated with doxorubicin or a combination of doxorubicin and visnagin and cell proliferation was quantified using the *in-vivo* cell proliferation assay described in Chapter 3. The combination of doxorubicin and visnagin was shown to prevent cardiac edema in the embryos but did not interfere with the doxorubicin-induced inhibition of T-ALL cell proliferation. These results suggest that visnagin could be used clinically to prevent cardiac toxicity in doxorubicin-treated patients without interfering with the anti-tumour activity of the drug (290). This study highlights the ability to simultaneously evaluate

anti-tumour activity and toxicity using the zebrafish XT model. This will be invaluable in helping prioritize compounds as we move toward drug-screening using the zebrafish XT model.

5.3 Molecular Mechanisms of PRP4K Functions

PRP4K has been linked to several cellular processes including regulation of the spindle assembly checkpoint, host-viral interaction, response to anti-cancer therapies, and anoikis. However, the mechanism through which PRP4K functions in these processes remains largely unknown. With alternative splicing occurring in an estimated 95% of human gene transcripts (21) it is possible that PRP4K is functioning, in part, to maintain proper splicing of the genes directly involved in each process. In this thesis, PRP4K was identified as a novel HER2 regulated mediator of taxane sensitivity in breast and ovarian cancer (Chapter 2). While increased cellular resistance to taxanes following PRP4K knockdown is consistent with defects in the spindle assembly checkpoint (37), several alternative splice events have been linked to taxane resistance which could be impacted by the loss of a splicing kinase like PRP4K. For example, survivin, a member of the inhibitor of apoptosis (IAP) protein family, is expressed as five different isoforms (WT, 2B, 3B, Δ Ex3 and 2 α) arising from alternative splicing of the survivin (*BIRC-5*) gene (292-294). Increasing evidence suggests that the survivin splice variants each have different, and sometimes opposite, biological functions (294-296). In particular, increased expression of the survivin-2B splice variant is associated with increased resistance to taxanes in human ovarian cancer cell lines and poor progression-free survival in epithelial ovarian cancer patients treated with taxanes (297). Other proteins with splice variants

linked to taxane resistance include Shugoshin-like 1 (SGOL-1) (298), caspase 9 (20), and Tau (299). Understanding how the loss of PRP4K affects the splicing of these genes could provide an additional mechanism through which PRP4K regulates the cellular response to taxanes.

A novel role for PRP4K in the regulation of anoikis which appears to be mediated by the internalization and degradation of Cav-1 following cell detachment was identified in this thesis (Chapter 4). The endocytic pathway through which Cav-1 is degraded also relies on regulated alternative splicing as several endocytic adaptor proteins are expressed as multiple splice variants which can impact the rate of endocytosis. For example, at least 11 splice variants have been identified for intersectin-1 (ITSN1), an adaptor protein involved in multiple aspects of clathrin-mediated endocytosis (300,301). While the exact function of each individual splice variant remains unknown, several of the variants have been suggested to be possible targets for nonsense mediated decay (300). With loss of ITSN1 shown to reduce caveolae-dependent endocytosis in endothelial cells (302,303), an increase in nonsense mediated decay targeted ITSN1 splice variants could result in inhibited Cav-1 internalization following detachment. Other endocytic adaptor proteins with splice variants that can alter the rate of endocytosis include Rab15 (304) and SH3-domain GRB2-like (endophilin) interacting protein 1 (SGIP1) (305).

Determining how changes in PRP4K expression affect alternative pre-mRNA splicing will be important in elucidating the mechanisms of the various functions of PRP4K.

5.4 Ascites Development and Chemoresistance

More than one third of ovarian cancer patients present with an accumulation of fluid in the peritoneal cavity, known as ascites, at the time of diagnosis (306,307). The accumulation of fluid is believed to result from a combination of the altered vascular permeability of tumour microvasculature (308) and tumour-mediated obstruction of lymphatic drainage (309). Treatment for ascites is limited to treatment of the underlying disease; that is, intravenous treatment with a combination of platinum and taxol-based chemotherapy. While the clinical response to first-line chemotherapy is quite high, ranging from 70 to 80% (310-312), the majority of patients (50-75%) relapse due to the development of chemoresistant disease (313). In most cases, recurrent disease is accompanied by intractable ascites requiring frequent paracentesis for temporary relief of symptoms (307). It has been suggested that the development of ascites upon recurrence has to do with an increased number of metastases in the peritoneal cavity (transcoelomic metastases), as reduction in peritoneal tumour bulk corresponds with a reduction in the volume of ascites (314).

PRP4K was identified as a novel HER2-regulated mediator of taxane sensitivity in breast and ovarian cancer in this thesis (Chapter 2). PRP4K levels decrease in cells which have acquired a resistance to paclitaxel both *in vitro* and *in vivo*. Importantly, PRP4K protein levels are decreased in ascites-derived tumour cells isolated from a high-grade serous ovarian cancer patient following relapse from taxane-based therapy, as compared to a matched cell line derived from the solid tumour at the time of diagnosis. The knockdown of PRP4K was found to increase resistance to anoikis in breast and

ovarian cancer cell lines grown either under conditions of low attachment (Chapter 4) or in a zebrafish xenotransplantation model (Chapter 3). Given that acquisition of anoikis resistance is a prerequisite for epithelial ovarian cancer cells to survive in ascitic fluid, PRP4K could provide a link between chemoresistance and intractable ascites. Ovarian tumours treated with a taxane-based chemotherapy regimen could acquire drug resistance through the downregulation of PRP4K. As a consequence of this downregulation, cells would also lose the ability to degrade Cav-1 following detachment from the primary tumour, resulting in evasion of anoikis. The ability to survive suspended in ascitic fluid would promote transcoelomic metastasis resulting in the increase in ascites development commonly observed in recurrent disease.

While transcoelomic metastasis in ovarian cancer provides an example of how loss of PRP4K could potentially impact cancer progression, this concept could be applied to any cancer in which taxanes are used as a first-line therapy. It should be noted, however, that loss of PRP4K does not induce EMT. Therefore, in tumours which require intravasation to metastasize, loss of PRP4K alone is likely not sufficient to induce metastasis.

Overall, the work described in this thesis furthers our understanding of the role of PRP4K in cancer treatment and identifies a novel role for PRP4K with implications for cancer progression and relapsed disease.

Bibliography

1. Rosenberg, G. H., Alahari, S. K., and Kaufer, N. F. (1991) prp4 from *Schizosaccharomyces pombe*, a mutant deficient in pre-mRNA splicing isolated using genes containing artificial introns. *Mol Gen Genet* **226**, 305-309
2. Grimm, C., Kohli, J., Murray, J., and Maundrell, K. (1988) Genetic engineering of *Schizosaccharomyces pombe*: a system for gene disruption and replacement using the ura4 gene as a selectable marker. *Mol Gen Genet* **215**, 81-86
3. Warner, J. R. (1987) Applying genetics to the splicing problem. *Genes Dev* **1**, 1-3
4. Ares, M., Jr., Grate, L., and Pauling, M. H. (1999) A handful of intron-containing genes produces the lion's share of yeast mRNA. *RNA* **5**, 1138-1139
5. Hartwell, L. H., McLaughlin, C. S., and Warner, J. R. (1970) Identification of ten genes that control ribosome formation in yeast. *Mol Gen Genet* **109**, 42-56
6. Warner, J. R., and Gorenstein, C. (1978) Yeast has a true stringent response. *Nature* **275**, 338-339
7. Rosbash, M., Harris, P. K., Woolford, J. L., Jr., and Teem, J. L. (1981) The effect of temperature-sensitive RNA mutants on the transcription products from cloned ribosomal protein genes of yeast. *Cell* **24**, 679-686
8. Potashkin, J., Li, R., and Frendewey, D. (1989) Pre-mRNA splicing mutants of *Schizosaccharomyces pombe*. *EMBO J* **8**, 551-559
9. Alahari, S. K., Schmidt, H., and Kaufer, N. F. (1993) The fission yeast prp4+ gene involved in pre-mRNA splicing codes for a predicted serine/threonine kinase and is essential for growth. *Nucleic Acids Res* **21**, 4079-4083
10. Kojima, T., Zama, T., Wada, K., Onogi, H., and Hagiwara, M. (2001) Cloning of human PRP4 reveals interaction with Clk1. *J Biol Chem* **276**, 32247-32256

11. Dellaire, G., Makarov, E. M., Cowger, J. M., Longman, D., Sutherland, H. G. E., Luhrmann, R., Torchia, J., and Bickmore, W. A. (2002) Mammalian PRP4 Kinase Copurifies and Interacts with Components of Both the U5 snRNP and the N-CoR Deacetylase Complexes. *Molecular and Cellular Biology* **22**, 5141-5156
12. Gross, T., Lutzberger, M., Weigmann, H., Klingenhoff, A., Shenoy, S., and Kaufner, N. F. (1997) Functional analysis of the fission yeast Prp4 protein kinase involved in pre-mRNA splicing and isolation of a putative mammalian homologue. *Nucleic Acids Res* **25**, 1028-1035
13. Schneider, M., Hsiao, H. H., Will, C. L., Giet, R., Urlaub, H., and Luhrmann, R. (2010) Human PRP4 kinase is required for stable tri-snRNP association during spliceosomal B complex formation. *Nat Struct Mol Biol* **17**, 216-221
14. Wahl, M. C., Will, C. L., and Luhrmann, R. (2009) The spliceosome: design principles of a dynamic RNP machine. *Cell* **136**, 701-718
15. Tacke, R., Chen, Y., and Manley, J. L. (1997) Sequence-specific RNA binding by an SR protein requires RS domain phosphorylation: creation of an SRp40-specific splicing enhancer. *Proc Natl Acad Sci U S A* **94**, 1148-1153
16. Cho, S., Hoang, A., Sinha, R., Zhong, X. Y., Fu, X. D., Krainer, A. R., and Ghosh, G. (2011) Interaction between the RNA binding domains of Ser-Arg splicing factor 1 and U1-70K snRNP protein determines early spliceosome assembly. *Proc Natl Acad Sci U S A* **108**, 8233-8238
17. Makarova, O. V., Makarov, E. M., and Luhrmann, R. (2001) The 65 and 110 kDa SR-related proteins of the U4/U6.U5 tri-snRNP are essential for the assembly of mature spliceosomes. *EMBO J* **20**, 2553-2563
18. Mathew, R., Hartmuth, K., Mohlmann, S., Urlaub, H., Ficner, R., and Luhrmann, R. (2008) Phosphorylation of human PRP28 by SRPK2 is required for integration of the U4/U6-U5 tri-snRNP into the spliceosome. *Nat Struct Mol Biol* **15**, 435-443
19. Goncalves, V., Henriques, A., Pereira, J., Neves Costa, A., Moyer, M. P., Moita, L. F., Gama-Carvalho, M., Matos, P., and Jordan, P. (2014) Phosphorylation of SRSF1 by SRPK1 regulates alternative splicing of tumor-related Rac1b in colorectal cells. *RNA* **20**, 474-482

20. Shultz, J. C., Goehe, R. W., Murudkar, C. S., Wijesinghe, D. S., Mayton, E. K., Massiello, A., Hawkins, A. J., Mukerjee, P., Pinkerman, R. L., Park, M. A., and Chalfant, C. E. (2011) SRSF1 regulates the alternative splicing of caspase 9 via a novel intronic splicing enhancer affecting the chemotherapeutic sensitivity of non-small cell lung cancer cells. *Mol Cancer Res* **9**, 889-900
21. Pan, Q., Shai, O., Lee, L. J., Frey, B. J., and Blencowe, B. J. (2008) Deep surveying of alternative splicing complexity in the human transcriptome by high-throughput sequencing. *Nat Genet* **40**, 1413-1415
22. Keren, H., Lev-Maor, G., and Ast, G. (2010) Alternative splicing and evolution: diversification, exon definition and function. *Nat Rev Genet* **11**, 345-355
23. Hughes, T. A. (2006) Regulation of gene expression by alternative untranslated regions. *Trends Genet* **22**, 119-122
24. Lin, S., and Fu, X. D. (2007) SR proteins and related factors in alternative splicing. *Adv Exp Med Biol* **623**, 107-122
25. Kataoka, N., Bachorik, J. L., and Dreyfuss, G. (1999) Transportin-SR, a nuclear import receptor for SR proteins. *J Cell Biol* **145**, 1145-1152
26. Lai, M. C., Lin, R. I., and Tarn, W. Y. (2001) Transportin-SR2 mediates nuclear import of phosphorylated SR proteins. *Proc Natl Acad Sci U S A* **98**, 10154-10159
27. Misteli, T., Caceres, J. F., Clement, J. Q., Krainer, A. R., Wilkinson, M. F., and Spector, D. L. (1998) Serine phosphorylation of SR proteins is required for their recruitment to sites of transcription in vivo. *J Cell Biol* **143**, 297-307
28. Ngo, J. C., Chakrabarti, S., Ding, J. H., Velazquez-Dones, A., Nolen, B., Aubol, B. E., Adams, J. A., Fu, X. D., and Ghosh, G. (2005) Interplay between SRPK and Clk/Sty kinases in phosphorylation of the splicing factor ASF/SF2 is regulated by a docking motif in ASF/SF2. *Mol Cell* **20**, 77-89
29. Huang, Y., and Steitz, J. A. (2001) Splicing factors SRp20 and 9G8 promote the nucleocytoplasmic export of mRNA. *Mol Cell* **7**, 899-905
30. Huang, Y., Gattoni, R., Stevenin, J., and Steitz, J. A. (2003) SR splicing factors serve as adapter proteins for TAP-dependent mRNA export. *Mol Cell* **11**, 837-843

31. Sanford, J. R., Gray, N. K., Beckmann, K., and Caceres, J. F. (2004) A novel role for shuttling SR proteins in mRNA translation. *Genes Dev* **18**, 755-768
32. Rieder, C. L., Cole, R. W., Khodjakov, A., and Sluder, G. (1995) The checkpoint delaying anaphase in response to chromosome monoorientation is mediated by an inhibitory signal produced by unattached kinetochores. *J Cell Biol* **130**, 941-948
33. Uchida, K. S., Takagaki, K., Kumada, K., Hirayama, Y., Noda, T., and Hirota, T. (2009) Kinetochores stretching inactivates the spindle assembly checkpoint. *J Cell Biol* **184**, 383-390
34. Vigneron, S., Prieto, S., Bernis, C., Labbe, J. C., Castro, A., and Lorca, T. (2004) Kinetochores localization of spindle checkpoint proteins: who controls whom? *Mol Biol Cell* **15**, 4584-4596
35. Chen, R. H., Shevchenko, A., Mann, M., and Murray, A. W. (1998) Spindle checkpoint protein Xmad1 recruits Xmad2 to unattached kinetochores. *J Cell Biol* **143**, 283-295
36. Musacchio, A., and Salmon, E. D. (2007) The spindle-assembly checkpoint in space and time. *Nat Rev Mol Cell Biol* **8**, 379-393
37. Montembault, E., Dutertre, S., Prigent, C., and Giet, R. (2007) PRP4 is a spindle assembly checkpoint protein required for MPS1, MAD1, and MAD2 localization to the kinetochores. *J Cell Biol* **179**, 601-609
38. Nisole, S., and Saib, A. (2004) Early steps of retrovirus replicative cycle. *Retrovirology* **1**, 9
39. Schwartz, S., Felber, B. K., Benko, D. M., Fenyo, E. M., and Pavlakis, G. N. (1990) Cloning and functional analysis of multiply spliced mRNA species of human immunodeficiency virus type 1. *J Virol* **64**, 2519-2529
40. Purcell, D. F., and Martin, M. A. (1993) Alternative splicing of human immunodeficiency virus type 1 mRNA modulates viral protein expression, replication, and infectivity. *J Virol* **67**, 6365-6378
41. Frankel, A. D., and Young, J. A. (1998) HIV-1: fifteen proteins and an RNA. *Annu Rev Biochem* **67**, 1-25

42. Stoltzfus, C. M., and Madsen, J. M. (2006) Role of viral splicing elements and cellular RNA binding proteins in regulation of HIV-1 alternative RNA splicing. *Curr HIV Res* **4**, 43-55
43. Askjaer, P., Jensen, T. H., Nilsson, J., Englmeier, L., and Kjems, J. (1998) The specificity of the CRM1-Rev nuclear export signal interaction is mediated by RanGTP. *J Biol Chem* **273**, 33414-33422
44. Berger, J., Aepinus, C., Dobrovnik, M., Fleckenstein, B., Hauber, J., and Bohnlein, E. (1991) Mutational analysis of functional domains in the HIV-1 Rev trans-regulatory protein. *Virology* **183**, 630-635
45. Fischer, U., Huber, J., Boelens, W. C., Mattaj, I. W., and Luhrmann, R. (1995) The HIV-1 Rev activation domain is a nuclear export signal that accesses an export pathway used by specific cellular RNAs. *Cell* **82**, 475-483
46. Kjems, J., and Sharp, P. A. (1993) The basic domain of Rev from human immunodeficiency virus type 1 specifically blocks the entry of U4/U6.U5 small nuclear ribonucleoprotein in spliceosome assembly. *J Virol* **67**, 4769-4776
47. Bennett, E. M., Lever, A. M., and Allen, J. F. (2004) Human immunodeficiency virus type 2 Gag interacts specifically with PRP4, a serine-threonine kinase, and inhibits phosphorylation of splicing factor SF2. *J Virol* **78**, 11303-11312
48. Freed, E. O. (1998) HIV-1 gag proteins: diverse functions in the virus life cycle. *Virology* **251**, 1-15
49. Shehzad, A., Park, J. W., Lee, J., and Lee, Y. S. (2013) Curcumin induces radiosensitivity of in vitro and in vivo cancer models by modulating pre-mRNA processing factor 4 (Prp4). *Chem Biol Interact* **206**, 394-402
50. Shehzad, A., Lee, J., Huh, T. L., and Lee, Y. S. (2013) Curcumin induces apoptosis in human colorectal carcinoma (HCT-15) cells by regulating expression of Prp4 and p53. *Mol Cells* **35**, 526-532
51. Nohl, H., Kozlov, A. V., Gille, L., and Staniek, K. (2003) Cell respiration and formation of reactive oxygen species: facts and artefacts. *Biochem Soc Trans* **31**, 1308-1311

52. Waris, G., and Ahsan, H. (2006) Reactive oxygen species: role in the development of cancer and various chronic conditions. *J Carcinog* **5**, 14
53. Sinha, K., Das, J., Pal, P. B., and Sil, P. C. (2013) Oxidative stress: the mitochondria-dependent and mitochondria-independent pathways of apoptosis. *Arch Toxicol* **87**, 1157-1180
54. Liou, G. Y., and Storz, P. (2010) Reactive oxygen species in cancer. *Free Radic Res* **44**, 479-496
55. Swanton, C., Marani, M., Pardo, O., Warne, P. H., Kelly, G., Sahai, E., Elustondo, F., Chang, J., Temple, J., Ahmed, A. A., Brenton, J. D., Downward, J., and Nicke, B. (2007) Regulators of mitotic arrest and ceramide metabolism are determinants of sensitivity to paclitaxel and other chemotherapeutic drugs. *Cancer Cell* **11**, 498-512
56. Duan, Z., Weinstein, E. J., Ji, D., Ames, R. Y., Choy, E., Mankin, H., and Hornicek, F. J. (2008) Lentiviral short hairpin RNA screen of genes associated with multidrug resistance identifies PRP-4 as a new regulator of chemoresistance in human ovarian cancer. *Mol Cancer Ther* **7**, 2377-2385
57. Wani, M. C., Taylor, H. L., Wall, M. E., Coggon, P., and McPhail, A. T. (1971) Plant antitumor agents. VI. The isolation and structure of taxol, a novel antileukemic and antitumor agent from *Taxus brevifolia*. *J Am Chem Soc* **93**, 2325-2327
58. Wani, M. C., and Horwitz, S. B. (2014) Nature as a remarkable chemist: a personal story of the discovery and development of Taxol. *Anticancer Drugs* **25**, 482-487
59. McGrogan, B. T., Gilmartin, B., Carney, D. N., and McCann, A. (2008) Taxanes, microtubules and chemoresistant breast cancer. *Biochim Biophys Acta* **1785**, 96-132
60. Seetalarom, K., Kudelka, A. P., Verschraegen, C. F., and Kavanagh, J. J. (1997) Taxanes in ovarian cancer treatment. *Curr Opin Obstet Gynecol* **9**, 14-20
61. Kollman, J. M., Polka, J. K., Zelter, A., Davis, T. N., and Agard, D. A. (2010) Microtubule nucleating gamma-TuSC assembles structures with 13-fold microtubule-like symmetry. *Nature* **466**, 879-882

62. Nogales, E., Whittaker, M., Milligan, R. A., and Downing, K. H. (1999) High-resolution model of the microtubule. *Cell* **96**, 79-88
63. Holy, T. E., and Leibler, S. (1994) Dynamic instability of microtubules as an efficient way to search in space. *Proc Natl Acad Sci U S A* **91**, 5682-5685
64. Snyder, J. P., Nettles, J. H., Cornett, B., Downing, K. H., and Nogales, E. (2001) The binding conformation of Taxol in beta-tubulin: a model based on electron crystallographic density. *Proc Natl Acad Sci U S A* **98**, 5312-5316
65. Gascoigne, K. E., and Taylor, S. S. (2009) How do anti-mitotic drugs kill cancer cells? *J Cell Sci* **122**, 2579-2585
66. Woods, C. M., Zhu, J., McQueney, P. A., Bollag, D., and Lazarides, E. (1995) Taxol-induced mitotic block triggers rapid onset of a p53-independent apoptotic pathway. *Mol Med* **1**, 506-526
67. Brito, D. A., and Rieder, C. L. (2006) Mitotic checkpoint slippage in humans occurs via cyclin B destruction in the presence of an active checkpoint. *Curr Biol* **16**, 1194-1200
68. Gerlach, J. H., Endicott, J. A., Juranka, P. F., Henderson, G., Sarangi, F., Deuchars, K. L., and Ling, V. (1986) Homology between P-glycoprotein and a bacterial haemolysin transport protein suggests a model for multidrug resistance. *Nature* **324**, 485-489
69. Fojo, A. T., and Menefee, M. (2005) Microtubule targeting agents: basic mechanisms of multidrug resistance (MDR). *Semin Oncol* **32**, S3-8
70. Dean, M., Rzhetsky, A., and Allikmets, R. (2001) The human ATP-binding cassette (ABC) transporter superfamily. *Genome Res* **11**, 1156-1166
71. Hamada, H., and Tsuruo, T. (1986) Functional role for the 170- to 180-kDa glycoprotein specific to drug-resistant tumor cells as revealed by monoclonal antibodies. *Proc Natl Acad Sci U S A* **83**, 7785-7789
72. Kartner, N., Shales, M., Riordan, J. R., and Ling, V. (1983) Daunorubicin-resistant Chinese hamster ovary cells expressing multidrug resistance and a cell-surface P-glycoprotein. *Cancer Res* **43**, 4413-4419

73. Mickisch, G. H., Pai, L. H., Gottesman, M. M., and Pastan, I. (1992) Monoclonal antibody MRK16 reverses the multidrug resistance of multidrug-resistant transgenic mice. *Cancer Res* **52**, 4427-4432
74. Senior, A. E., and Bhagat, S. (1998) P-glycoprotein shows strong catalytic cooperativity between the two nucleotide sites. *Biochemistry* **37**, 831-836
75. Ramachandra, M., Ambudkar, S. V., Chen, D., Hrycyna, C. A., Dey, S., Gottesman, M. M., and Pastan, I. (1998) Human P-glycoprotein exhibits reduced affinity for substrates during a catalytic transition state. *Biochemistry* **37**, 5010-5019
76. Noguchi, S. (2006) Predictive factors for response to docetaxel in human breast cancers. *Cancer Sci* **97**, 813-820
77. Trock, B. J., Leonessa, F., and Clarke, R. (1997) Multidrug resistance in breast cancer: a meta-analysis of MDR1/gp170 expression and its possible functional significance. *J Natl Cancer Inst* **89**, 917-931
78. Giannakakou, P., Sackett, D. L., Kang, Y. K., Zhan, Z., Buters, J. T., Fojo, T., and Poruchynsky, M. S. (1997) Paclitaxel-resistant human ovarian cancer cells have mutant beta-tubulins that exhibit impaired paclitaxel-driven polymerization. *J Biol Chem* **272**, 17118-17125
79. Goncalves, A., Braguer, D., Kamath, K., Martello, L., Briand, C., Horwitz, S., Wilson, L., and Jordan, M. A. (2001) Resistance to Taxol in lung cancer cells associated with increased microtubule dynamics. *Proc Natl Acad Sci U S A* **98**, 11737-11742
80. Hari, M., Loganzo, F., Annable, T., Tan, X., Musto, S., Morilla, D. B., Nettles, J. H., Snyder, J. P., and Greenberger, L. M. (2006) Paclitaxel-resistant cells have a mutation in the paclitaxel-binding region of beta-tubulin (Asp26Glu) and less stable microtubules. *Mol Cancer Ther* **5**, 270-278
81. Monzo, M., Rosell, R., Sanchez, J. J., Lee, J. S., O'Brate, A., Gonzalez-Larriba, J. L., Alberola, V., Lorenzo, J. C., Nunez, L., Ro, J. Y., and Martin, C. (1999) Paclitaxel resistance in non-small-cell lung cancer associated with beta-tubulin gene mutations. *J Clin Oncol* **17**, 1786-1793

82. Kelley, M. J., Li, S., and Harpole, D. H. (2001) Genetic analysis of the beta-tubulin gene, TUBB, in non-small-cell lung cancer. *J Natl Cancer Inst* **93**, 1886-1888
83. Kohonen-Corish, M. R., Qin, H., Daniel, J. J., Cooper, W. A., Rivory, L., McCaughan, B., Millward, M. J., and Trent, R. J. (2002) Lack of beta-tubulin gene mutations in early stage lung cancer. *Int J Cancer* **101**, 398-399
84. Sale, S., Oefner, P. J., and Sikic, B. I. (2002) Re: genetic analysis of the beta-tubulin gene, TUBB, in non-small-cell lung cancer. *J Natl Cancer Inst* **94**, 776-777; author reply 777
85. Tsurutani, J., Komiya, T., Uejima, H., Tada, H., Syunichi, N., Oka, M., Kohno, S., Fukuoka, M., and Nakagawa, K. (2002) Mutational analysis of the beta-tubulin gene in lung cancer. *Lung Cancer* **35**, 11-16
86. Sullivan, K. F. (1988) Structure and utilization of tubulin isotypes. *Annu Rev Cell Biol* **4**, 687-716
87. Derry, W. B., Wilson, L., Khan, I. A., Luduena, R. F., and Jordan, M. A. (1997) Taxol differentially modulates the dynamics of microtubules assembled from unfractionated and purified beta-tubulin isotypes. *Biochemistry* **36**, 3554-3562
88. Seve, P., and Dumontet, C. (2008) Is class III beta-tubulin a predictive factor in patients receiving tubulin-binding agents? *Lancet Oncol* **9**, 168-175
89. Narvi, E., Jaakkola, K., Winsel, S., Oetken-Lindholm, C., Halonen, P., Kallio, L., and Kallio, M. J. (2013) Altered TUBB3 expression contributes to the epothilone response of mitotic cells. *Br J Cancer* **108**, 82-90
90. Belmont, L. D., and Mitchison, T. J. (1996) Identification of a protein that interacts with tubulin dimers and increases the catastrophe rate of microtubules. *Cell* **84**, 623-631
91. Gardner, M. K., Zanic, M., and Howard, J. (2013) Microtubule catastrophe and rescue. *Curr Opin Cell Biol* **25**, 14-22

92. Alli, E., Bash-Babula, J., Yang, J. M., and Hait, W. N. (2002) Effect of stathmin on the sensitivity to antimicrotubule drugs in human breast cancer. *Cancer Res* **62**, 6864-6869
93. Holmfeldt, P., Brattsand, G., and Gullberg, M. (2002) MAP4 counteracts microtubule catastrophe promotion but not tubulin-sequestering activity in intact cells. *Curr Biol* **12**, 1034-1039
94. Zhang, C. C., Yang, J. M., White, E., Murphy, M., Levine, A., and Hait, W. N. (1998) The role of MAP4 expression in the sensitivity to paclitaxel and resistance to vinca alkaloids in p53 mutant cells. *Oncogene* **16**, 1617-1624
95. Kar, S., Fan, J., Smith, M. J., Goedert, M., and Amos, L. A. (2003) Repeat motifs of tau bind to the insides of microtubules in the absence of taxol. *EMBO J* **22**, 70-77
96. Smoter, M., Bodnar, L., Duchnowska, R., Stec, R., Grala, B., and Szczylik, C. (2011) The role of Tau protein in resistance to paclitaxel. *Cancer Chemother Pharmacol* **68**, 553-557
97. Spicakova, T., O'Brien, M. M., Duran, G. E., Sweet-Cordero, A., and Sikic, B. I. (2010) Expression and silencing of the microtubule-associated protein Tau in breast cancer cells. *Mol Cancer Ther* **9**, 2970-2981
98. Kirkin, V., Joos, S., and Zornig, M. (2004) The role of Bcl-2 family members in tumorigenesis. *Biochim Biophys Acta* **1644**, 229-249
99. Ferlini, C., Raspaglio, G., Mozzetti, S., Distefano, M., Filippetti, F., Martinelli, E., Ferrandina, G., Gallo, D., Ranelletti, F. O., and Scambia, G. (2003) Bcl-2 down-regulation is a novel mechanism of paclitaxel resistance. *Mol Pharmacol* **64**, 51-58
100. Ferlini, C., Cicchillitti, L., Raspaglio, G., Bartollino, S., Cimitan, S., Bertucci, C., Mozzetti, S., Gallo, D., Persico, M., Fattorusso, C., Campiani, G., and Scambia, G. (2009) Paclitaxel directly binds to Bcl-2 and functionally mimics activity of Nur77. *Cancer Res* **69**, 6906-6914
101. Sudo, T., Nitta, M., Saya, H., and Ueno, N. T. (2004) Dependence of paclitaxel sensitivity on a functional spindle assembly checkpoint. *Cancer Res* **64**, 2502-2508

102. Lee, E. A., Keutmann, M. K., Dowling, M. L., Harris, E., Chan, G., and Kao, G. D. (2004) Inactivation of the mitotic checkpoint as a determinant of the efficacy of microtubule-targeted drugs in killing human cancer cells. *Mol Cancer Ther* **3**, 661-669
103. Tao, W., South, V. J., Zhang, Y., Davide, J. P., Farrell, L., Kohl, N. E., Sepp-Lorenzino, L., and Lobell, R. B. (2005) Induction of apoptosis by an inhibitor of the mitotic kinesin KSP requires both activation of the spindle assembly checkpoint and mitotic slippage. *Cancer Cell* **8**, 49-59
104. Anand, S., Penrhyn-Lowe, S., and Venkitaraman, A. R. (2003) AURORA-A amplification overrides the mitotic spindle assembly checkpoint, inducing resistance to Taxol. *Cancer Cell* **3**, 51-62
105. Slamon, D. J., Clark, G. M., Wong, S. G., Levin, W. J., Ullrich, A., and McGuire, W. L. (1987) Human breast cancer: correlation of relapse and survival with amplification of the HER-2/neu oncogene. *Science* **235**, 177-182
106. Slamon, D. J., Godolphin, W., Jones, L. A., Holt, J. A., Wong, S. G., Keith, D. E., Levin, W. J., Stuart, S. G., Udove, J., Ullrich, A., and et al. (1989) Studies of the HER-2/neu proto-oncogene in human breast and ovarian cancer. *Science* **244**, 707-712
107. Lonardo, F., Di Marco, E., King, C. R., Pierce, J. H., Segatto, O., Aaronson, S. A., and Di Fiore, P. P. (1990) The normal erbB-2 product is an atypical receptor-like tyrosine kinase with constitutive activity in the absence of ligand. *New Biol* **2**, 992-1003
108. Harari, D., and Yarden, Y. (2000) Molecular mechanisms underlying ErbB2/HER2 action in breast cancer. *Oncogene* **19**, 6102-6114
109. Garrett, T. P., McKern, N. M., Lou, M., Elleman, T. C., Adams, T. E., Lovrecz, G. O., Kofler, M., Jorissen, R. N., Nice, E. C., Burgess, A. W., and Ward, C. W. (2003) The crystal structure of a truncated ErbB2 ectodomain reveals an active conformation, poised to interact with other ErbB receptors. *Mol Cell* **11**, 495-505
110. Cho, H. S., Mason, K., Ramyar, K. X., Stanley, A. M., Gabelli, S. B., Denney, D. W., Jr., and Leahy, D. J. (2003) Structure of the extracellular region of HER2 alone and in complex with the Herceptin Fab. *Nature* **421**, 756-760

111. Venter, D. J., Tuzi, N. L., Kumar, S., and Gullick, W. J. (1987) Overexpression of the c-erbB-2 oncoprotein in human breast carcinomas: immunohistological assessment correlates with gene amplification. *Lancet* **2**, 69-72
112. Kallioniemi, O. P., Kallioniemi, A., Kurisu, W., Thor, A., Chen, L. C., Smith, H. S., Waldman, F. M., Pinkel, D., and Gray, J. W. (1992) ERBB2 amplification in breast cancer analyzed by fluorescence in situ hybridization. *Proc Natl Acad Sci U S A* **89**, 5321-5325
113. Iqbal, N., and Iqbal, N. (2014) Human Epidermal Growth Factor Receptor 2 (HER2) in Cancers: Overexpression and Therapeutic Implications. *Mol Biol Int* **2014**, 852748
114. Soltoff, S. P., Carraway, K. L., 3rd, Prigent, S. A., Gullick, W. G., and Cantley, L. C. (1994) ErbB3 is involved in activation of phosphatidylinositol 3-kinase by epidermal growth factor. *Mol Cell Biol* **14**, 3550-3558
115. Datta, S. R., Dudek, H., Tao, X., Masters, S., Fu, H., Gotoh, Y., and Greenberg, M. E. (1997) Akt phosphorylation of BAD couples survival signals to the cell-intrinsic death machinery. *Cell* **91**, 231-241
116. Gottlieb, T. M., Leal, J. F., Seger, R., Taya, Y., and Oren, M. (2002) Cross-talk between Akt, p53 and Mdm2: possible implications for the regulation of apoptosis. *Oncogene* **21**, 1299-1303
117. Zhou, B. P., Liao, Y., Xia, W., Zou, Y., Spohn, B., and Hung, M. C. (2001) HER-2/neu induces p53 ubiquitination via Akt-mediated MDM2 phosphorylation. *Nat Cell Biol* **3**, 973-982
118. Mayo, L. D., and Donner, D. B. (2001) A phosphatidylinositol 3-kinase/Akt pathway promotes translocation of Mdm2 from the cytoplasm to the nucleus. *Proc Natl Acad Sci U S A* **98**, 11598-11603
119. Wiza, C., Nascimento, E. B., and Ouwens, D. M. (2012) Role of PRAS40 in Akt and mTOR signaling in health and disease. *Am J Physiol Endocrinol Metab* **302**, E1453-1460
120. Inoki, K., Li, Y., Zhu, T., Wu, J., and Guan, K. L. (2002) TSC2 is phosphorylated and inhibited by Akt and suppresses mTOR signalling. *Nat Cell Biol* **4**, 648-657

121. Vivanco, I., and Sawyers, C. L. (2002) The phosphatidylinositol 3-Kinase AKT pathway in human cancer. *Nat Rev Cancer* **2**, 489-501
122. Schulze, W. X., Deng, L., and Mann, M. (2005) Phosphotyrosine interactome of the ErbB-receptor kinase family. *Mol Syst Biol* **1**, 2005 0008
123. Margolis, B., and Skolnik, E. Y. (1994) Activation of Ras by receptor tyrosine kinases. *J Am Soc Nephrol* **5**, 1288-1299
124. McCubrey, J. A., Steelman, L. S., Chappell, W. H., Abrams, S. L., Wong, E. W., Chang, F., Lehmann, B., Terrian, D. M., Milella, M., Tafuri, A., Stivala, F., Libra, M., Basecke, J., Evangelisti, C., Martelli, A. M., and Franklin, R. A. (2007) Roles of the Raf/MEK/ERK pathway in cell growth, malignant transformation and drug resistance. *Biochim Biophys Acta* **1773**, 1263-1284
125. Kolch, W. (2000) Meaningful relationships: the regulation of the Ras/Raf/MEK/ERK pathway by protein interactions. *Biochem J* **351 Pt 2**, 289-305
126. Yu, D., Liu, B., Tan, M., Li, J., Wang, S. S., and Hung, M. C. (1996) Overexpression of c-erbB-2/neu in breast cancer cells confers increased resistance to Taxol via mdr-1-independent mechanisms. *Oncogene* **13**, 1359-1365
127. Baselga, J., Seidman, A. D., Rosen, P. P., and Norton, L. (1997) HER2 overexpression and paclitaxel sensitivity in breast cancer: therapeutic implications. *Oncology (Williston Park)* **11**, 43-48
128. Di Leo, A., Chan, S., Paesmans, M., Friedrichs, K., Pinter, T., Cocquyt, V., Murray, E., Bodrogi, I., Walpole, E., Lesperance, B., Korec, S., Crown, J., Simmonds, P., Von Minckwitz, G., Leroy, J. Y., Durbecq, V., Isola, J., Aapro, M., Piccart, M. J., and Larsimont, D. (2004) HER-2/neu as a predictive marker in a population of advanced breast cancer patients randomly treated either with single-agent doxorubicin or single-agent docetaxel. *Breast Cancer Res Treat* **86**, 197-206
129. Konecny, G. E., Thomssen, C., Luck, H. J., Untch, M., Wang, H. J., Kuhn, W., Eidtmann, H., du Bois, A., Olbricht, S., Steinfeld, D., Mobus, V., von Minckwitz, G., Dandekar, S., Ramos, L., Pauletti, G., Pegram, M. D., Janicke, F., and Slamon, D. J. (2004) Her-2/neu gene amplification and response to paclitaxel in patients with metastatic breast cancer. *J Natl Cancer Inst* **96**, 1141-1151

130. Martin, M., Pienkowski, T., Mackey, J., Pawlicki, M., Guastalla, J. P., Weaver, C., Tomiak, E., Al-Tweigeri, T., Chap, L., Juhos, E., Guevin, R., Howell, A., Fornander, T., Hainsworth, J., Coleman, R., Vinholes, J., Modiano, M., Pinter, T., Tang, S. C., Colwell, B., Prady, C., Provencher, L., Walde, D., Rodriguez-Lescure, A., Hugh, J., Loret, C., Rupin, M., Blitz, S., Jacobs, P., Murawsky, M., Riva, A., Vogel, C., and Breast Cancer International Research Group, I. (2005) Adjuvant docetaxel for node-positive breast cancer. *N Engl J Med* **352**, 2302-2313
131. Hayes, D. F., Thor, A. D., Dressler, L. G., Weaver, D., Edgerton, S., Cowan, D., Broadwater, G., Goldstein, L. J., Martino, S., Ingle, J. N., Henderson, I. C., Norton, L., Winer, E. P., Hudis, C. A., Ellis, M. J., Berry, D. A., Cancer, and Leukemia Group, B. I. (2007) HER2 and response to paclitaxel in node-positive breast cancer. *N Engl J Med* **357**, 1496-1506
132. Camerini, A., Donati, S., Viacava, P., Siclari, O., Puccetti, C., Tartarelli, G., Valsuani, C., De Luca, F., Martini, L., Cavazzana, A., and Amoroso, D. (2011) Evaluation of HER2 and p53 expression in predicting response to docetaxel-based first-line chemotherapy in advanced breast cancer. *J Exp Clin Cancer Res* **30**, 38
133. Le Page, C., Marineau, A., Bonza, P. K., Rahimi, K., Cyr, L., Labouba, I., Madore, J., Delvoye, N., Mes-Masson, A. M., Provencher, D. M., and Cailhier, J. F. (2012) BTN3A2 expression in epithelial ovarian cancer is associated with higher tumor infiltrating T cells and a better prognosis. *PLoS One* **7**, e38541
134. Svtelis, A., Bianco, S., Madore, J., Huppe, G., Nordell-Markovits, A., Mes-Masson, A. M., and Gevry, N. (2011) H3K27 demethylation by JMJD3 at a poised enhancer of anti-apoptotic gene BCL2 determines ERalpha ligand dependency. *EMBO J* **30**, 3947-3961
135. Letourneau, I. J., Quinn, M. C., Wang, L. L., Portelance, L., Caceres, K. Y., Cyr, L., Delvoye, N., Meunier, L., de Ladurantaye, M., Shen, Z., Arcand, S. L., Tonin, P. N., Provencher, D. M., and Mes-Masson, A. M. (2012) Derivation and characterization of matched cell lines from primary and recurrent serous ovarian cancer. *BMC Cancer* **12**, 379
136. Labugger, R., Organ, L., Collier, C., Atar, D., and Van Eyk, J. E. (2000) Extensive troponin I and T modification detected in serum from patients with acute myocardial infarction. *Circulation* **102**, 1221-1226

137. Bedard, K., Attar, H., Bonnefont, J., Jaquet, V., Borel, C., Plastre, O., Stasia, M. J., Antonarakis, S. E., and Krause, K. H. (2009) Three common polymorphisms in the CYBA gene form a haplotype associated with decreased ROS generation. *Hum Mutat* **30**, 1123-1133
138. Kanda, T., Sullivan, K. F., and Wahl, G. M. (1998) Histone-GFP fusion protein enables sensitive analysis of chromosome dynamics in living mammalian cells. *Curr Biol* **8**, 377-385
139. Li, Y. M., Pan, Y., Wei, Y., Cheng, X., Zhou, B. P., Tan, M., Zhou, X., Xia, W., Hortobagyi, G. N., Yu, D., and Hung, M. C. (2004) Upregulation of CXCR4 is essential for HER2-mediated tumor metastasis. *Cancer Cell* **6**, 459-469
140. Salsman, J., Pinder, J., Tse, B., Corkery, D., and Dellaire, G. (2013) The translation initiation factor 3 subunit eIF3K interacts with PML and associates with PML nuclear bodies. *Exp Cell Res* **319**, 2554-2565
141. Gao, Q., Mechin, I., Kothari, N., Guo, Z., Deng, G., Haas, K., McManus, J., Hoffmann, D., Wang, A., Wiederschain, D., Rocnik, J., Czechtizky, W., Chen, X., McLean, L., Arlt, H., Harper, D., Liu, F., Majid, T., Patel, V., Lengauer, C., Garcia-Echeverria, C., Zhang, B., Cheng, H., Dorsch, M., and Huang, S. M. (2013) Evaluation of cancer dependence and druggability of PRP4 kinase using cellular, biochemical, and structural approaches. *J Biol Chem* **288**, 30125-30138
142. Le Page, C., Ouellet, V., Quinn, M. C., Tonin, P. N., Provencher, D. M., and Mes-Masson, A. M. (2008) BTF4/BTNA3.2 and GCS as candidate mRNA prognostic markers in epithelial ovarian cancer. *Cancer Epidemiol Biomarkers Prev* **17**, 913-920
143. Nguyen, D. M., Chen, G. A., Reddy, R., Tsai, W., Schrump, W. D., Cole, G., Jr., and Schrump, D. S. (2004) Potentiation of paclitaxel cytotoxicity in lung and esophageal cancer cells by pharmacologic inhibition of the phosphoinositide 3-kinase/protein kinase B (Akt)-mediated signaling pathway. *J Thorac Cardiovasc Surg* **127**, 365-375
144. Gianni, L., Kearns, C. M., Giani, A., Capri, G., Vigano, L., Lacatelli, A., Bonadonna, G., and Egorin, M. J. (1995) Nonlinear pharmacokinetics and metabolism of paclitaxel and its pharmacokinetic/pharmacodynamic relationships in humans. *J Clin Oncol* **13**, 180-190

145. Lassus, H., Leminen, A., Vayrynen, A., Cheng, G., Gustafsson, J. A., Isola, J., and Butzow, R. (2004) ERBB2 amplification is superior to protein expression status in predicting patient outcome in serous ovarian carcinoma. *Gynecol Oncol* **92**, 31-39
146. Raspollini, M. R., Amunni, G., Villanucci, A., Castiglione, F., Rossi Degl'Innocenti, D., Baroni, G., Paglierani, M., and Taddei, G. L. (2006) HER-2/neu and bcl-2 in ovarian carcinoma: clinicopathologic, immunohistochemical, and molecular study in patients with shorter and longer survival. *Appl Immunohistochem Mol Morphol* **14**, 181-186
147. Slamon, D. J., Leyland-Jones, B., Shak, S., Fuchs, H., Paton, V., Bajamonde, A., Fleming, T., Eiermann, W., Wolter, J., Pegram, M., Baselga, J., and Norton, L. (2001) Use of chemotherapy plus a monoclonal antibody against HER2 for metastatic breast cancer that overexpresses HER2. *N Engl J Med* **344**, 783-792
148. Romond, E. H., Perez, E. A., Bryant, J., Suman, V. J., Geyer, C. E., Jr., Davidson, N. E., Tan-Chiu, E., Martino, S., Paik, S., Kaufman, P. A., Swain, S. M., Pisansky, T. M., Fehrenbacher, L., Kutteh, L. A., Vogel, V. G., Visscher, D. W., Yothers, G., Jenkins, R. B., Brown, A. M., Dakhil, S. R., Mamounas, E. P., Lingle, W. L., Klein, P. M., Ingle, J. N., and Wolmark, N. (2005) Trastuzumab plus adjuvant chemotherapy for operable HER2-positive breast cancer. *N Engl J Med* **353**, 1673-1684
149. Alba, E., Albanell, J., de la Haba, J., Barnadas, A., Calvo, L., Sanchez-Rovira, P., Ramos, M., Rojo, F., Burgues, O., Carrasco, E., Caballero, R., Porras, I., Tibau, A., Camara, M. C., and Lluch, A. (2014) Trastuzumab or lapatinib with standard chemotherapy for HER2-positive breast cancer: results from the GEICAM/2006-14 trial. *Br J Cancer* **110**, 1139-1147
150. Guarneri, V., Frassoldati, A., Bottini, A., Cagossi, K., Bisagni, G., Sarti, S., Ravaioli, A., Cavanna, L., Giardina, G., Musolino, A., Untch, M., Orlando, L., Artioli, F., Boni, C., Generali, D. G., Serra, P., Bagnalasta, M., Marini, L., Piacentini, F., D'Amico, R., and Conte, P. (2012) Preoperative chemotherapy plus trastuzumab, lapatinib, or both in human epidermal growth factor receptor 2-positive operable breast cancer: results of the randomized phase II CHER-LOB study. *J Clin Oncol* **30**, 1989-1995
151. Cahill, D. P., Lengauer, C., Yu, J., Riggins, G. J., Willson, J. K., Markowitz, S. D., Kinzler, K. W., and Vogelstein, B. (1998) Mutations of mitotic checkpoint genes in human cancers. *Nature* **392**, 300-303

152. Joensuu, H., Isola, J., Lundin, M., Salminen, T., Holli, K., Kataja, V., Pylkkanen, L., Turpeenniemi-Hujanen, T., von Smitten, K., and Lundin, J. (2003) Amplification of erbB2 and erbB2 expression are superior to estrogen receptor status as risk factors for distant recurrence in pT1N0M0 breast cancer: a nationwide population-based study. *Clin Cancer Res* **9**, 923-930
153. Berchuck, A., Kamel, A., Whitaker, R., Kerns, B., Olt, G., Kinney, R., Soper, J. T., Dodge, R., Clarke-Pearson, D. L., Marks, P., and et al. (1990) Overexpression of HER-2/neu is associated with poor survival in advanced epithelial ovarian cancer. *Cancer Res* **50**, 4087-4091
154. Hisaoka, K. K. (1958) The effects of 2-acetylaminofluorene on the embryonic development of the zebrafish. II. Histochemical studies. *Cancer Res* **18**, 664-667
155. Streisinger, G., Walker, C., Dower, N., Knauber, D., and Singer, F. (1981) Production of clones of homozygous diploid zebra fish (*Brachydanio rerio*). *Nature* **291**, 293-296

156. Howe, K., Clark, M. D., Torroja, C. F., Tarrance, J., Berthelot, C., Muffato, M., Collins, J. E., Humphray, S., McLaren, K., Matthews, L., McLaren, S., Sealy, I., Caccamo, M., Churcher, C., Scott, C., Barrett, J. C., Koch, R., Rauch, G. J., White, S., Chow, W., Kilian, B., Quintais, L. T., Guerra-Assuncao, J. A., Zhou, Y., Gu, Y., Yen, J., Vogel, J. H., Eyre, T., Redmond, S., Banerjee, R., Chi, J., Fu, B., Langley, E., Maguire, S. F., Laird, G. K., Lloyd, D., Kenyon, E., Donaldson, S., Sehra, H., Almeida-King, J., Loveland, J., Trevanion, S., Jones, M., Quail, M., Willey, D., Hunt, A., Burton, J., Sims, S., McLay, K., Plumb, B., Davis, J., Clee, C., Oliver, K., Clark, R., Riddle, C., Elliot, D., Threadgold, G., Harden, G., Ware, D., Begum, S., Mortimore, B., Kerry, G., Heath, P., Phillimore, B., Tracey, A., Corby, N., Dunn, M., Johnson, C., Wood, J., Clark, S., Pelan, S., Griffiths, G., Smith, M., Glithero, R., Howden, P., Barker, N., Lloyd, C., Stevens, C., Harley, J., Holt, K., Panagiotidis, G., Lovell, J., Beasley, H., Henderson, C., Gordon, D., Auger, K., Wright, D., Collins, J., Raisen, C., Dyer, L., Leung, K., Robertson, L., Ambridge, K., Leongamornlert, D., McGuire, S., Gilderthorp, R., Griffiths, C., Manthradi, D., Nichol, S., Barker, G., Whitehead, S., Kay, M., Brown, J., Murnane, C., Gray, E., Humphries, M., Sycamore, N., Barker, D., Saunders, D., Wallis, J., Babbage, A., Hammond, S., Mashreghi-Mohammadi, M., Barr, L., Martin, S., Wray, P., Ellington, A., Matthews, N., Ellwood, M., Woodmansey, R., Clark, G., Cooper, J., Tromans, A., Grafham, D., Skuce, C., Pandian, R., Andrews, R., Harrison, E., Kimberley, A., Garnett, J., Fosker, N., Hall, R., Garner, P., Kelly, D., Bird, C., Palmer, S., Gehring, I., Berger, A., Dooley, C. M., Ersan-Urun, Z., Eser, C., Geiger, H., Geisler, M., Karotki, L., Kim, A., Konantz, J., Konantz, M., Oberlander, M., Rudolph-Geiger, S., Teucke, M., Lanz, C., Raddatz, G., Osoegawa, K., Zhu, B., Rapp, A., Widaa, S., Langford, C., Yang, F., Schuster, S. C., Carter, N. P., Harrow, J., Ning, Z., Herrero, J., Searle, S. M., Enright, A., Geisler, R., Plasterk, R. H., Lee, C., Westerfield, M., de Jong, P. J., Zon, L. I., Postlethwait, J. H., Nusslein-Volhard, C., Hubbard, T. J., Roest Crollius, H., Rogers, J., and Stemple, D. L. (2013) The zebrafish reference genome sequence and its relationship to the human genome. *Nature* **496**, 498-503
157. Pliss, G. B., Zabezhinski, M. A., Petrov, A. S., and Khudoley, V. V. (1982) Peculiarities of N-nitramines carcinogenic action. *Arch Geschwulstforsch* **52**, 629-634
158. Amatruda, J. F., Shepard, J. L., Stern, H. M., and Zon, L. I. (2002) Zebrafish as a cancer model system. *Cancer Cell* **1**, 229-231
159. Lam, S. H., and Gong, Z. (2006) Modeling liver cancer using zebrafish: a comparative oncogenomics approach. *Cell Cycle* **5**, 573-577
160. Patton, E. E., and Zon, L. I. (2001) The art and design of genetic screens: zebrafish. *Nat Rev Genet* **2**, 956-966

161. Driever, W., Solnica-Krezel, L., Schier, A. F., Neuhauss, S. C., Malicki, J., Stemple, D. L., Stainier, D. Y., Zwartkruis, F., Abdelilah, S., Rangini, Z., Belak, J., and Boggs, C. (1996) A genetic screen for mutations affecting embryogenesis in zebrafish. *Development* **123**, 37-46
162. Haffter, P., Granato, M., Brand, M., Mullins, M. C., Hammerschmidt, M., Kane, D. A., Odenthal, J., van Eeden, F. J., Jiang, Y. J., Heisenberg, C. P., Kelsh, R. N., Furutani-Seiki, M., Vogelsang, E., Beuchle, D., Schach, U., Fabian, C., and Nusslein-Volhard, C. (1996) The identification of genes with unique and essential functions in the development of the zebrafish, *Danio rerio*. *Development* **123**, 1-36
163. Frazer, J. K., Meeker, N. D., Rudner, L., Bradley, D. F., Smith, A. C., Demarest, B., Joshi, D., Locke, E. E., Hutchinson, S. A., Tripp, S., Perkins, S. L., and Trede, N. S. (2009) Heritable T-cell malignancy models established in a zebrafish phenotypic screen. *Leukemia* **23**, 1825-1835
164. Shepard, J. L., Amatruda, J. F., Stern, H. M., Subramanian, A., Finkelstein, D., Ziai, J., Finley, K. R., Pfaff, K. L., Hersey, C., Zhou, Y., Barut, B., Freedman, M., Lee, C., Spitsbergen, J., Neuberg, D., Weber, G., Golub, T. R., Glickman, J. N., Kutok, J. L., Aster, J. C., and Zon, L. I. (2005) A zebrafish *bmyb* mutation causes genome instability and increased cancer susceptibility. *Proc Natl Acad Sci U S A* **102**, 13194-13199
165. Amsterdam, A., Burgess, S., Golling, G., Chen, W., Sun, Z., Townsend, K., Farrington, S., Haldi, M., and Hopkins, N. (1999) A large-scale insertional mutagenesis screen in zebrafish. *Genes Dev* **13**, 2713-2724
166. Amsterdam, A., Sadler, K. C., Lai, K., Farrington, S., Bronson, R. T., Lees, J. A., and Hopkins, N. (2004) Many ribosomal protein genes are cancer genes in zebrafish. *PLoS Biol* **2**, E139
167. Berghmans, S., Murphey, R. D., Wienholds, E., Neuberg, D., Kutok, J. L., Fletcher, C. D., Morris, J. P., Liu, T. X., Schulte-Merker, S., Kanki, J. P., Plasterk, R., Zon, L. I., and Look, A. T. (2005) *tp53* mutant zebrafish develop malignant peripheral nerve sheath tumors. *Proc Natl Acad Sci U S A* **102**, 407-412
168. Stern, H. M., Murphey, R. D., Shepard, J. L., Amatruda, J. F., Straub, C. T., Pfaff, K. L., Weber, G., Tallarico, J. A., King, R. W., and Zon, L. I. (2005) Small molecules that delay S phase suppress a zebrafish *bmyb* mutant. *Nat Chem Biol* **1**, 366-370

169. Langenau, D. M., Traver, D., Ferrando, A. A., Kutok, J. L., Aster, J. C., Kanki, J. P., Lin, S., Prochownik, E., Trede, N. S., Zon, L. I., and Look, A. T. (2003) Myc-induced T cell leukemia in transgenic zebrafish. *Science* **299**, 887-890
170. Langenau, D. M., Feng, H., Berghmans, S., Kanki, J. P., Kutok, J. L., and Look, A. T. (2005) Cre/lox-regulated transgenic zebrafish model with conditional myc-induced T cell acute lymphoblastic leukemia. *Proc Natl Acad Sci U S A* **102**, 6068-6073
171. Feng, H., Langenau, D. M., Madge, J. A., Quinkertz, A., Gutierrez, A., Neuberg, D. S., Kanki, J. P., and Look, A. T. (2007) Heat-shock induction of T-cell lymphoma/leukaemia in conditional Cre/lox-regulated transgenic zebrafish. *Br J Haematol* **138**, 169-175
172. Sabaawy, H. E., Azuma, M., Embree, L. J., Tsai, H. J., Starost, M. F., and Hickstein, D. D. (2006) TEL-AML1 transgenic zebrafish model of precursor B cell acute lymphoblastic leukemia. *Proc Natl Acad Sci U S A* **103**, 15166-15171
173. Yang, H. W., Kutok, J. L., Lee, N. H., Piao, H. Y., Fletcher, C. D., Kanki, J. P., and Look, A. T. (2004) Targeted expression of human MYCN selectively causes pancreatic neuroendocrine tumors in transgenic zebrafish. *Cancer Res* **64**, 7256-7262
174. Patton, E. E., Widlund, H. R., Kutok, J. L., Kopani, K. R., Amatruda, J. F., Murphey, R. D., Berghmans, S., Mayhall, E. A., Traver, D., Fletcher, C. D., Aster, J. C., Granter, S. R., Look, A. T., Lee, C., Fisher, D. E., and Zon, L. I. (2005) BRAF mutations are sufficient to promote nevi formation and cooperate with p53 in the genesis of melanoma. *Curr Biol* **15**, 249-254
175. Langenau, D. M., Keefe, M. D., Storer, N. Y., Guyon, J. R., Kutok, J. L., Le, X., Goessling, W., Neuberg, D. S., Kunkel, L. M., and Zon, L. I. (2007) Effects of RAS on the genesis of embryonal rhabdomyosarcoma. *Genes Dev* **21**, 1382-1395
176. Lee, L. M., Seftor, E. A., Bonde, G., Cornell, R. A., and Hendrix, M. J. (2005) The fate of human malignant melanoma cells transplanted into zebrafish embryos: assessment of migration and cell division in the absence of tumor formation. *Dev Dyn* **233**, 1560-1570

177. Topczewska, J. M., Postovit, L. M., Margaryan, N. V., Sam, A., Hess, A. R., Wheaton, W. W., Nickoloff, B. J., Topczewski, J., and Hendrix, M. J. (2006) Embryonic and tumorigenic pathways converge via Nodal signaling: role in melanoma aggressiveness. *Nat Med* **12**, 925-932
178. Haldi, M., Ton, C., Seng, W. L., and McGrath, P. (2006) Human melanoma cells transplanted into zebrafish proliferate, migrate, produce melanin, form masses and stimulate angiogenesis in zebrafish. *Angiogenesis* **9**, 139-151
179. Lam, S. H., Chua, H. L., Gong, Z., Lam, T. J., and Sin, Y. M. (2004) Development and maturation of the immune system in zebrafish, *Danio rerio*: a gene expression profiling, in situ hybridization and immunological study. *Dev Comp Immunol* **28**, 9-28
180. Nicoli, S., Ribatti, D., Cotelli, F., and Presta, M. (2007) Mammalian tumor xenografts induce neovascularization in zebrafish embryos. *Cancer Res* **67**, 2927-2931
181. Liao, F., Li, Y., O'Connor, W., Zanetta, L., Bassi, R., Santiago, A., Overholser, J., Hooper, A., Mignatti, P., Dejana, E., Hicklin, D. J., and Bohlen, P. (2000) Monoclonal antibody to vascular endothelial-cadherin is a potent inhibitor of angiogenesis, tumor growth, and metastasis. *Cancer Res* **60**, 6805-6810
182. Kellokumpu-Lehtinen, P., Talpaz, M., Harris, D., Van, Q., Kurzrock, R., and Estrov, Z. (1996) Leukemia-inhibitory factor stimulates breast, kidney and prostate cancer cell proliferation by paracrine and autocrine pathways. *Int J Cancer* **66**, 515-519
183. Queen, M. M., Ryan, R. E., Holzer, R. G., Keller-Peck, C. R., and Jorcyk, C. L. (2005) Breast cancer cells stimulate neutrophils to produce oncostatin M: potential implications for tumor progression. *Cancer Res* **65**, 8896-8904
184. Guo, Y., Xu, F., Lu, T., Duan, Z., and Zhang, Z. (2012) Interleukin-6 signaling pathway in targeted therapy for cancer. *Cancer Treat Rev* **38**, 904-910
185. Welsh, P. L., and King, M. C. (2001) BRCA1 and BRCA2 and the genetics of breast and ovarian cancer. *Hum Mol Genet* **10**, 705-713

186. Meyer, A., and Schartl, M. (1999) Gene and genome duplications in vertebrates: the one-to-four (-to-eight in fish) rule and the evolution of novel gene functions. *Curr Opin Cell Biol* **11**, 699-704
187. Faucherre, A., Taylor, G. S., Overvoorde, J., Dixon, J. E., and Hertog, J. (2008) Zebrafish pten genes have overlapping and non-redundant functions in tumorigenesis and embryonic development. *Oncogene* **27**, 1079-1086
188. DeNardo, D. G., and Coussens, L. M. (2007) Inflammation and breast cancer. Balancing immune response: crosstalk between adaptive and innate immune cells during breast cancer progression. *Breast Cancer Res* **9**, 212
189. Lakshmi Narendra, B., Eshvendar Reddy, K., Shantikumar, S., and Ramakrishna, S. (2013) Immune system: a double-edged sword in cancer. *Inflamm Res* **62**, 823-834
190. Witz, I. P. (2008) Tumor-microenvironment interactions: dangerous liaisons. *Adv Cancer Res* **100**, 203-229
191. White, R. M., Sessa, A., Burke, C., Bowman, T., LeBlanc, J., Ceol, C., Bourque, C., Dovey, M., Goessling, W., Burns, C. E., and Zon, L. I. (2008) Transparent adult zebrafish as a tool for in vivo transplantation analysis. *Cell Stem Cell* **2**, 183-189
192. Westerfield, M. (1995) *The Zebrafish Book. A Guide for the Laboratory Use of Zebrafish (Danio rerio)* University of Oregon Press, Eugene, OR
193. Rowley, J. D. (1973) Letter: A new consistent chromosomal abnormality in chronic myelogenous leukaemia identified by quinacrine fluorescence and Giemsa staining. *Nature* **243**, 290-293
194. Druker, B. J., Guilhot, F., O'Brien, S. G., Gathmann, I., Kantarjian, H., Gattermann, N., Deininger, M. W., Silver, R. T., Goldman, J. M., Stone, R. M., Cervantes, F., Hochhaus, A., Powell, B. L., Gabrilove, J. L., Rousselot, P., Reiffers, J., Cornelissen, J. J., Hughes, T., Agis, H., Fischer, T., Verhoef, G., Shepherd, J., Saglio, G., Gratwohl, A., Nielsen, J. L., Radich, J. P., Simonsson, B., Taylor, K., Baccarani, M., So, C., Letvak, L., Larson, R. A., and Investigators, I. (2006) Five-year follow-up of patients receiving imatinib for chronic myeloid leukemia. *N Engl J Med* **355**, 2408-2417

195. de The, H., and Chen, Z. (2010) Acute promyelocytic leukaemia: novel insights into the mechanisms of cure. *Nat Rev Cancer* **10**, 775-783
196. De Botton, S., Dombret, H., Sanz, M., Miguel, J. S., Caillot, D., Zittoun, R., Gardembas, M., Stamatoulas, A., Conde, E., Guerci, A., Gardin, C., Geiser, K., Makhoul, D. C., Reman, O., de la Serna, J., Lefrere, F., Chomienne, C., Chastang, C., Degos, L., and Fenaux, P. (1998) Incidence, clinical features, and outcome of all trans-retinoic acid syndrome in 413 cases of newly diagnosed acute promyelocytic leukemia. The European APL Group. *Blood* **92**, 2712-2718
197. Fenaux, P., Chevret, S., Guerci, A., Fegueux, N., Dombret, H., Thomas, X., Sanz, M., Link, H., Maloisel, F., Gardin, C., Bordessoule, D., Stoppa, A. M., Sadoun, A., Muus, P., Wandt, H., Mineur, P., Whittaker, J. A., Fey, M., Daniel, M. T., Castaigne, S., and Degos, L. (2000) Long-term follow-up confirms the benefit of all-trans retinoic acid in acute promyelocytic leukemia. European APL group. *Leukemia* **14**, 1371-1377
198. Pruvot, B., Jacquet, A., Droin, N., Auberger, P., Bouscary, D., Tamburini, J., Muller, M., Fontenay, M., Chluba, J., and Solary, E. (2011) Leukemic cell xenograft in zebrafish embryo for investigating drug efficacy. *Haematologica* **96**, 612-616
199. Smithen, D. A., Forrester, A. M., Corkery, D. P., Dellaire, G., Colpitts, J., McFarland, S. A., Berman, J. N., and Thompson, A. (2013) Investigations regarding the utility of prodigiosenes to treat leukemia. *Org Biomol Chem* **11**, 62-68
200. Bentley, V. L., Veinotte, C. J., Corkery, D. P., Pinder, J. B., LeBlanc, M. A., Bedard, K., Weng, A. P., Berman, J. N., and Dellaire, G. (2015) Focused chemical genomics using zebrafish xenotransplantation as a pre-clinical therapeutic platform for T-cell acute lymphoblastic leukemia. *Haematologica* **100**, 70-76
201. Tang, Q., Abdelfattah, N. S., Blackburn, J. S., Moore, J. C., Martinez, S. A., Moore, F. E., Lobbardi, R., Tenente, I. M., Ignatius, M. S., Berman, J. N., Liwski, R. S., Houvras, Y., and Langenau, D. M. (2014) Optimized cell transplantation using adult rag2 mutant zebrafish. *Nat Methods* **11**, 821-824
202. Shannon, A. M., Bouchier-Hayes, D. J., Condrón, C. M., and Toomey, D. (2003) Tumour hypoxia, chemotherapeutic resistance and hypoxia-related therapies. *Cancer Treat Rev* **29**, 297-307

203. Frisch, S. M., and Francis, H. (1994) Disruption of epithelial cell-matrix interactions induces apoptosis. *J Cell Biol* **124**, 619-626
204. Frisch, S. M., and Ruoslahti, E. (1997) Integrins and anoikis. *Curr Opin Cell Biol* **9**, 701-706
205. Giancotti, F. G. (2000) Complexity and specificity of integrin signalling. *Nat Cell Biol* **2**, E13-14
206. Meredith, J. E., Jr., Fazeli, B., and Schwartz, M. A. (1993) The extracellular matrix as a cell survival factor. *Mol Biol Cell* **4**, 953-961
207. Naldini, L., Weidner, K. M., Vigna, E., Gaudino, G., Bardelli, A., Ponzetto, C., Narsimhan, R. P., Hartmann, G., Zarnegar, R., Michalopoulos, G. K., and et al. (1991) Scatter factor and hepatocyte growth factor are indistinguishable ligands for the MET receptor. *EMBO J* **10**, 2867-2878
208. Wei, M. C., Zong, W. X., Cheng, E. H., Lindsten, T., Panoutsakopoulou, V., Ross, A. J., Roth, K. A., MacGregor, G. R., Thompson, C. B., and Korsmeyer, S. J. (2001) Proapoptotic BAX and BAK: a requisite gateway to mitochondrial dysfunction and death. *Science* **292**, 727-730
209. Pop, C., Timmer, J., Sperandio, S., and Salvesen, G. S. (2006) The apoptosome activates caspase-9 by dimerization. *Mol Cell* **22**, 269-275
210. Zou, H., Henzel, W. J., Liu, X., Lutschg, A., and Wang, X. (1997) Apaf-1, a human protein homologous to *C. elegans* CED-4, participates in cytochrome c-dependent activation of caspase-3. *Cell* **90**, 405-413
211. Reginato, M. J., Mills, K. R., Paulus, J. K., Lynch, D. K., Sgroi, D. C., Debnath, J., Muthuswamy, S. K., and Brugge, J. S. (2003) Integrins and EGFR coordinately regulate the pro-apoptotic protein Bim to prevent anoikis. *Nat Cell Biol* **5**, 733-740
212. Puthalakath, H., Huang, D. C., O'Reilly, L. A., King, S. M., and Strasser, A. (1999) The proapoptotic activity of the Bcl-2 family member Bim is regulated by interaction with the dynein motor complex. *Mol Cell* **3**, 287-296

213. Merino, D., Giam, M., Hughes, P. D., Siggs, O. M., Heger, K., O'Reilly, L. A., Adams, J. M., Strasser, A., Lee, E. F., Fairlie, W. D., and Bouillet, P. (2009) The role of BH3-only protein Bim extends beyond inhibiting Bcl-2-like prosurvival proteins. *J Cell Biol* **186**, 355-362
214. Gavathiotis, E., Suzuki, M., Davis, M. L., Pitter, K., Bird, G. H., Katz, S. G., Tu, H. C., Kim, H., Cheng, E. H., Tjandra, N., and Walensky, L. D. (2008) BAX activation is initiated at a novel interaction site. *Nature* **455**, 1076-1081
215. Czabotar, P. E., Colman, P. M., and Huang, D. C. (2009) Bax activation by Bim? *Cell Death Differ* **16**, 1187-1191
216. Chen, L., Willis, S. N., Wei, A., Smith, B. J., Fletcher, J. I., Hinds, M. G., Colman, P. M., Day, C. L., Adams, J. M., and Huang, D. C. (2005) Differential targeting of prosurvival Bcl-2 proteins by their BH3-only ligands allows complementary apoptotic function. *Mol Cell* **17**, 393-403
217. Willis, S. N., Chen, L., Dewson, G., Wei, A., Naik, E., Fletcher, J. I., Adams, J. M., and Huang, D. C. (2005) Proapoptotic Bak is sequestered by Mcl-1 and Bcl-xL, but not Bcl-2, until displaced by BH3-only proteins. *Genes Dev* **19**, 1294-1305
218. Martin, D. A., Siegel, R. M., Zheng, L., and Lenardo, M. J. (1998) Membrane oligomerization and cleavage activates the caspase-8 (FLICE/MACHalpha1) death signal. *J Biol Chem* **273**, 4345-4349
219. Yang, X., Chang, H. Y., and Baltimore, D. (1998) Autoproteolytic activation of pro-caspases by oligomerization. *Mol Cell* **1**, 319-325
220. Marconi, A., Atzei, P., Panza, C., Fila, C., Tiberio, R., Truzzi, F., Wachter, T., Leverkus, M., and Pincelli, C. (2004) FLICE/caspase-8 activation triggers anoikis induced by beta1-integrin blockade in human keratinocytes. *J Cell Sci* **117**, 5815-5823
221. Aoudjit, F., and Vuori, K. (2001) Matrix attachment regulates Fas-induced apoptosis in endothelial cells: a role for c-flip and implications for anoikis. *J Cell Biol* **152**, 633-643

222. Stupack, D. G., Puente, X. S., Boutsaboualoy, S., Storgard, C. M., and Cheresch, D. A. (2001) Apoptosis of adherent cells by recruitment of caspase-8 to unligated integrins. *J Cell Biol* **155**, 459-470
223. Gabarra-Niecko, V., Schaller, M. D., and Dunty, J. M. (2003) FAK regulates biological processes important for the pathogenesis of cancer. *Cancer Metastasis Rev* **22**, 359-374
224. Cooper, L. A., Shen, T. L., and Guan, J. L. (2003) Regulation of focal adhesion kinase by its amino-terminal domain through an autoinhibitory interaction. *Mol Cell Biol* **23**, 8030-8041
225. Lietha, D., Cai, X., Ceccarelli, D. F., Li, Y., Schaller, M. D., and Eck, M. J. (2007) Structural basis for the autoinhibition of focal adhesion kinase. *Cell* **129**, 1177-1187
226. Chen, H. C., and Guan, J. L. (1994) Association of focal adhesion kinase with its potential substrate phosphatidylinositol 3-kinase. *Proc Natl Acad Sci U S A* **91**, 10148-10152
227. Xing, Z., Chen, H. C., Nowlen, J. K., Taylor, S. J., Shalloway, D., and Guan, J. L. (1994) Direct interaction of v-Src with the focal adhesion kinase mediated by the Src SH2 domain. *Mol Biol Cell* **5**, 413-421
228. Schlaepfer, D. D., Hanks, S. K., Hunter, T., and van der Geer, P. (1994) Integrin-mediated signal transduction linked to Ras pathway by GRB2 binding to focal adhesion kinase. *Nature* **372**, 786-791
229. Zarich, N., Oliva, J. L., Martinez, N., Jorge, R., Ballester, A., Gutierrez-Eisman, S., Garcia-Vargas, S., and Rojas, J. M. (2006) Grb2 is a negative modulator of the intrinsic Ras-GEF activity of hSos1. *Mol Biol Cell* **17**, 3591-3597
230. Taddei, M. L., Giannoni, E., Fiaschi, T., and Chiarugi, P. (2012) Anoikis: an emerging hallmark in health and diseases. *J Pathol* **226**, 380-393
231. Valastyan, S., and Weinberg, R. A. (2011) Tumor metastasis: molecular insights and evolving paradigms. *Cell* **147**, 275-292

232. Kalluri, R., and Weinberg, R. A. (2009) The basics of epithelial-mesenchymal transition. *J Clin Invest* **119**, 1420-1428
233. Yang, J., Mani, S. A., Donaher, J. L., Ramaswamy, S., Itzykson, R. A., Come, C., Savagner, P., Gitelman, I., Richardson, A., and Weinberg, R. A. (2004) Twist, a master regulator of morphogenesis, plays an essential role in tumor metastasis. *Cell* **117**, 927-939
234. Cano, A., Perez-Moreno, M. A., Rodrigo, I., Locascio, A., Blanco, M. J., del Barrio, M. G., Portillo, F., and Nieto, M. A. (2000) The transcription factor snail controls epithelial-mesenchymal transitions by repressing E-cadherin expression. *Nat Cell Biol* **2**, 76-83
235. Kwok, W. K., Ling, M. T., Lee, T. W., Lau, T. C., Zhou, C., Zhang, X., Chua, C. W., Chan, K. W., Chan, F. L., Glackin, C., Wong, Y. C., and Wang, X. (2005) Up-regulation of TWIST in prostate cancer and its implication as a therapeutic target. *Cancer Res* **65**, 5153-5162
236. Kajita, M., McClinic, K. N., and Wade, P. A. (2004) Aberrant expression of the transcription factors snail and slug alters the response to genotoxic stress. *Mol Cell Biol* **24**, 7559-7566
237. Escriva, M., Peiro, S., Herranz, N., Villagrasa, P., Dave, N., Montserrat-Sentis, B., Murray, S. A., Franci, C., Gridley, T., Virtanen, I., and Garcia de Herreros, A. (2008) Repression of PTEN phosphatase by Snail1 transcriptional factor during gamma radiation-induced apoptosis. *Mol Cell Biol* **28**, 1528-1540
238. Huber, M. A., Azoitei, N., Baumann, B., Grunert, S., Sommer, A., Pehamberger, H., Kraut, N., Beug, H., and Wirth, T. (2004) NF-kappaB is essential for epithelial-mesenchymal transition and metastasis in a model of breast cancer progression. *J Clin Invest* **114**, 569-581
239. Li, C. W., Xia, W., Huo, L., Lim, S. O., Wu, Y., Hsu, J. L., Chao, C. H., Yamaguchi, H., Yang, N. K., Ding, Q., Wang, Y., Lai, Y. J., LaBaff, A. M., Wu, T. J., Lin, B. R., Yang, M. H., Hortobagyi, G. N., and Hung, M. C. (2012) Epithelial-mesenchymal transition induced by TNF-alpha requires NF-kappaB-mediated transcriptional upregulation of Twist1. *Cancer Res* **72**, 1290-1300
240. Wu, Y., Deng, J., Rychahou, P. G., Qiu, S., Evers, B. M., and Zhou, B. P. (2009) Stabilization of snail by NF-kappaB is required for inflammation-induced cell migration and invasion. *Cancer Cell* **15**, 416-428

241. Nakshatri, H., Bhat-Nakshatri, P., Martin, D. A., Goulet, R. J., Jr., and Sledge, G. W., Jr. (1997) Constitutive activation of NF-kappaB during progression of breast cancer to hormone-independent growth. *Mol Cell Biol* **17**, 3629-3639
242. Bueso-Ramos, C. E., Rocha, F. C., Shishodia, S., Medeiros, L. J., Kantarjian, H. M., Vadhan-Raj, S., Estrov, Z., Smith, T. L., Nguyen, M. H., and Aggarwal, B. B. (2004) Expression of constitutively active nuclear-kappa B RelA transcription factor in blasts of acute myeloid leukemia. *Hum Pathol* **35**, 246-253
243. Thornburg, N. J., Pathmanathan, R., and Raab-Traub, N. (2003) Activation of nuclear factor-kappaB p50 homodimer/Bcl-3 complexes in nasopharyngeal carcinoma. *Cancer Res* **63**, 8293-8301
244. Toruner, M., Fernandez-Zapico, M., Sha, J. J., Pham, L., Urrutia, R., and Egan, L. J. (2006) Antianoikis effect of nuclear factor-kappaB through up-regulated expression of osteoprotegerin, BCL-2, and IAP-1. *J Biol Chem* **281**, 8686-8696
245. Hynes, R. O. (2002) Integrins: bidirectional, allosteric signaling machines. *Cell* **110**, 673-687
246. Barczyk, M., Carracedo, S., and Gullberg, D. (2010) Integrins. *Cell Tissue Res* **339**, 269-280
247. Plantefaber, L. C., and Hynes, R. O. (1989) Changes in integrin receptors on oncogenically transformed cells. *Cell* **56**, 281-290
248. Janes, S. M., and Watt, F. M. (2004) Switch from alphavbeta5 to alphavbeta6 integrin expression protects squamous cell carcinomas from anoikis. *J Cell Biol* **166**, 419-431
249. Desgrosellier, J. S., Barnes, L. A., Shields, D. J., Huang, M., Lau, S. K., Prevost, N., Tarin, D., Shattil, S. J., and Cheresch, D. A. (2009) An integrin alpha(v)beta(3)-c-Src oncogenic unit promotes anchorage-independence and tumor progression. *Nat Med* **15**, 1163-1169
250. Brabek, J., Constancio, S. S., Siesser, P. F., Shin, N. Y., Pozzi, A., and Hanks, S. K. (2005) Crk-associated substrate tyrosine phosphorylation sites are critical for invasion and metastasis of SRC-transformed cells. *Mol Cancer Res* **3**, 307-315

251. Cho, S. Y., and Klemke, R. L. (2000) Extracellular-regulated kinase activation and CAS/Crk coupling regulate cell migration and suppress apoptosis during invasion of the extracellular matrix. *J Cell Biol* **149**, 223-236
252. Albelda, S. M., Mette, S. A., Elder, D. E., Stewart, R., Damjanovich, L., Herlyn, M., and Buck, C. A. (1990) Integrin distribution in malignant melanoma: association of the beta 3 subunit with tumor progression. *Cancer Res* **50**, 6757-6764
253. McCabe, N. P., De, S., VasANJI, A., Brainard, J., and Byzova, T. V. (2007) Prostate cancer specific integrin alphavbeta3 modulates bone metastatic growth and tissue remodeling. *Oncogene* **26**, 6238-6243
254. Gruber, G., Hess, J., Stiefel, C., Aebersold, D. M., Zimmer, Y., Greiner, R. H., Studer, U., Altermatt, H. J., Hlushchuk, R., and Djonov, V. (2005) Correlation between the tumoral expression of beta3-integrin and outcome in cervical cancer patients who had undergone radiotherapy. *Br J Cancer* **92**, 41-46
255. Burnier, J. V., Wang, N., Michel, R. P., Hassanain, M., Li, S., Lu, Y., Metrakos, P., Anteck, E., Burnier, M. N., Ponton, A., Gallinger, S., and Brodt, P. (2011) Type IV collagen-initiated signals provide survival and growth cues required for liver metastasis. *Oncogene* **30**, 3766-3783
256. Brown, C. W., Brodsky, A. S., and Freiman, R. N. (2015) Notch3 overexpression promotes anoikis resistance in epithelial ovarian cancer via upregulation of COL4A2. *Mol Cancer Res* **13**, 78-85
257. del Pozo, M. A., Alderson, N. B., Kiosses, W. B., Chiang, H. H., Anderson, R. G., and Schwartz, M. A. (2004) Integrins regulate Rac targeting by internalization of membrane domains. *Science* **303**, 839-842
258. Del Pozo, M. A., and Schwartz, M. A. (2007) Rac, membrane heterogeneity, caveolin and regulation of growth by integrins. *Trends Cell Biol* **17**, 246-250
259. del Pozo, M. A., Balasubramanian, N., Alderson, N. B., Kiosses, W. B., Grande-Garcia, A., Anderson, R. G., and Schwartz, M. A. (2005) Phospho-caveolin-1 mediates integrin-regulated membrane domain internalization. *Nat Cell Biol* **7**, 901-908

260. Koleske, A. J., Baltimore, D., and Lisanti, M. P. (1995) Reduction of caveolin and caveolae in oncogenically transformed cells. *Proc Natl Acad Sci U S A* **92**, 1381-1385
261. Galbiati, F., Volonte, D., Engelman, J. A., Watanabe, G., Burk, R., Pestell, R. G., and Lisanti, M. P. (1998) Targeted downregulation of caveolin-1 is sufficient to drive cell transformation and hyperactivate the p42/44 MAP kinase cascade. *EMBO J* **17**, 6633-6648
262. Nijhawan, D., Fang, M., Traer, E., Zhong, Q., Gao, W., Du, F., and Wang, X. (2003) Elimination of Mcl-1 is required for the initiation of apoptosis following ultraviolet irradiation. *Genes Dev* **17**, 1475-1486
263. Woods, N. T., Yamaguchi, H., Lee, F. Y., Bhalla, K. N., and Wang, H. G. (2007) Anoikis, initiated by Mcl-1 degradation and Bim induction, is deregulated during oncogenesis. *Cancer Res* **67**, 10744-10752
264. Chunchacha, P., Pongrakhananon, V., Rojanasakul, Y., and Chanvorachote, P. (2012) Caveolin-1 regulates Mcl-1 stability and anoikis in lung carcinoma cells. *Am J Physiol Cell Physiol* **302**, C1284-1292
265. Hayer, A., Stoeber, M., Ritz, D., Engel, S., Meyer, H. H., and Helenius, A. (2010) Caveolin-1 is ubiquitinated and targeted to intraluminal vesicles in endolysosomes for degradation. *J Cell Biol* **191**, 615-629
266. Rungtabnapa, P., Nimmannit, U., Halim, H., Rojanasakul, Y., and Chanvorachote, P. (2011) Hydrogen peroxide inhibits non-small cell lung cancer cell anoikis through the inhibition of caveolin-1 degradation. *Am J Physiol Cell Physiol* **300**, C235-245
267. Chanvorachote, P., Nimmannit, U., Lu, Y., Talbott, S., Jiang, B. H., and Rojanasakul, Y. (2009) Nitric oxide regulates lung carcinoma cell anoikis through inhibition of ubiquitin-proteasomal degradation of caveolin-1. *J Biol Chem* **284**, 28476-28484
268. Mizushima, N. (2007) Autophagy: process and function. *Genes Dev* **21**, 2861-2873
269. Crotzer, V. L., and Blum, J. S. (2009) Autophagy and its role in MHC-mediated antigen presentation. *J Immunol* **182**, 3335-3341

270. Virgin, H. W., and Levine, B. (2009) Autophagy genes in immunity. *Nat Immunol* **10**, 461-470
271. Mizushima, N., and Klionsky, D. J. (2007) Protein turnover via autophagy: implications for metabolism. *Annu Rev Nutr* **27**, 19-40
272. Karantza-Wadsworth, V., Patel, S., Kravchuk, O., Chen, G., Mathew, R., Jin, S., and White, E. (2007) Autophagy mitigates metabolic stress and genome damage in mammary tumorigenesis. *Genes Dev* **21**, 1621-1635
273. Degenhardt, K., Mathew, R., Beaudoin, B., Bray, K., Anderson, D., Chen, G., Mukherjee, C., Shi, Y., Gelinas, C., Fan, Y., Nelson, D. A., Jin, S., and White, E. (2006) Autophagy promotes tumor cell survival and restricts necrosis, inflammation, and tumorigenesis. *Cancer Cell* **10**, 51-64
274. Aita, V. M., Liang, X. H., Murty, V. V., Pincus, D. L., Yu, W., Cayanis, E., Kalachikov, S., Gilliam, T. C., and Levine, B. (1999) Cloning and genomic organization of beclin 1, a candidate tumor suppressor gene on chromosome 17q21. *Genomics* **59**, 59-65
275. Liang, X. H., Jackson, S., Seaman, M., Brown, K., Kempkes, B., Hibshoosh, H., and Levine, B. (1999) Induction of autophagy and inhibition of tumorigenesis by beclin 1. *Nature* **402**, 672-676
276. Qu, X., Yu, J., Bhagat, G., Furuya, N., Hibshoosh, H., Troxel, A., Rosen, J., Eskelinen, E. L., Mizushima, N., Ohsumi, Y., Cattoretti, G., and Levine, B. (2003) Promotion of tumorigenesis by heterozygous disruption of the beclin 1 autophagy gene. *J Clin Invest* **112**, 1809-1820
277. Cadet, J., Ravanat, J. L., TavernaPorro, M., Menoni, H., and Angelov, D. (2012) Oxidatively generated complex DNA damage: tandem and clustered lesions. *Cancer Lett* **327**, 5-15
278. Dyavaiah, M., Rooney, J. P., Chittur, S. V., Lin, Q., and Begley, T. J. (2011) Autophagy-dependent regulation of the DNA damage response protein ribonucleotide reductase 1. *Mol Cancer Res* **9**, 462-475
279. Katayama, M., Kawaguchi, T., Berger, M. S., and Pieper, R. O. (2007) DNA damaging agent-induced autophagy produces a cytoprotective adenosine triphosphate surge in malignant glioma cells. *Cell Death Differ* **14**, 548-558

280. D'Angiolella, V., Santarpia, C., and Grieco, D. (2007) Oxidative stress overrides the spindle checkpoint. *Cell Cycle* **6**, 576-579
281. Mathew, R., Kongara, S., Beaudoin, B., Karp, C. M., Bray, K., Degenhardt, K., Chen, G., Jin, S., and White, E. (2007) Autophagy suppresses tumor progression by limiting chromosomal instability. *Genes Dev* **21**, 1367-1381
282. Fung, C., Lock, R., Gao, S., Salas, E., and Debnath, J. (2008) Induction of autophagy during extracellular matrix detachment promotes cell survival. *Mol Biol Cell* **19**, 797-806
283. Sun, L., Li, T., Wei, Q., Zhang, Y., Jia, X., Wan, Z., and Han, L. (2014) Upregulation of BNIP3 mediated by ERK/HIF-1alpha pathway induces autophagy and contributes to anoikis resistance of hepatocellular carcinoma cells. *Future Oncol* **10**, 1387-1398
284. Cai, Q., Yan, L., and Xu, Y. (2014) Anoikis resistance is a critical feature of highly aggressive ovarian cancer cells. *Oncogene* **0**
285. Franken, N. A., Rodermond, H. M., Stap, J., Haveman, J., and van Bree, C. (2006) Clonogenic assay of cells in vitro. *Nat Protoc* **1**, 2315-2319
286. Roby, K. F., Taylor, C. C., Sweetwood, J. P., Cheng, Y., Pace, J. L., Tawfik, O., Persons, D. L., Smith, P. G., and Terranova, P. F. (2000) Development of a syngeneic mouse model for events related to ovarian cancer. *Carcinogenesis* **21**, 585-591
287. Greenaway, J., Moorehead, R., Shaw, P., and Petrik, J. (2008) Epithelial-stromal interaction increases cell proliferation, survival and tumorigenicity in a mouse model of human epithelial ovarian cancer. *Gynecol Oncol* **108**, 385-394
288. Mani, S. A., Guo, W., Liao, M. J., Eaton, E. N., Ayyanan, A., Zhou, A. Y., Brooks, M., Reinhard, F., Zhang, C. C., Shipitsin, M., Campbell, L. L., Polyak, K., Brisken, C., Yang, J., and Weinberg, R. A. (2008) The epithelial-mesenchymal transition generates cells with properties of stem cells. *Cell* **133**, 704-715

289. Kang, H. G., Jenabi, J. M., Zhang, J., Keshelava, N., Shimada, H., May, W. A., Ng, T., Reynolds, C. P., Triche, T. J., and Sorensen, P. H. (2007) E-cadherin cell-cell adhesion in ewing tumor cells mediates suppression of anoikis through activation of the ErbB4 tyrosine kinase. *Cancer Res* **67**, 3094-3105
290. Liu, Y., Asnani, A., Zou, L., Bentley, V. L., Yu, M., Wang, Y., Dellaire, G., Sarkar, K. S., Dai, M., Chen, H. H., Sosnovik, D. E., Shin, J. T., Haber, D. A., Berman, J. N., Chao, W., and Peterson, R. T. (2014) Visnagin protects against doxorubicin-induced cardiomyopathy through modulation of mitochondrial malate dehydrogenase. *Sci Transl Med* **6**, 266ra170
291. Spitsbergen, J. M., and Kent, M. L. (2003) The state of the art of the zebrafish model for toxicology and toxicologic pathology research--advantages and current limitations. *Toxicol Pathol* **31 Suppl**, 62-87
292. Sampath, J., and Pelus, L. M. (2007) Alternative splice variants of survivin as potential targets in cancer. *Curr Drug Discov Technol* **4**, 174-191
293. Caldas, H., Jiang, Y., Holloway, M. P., Fangusaro, J., Mahotka, C., Conway, E. M., and Altura, R. A. (2005) Survivin splice variants regulate the balance between proliferation and cell death. *Oncogene* **24**, 1994-2007
294. Mahotka, C., Wenzel, M., Springer, E., Gabbert, H. E., and Gerharz, C. D. (1999) Survivin-deltaEx3 and survivin-2B: two novel splice variants of the apoptosis inhibitor survivin with different antiapoptotic properties. *Cancer Res* **59**, 6097-6102
295. Mahotka, C., Liebmann, J., Wenzel, M., Suschek, C. V., Schmitt, M., Gabbert, H. E., and Gerharz, C. D. (2002) Differential subcellular localization of functionally divergent survivin splice variants. *Cell Death Differ* **9**, 1334-1342
296. Noton, E. A., Colnaghi, R., Tate, S., Starck, C., Carvalho, A., Ko Ferrigno, P., and Wheatley, S. P. (2006) Molecular analysis of survivin isoforms: evidence that alternatively spliced variants do not play a role in mitosis. *J Biol Chem* **281**, 1286-1295
297. Vivas-Mejia, P. E., Rodriguez-Aguayo, C., Han, H. D., Shahzad, M. M., Valiyeva, F., Shibayama, M., Chavez-Reyes, A., Sood, A. K., and Lopez-Berestein, G. (2011) Silencing survivin splice variant 2B leads to antitumor activity in taxane--resistant ovarian cancer. *Clin Cancer Res* **17**, 3716-3726

298. Matsuura, S., Kahyo, T., Shinmura, K., Iwaizumi, M., Yamada, H., Funai, K., Kobayashi, J., Tanahashi, M., Niwa, H., Ogawa, H., Takahashi, T., Inui, N., Suda, T., Chida, K., Watanabe, Y., and Sugimura, H. (2013) SGOL1 variant B induces abnormal mitosis and resistance to taxane in non-small cell lung cancers. *Sci Rep* **3**, 3012
299. Wagner, P., Wang, B., Clark, E., Lee, H., Rouzier, R., and Puszta, L. (2005) Microtubule Associated Protein (MAP)-Tau: a novel mediator of paclitaxel sensitivity in vitro and in vivo. *Cell Cycle* **4**, 1149-1152
300. Tsyba, L., Skrypka, I., Rynditch, A., Nikolaienko, O., Ferenets, G., Fortna, A., and Gardiner, K. (2004) Alternative splicing of mammalian Intersectin 1: domain associations and tissue specificities. *Genomics* **84**, 106-113
301. Adams, A., Thorn, J. M., Yamabhai, M., Kay, B. K., and O'Bryan, J. P. (2000) Intersectin, an adaptor protein involved in clathrin-mediated endocytosis, activates mitogenic signaling pathways. *J Biol Chem* **275**, 27414-27420
302. Predescu, S. A., Predescu, D. N., Knezevic, I., Klein, I. K., and Malik, A. B. (2007) Intersectin-1s regulates the mitochondrial apoptotic pathway in endothelial cells. *J Biol Chem* **282**, 17166-17178
303. Predescu, S. A., Predescu, D. N., Timblin, B. K., Stan, R. V., and Malik, A. B. (2003) Intersectin regulates fission and internalization of caveolae in endothelial cells. *Mol Biol Cell* **14**, 4997-5010
304. Pham, T. V., Hartomo, T. B., Lee, M. J., Hasegawa, D., Ishida, T., Kawasaki, K., Kosaka, Y., Yamamoto, T., Morikawa, S., Yamamoto, N., Kubokawa, I., Mori, T., Yanai, T., Hayakawa, A., Takeshima, Y., Iijima, K., Matsuo, M., Nishio, H., and Nishimura, N. (2012) Rab15 alternative splicing is altered in spheres of neuroblastoma cells. *Oncol Rep* **27**, 2045-2049
305. Uezu, A., Horiuchi, A., Kanda, K., Kikuchi, N., Umeda, K., Tsujita, K., Suetsugu, S., Araki, N., Yamamoto, H., Takenawa, T., and Nakanishi, H. (2007) SGIP1alpha is an endocytic protein that directly interacts with phospholipids and Eps15. *J Biol Chem* **282**, 26481-26489
306. Ayantunde, A. A., and Parsons, S. L. (2007) Pattern and prognostic factors in patients with malignant ascites: a retrospective study. *Annals of Oncology* **18**, 945-949

307. Ahmed, N., and Stenvers, K. L. (2013) Getting to know ovarian cancer ascites: opportunities for targeted therapy-based translational research. *Front Oncol* **3**, 256
308. Adam, R. A., and Adam, Y. G. (2004) Malignant ascites: past, present, and future. *J Am Coll Surg* **198**, 999-1011
309. Feldman, G. B., Knapp, R. C., Order, S. E., and Hellman, S. (1972) The role of lymphatic obstruction in the formation of ascites in a murine ovarian carcinoma. *Cancer Res* **32**, 1663-1666
310. Bookman, M. A., McGuire, W. P., 3rd, Kilpatrick, D., Keenan, E., Hogan, W. M., Johnson, S. W., O'Dwyer, P., Rowinsky, E., Gallion, H. H., and Ozols, R. F. (1996) Carboplatin and paclitaxel in ovarian carcinoma: a phase I study of the Gynecologic Oncology Group. *J Clin Oncol* **14**, 1895-1902
311. McGuire, W. P., Hoskins, W. J., Brady, M. F., Kucera, P. R., Partridge, E. E., Look, K. Y., Clarke-Pearson, D. L., and Davidson, M. (1996) Cyclophosphamide and cisplatin compared with paclitaxel and cisplatin in patients with stage III and stage IV ovarian cancer. *N Engl J Med* **334**, 1-6
312. Ozols, R. F., Bundy, B. N., Greer, B. E., Fowler, J. M., Clarke-Pearson, D., Burger, R. A., Mannel, R. S., DeGeest, K., Hartenbach, E. M., Baergen, R., and Gynecologic Oncology, G. (2003) Phase III trial of carboplatin and paclitaxel compared with cisplatin and paclitaxel in patients with optimally resected stage III ovarian cancer: a Gynecologic Oncology Group study. *J Clin Oncol* **21**, 3194-3200
313. Herzog, T. J. (2004) Recurrent ovarian cancer: how important is it to treat to disease progression? *Clin Cancer Res* **10**, 7439-7449
314. Markman, M., Rowinsky, E., Hakes, T., Reichman, B., Jones, W., Lewis, J. L., Jr., Rubin, S., Curtin, J., Barakat, R., Phillips, M., and et al. (1992) Phase I trial of intraperitoneal taxol: a Gynecologic Oncology Group study. *J Clin Oncol* **10**, 1485-1491

Appendix A Copyright Agreements



Permissions

T & F Reference Number: P070115-04

7/1/2015

Dale Corkery
5859 University Ave.
Halifax, NS B3H 4H7
Canada
dale.corkery@dal.ca

Dear Mr. Corkery,

We are in receipt of your request to reproduce your article

Dale P. Corkery, Alice C. Holly, Sara Lahsae, Graham Dellaire (2015)
Connecting the speckles: Splicing kinases and their role in tumorigenesis and treatment response
Nucleus (online)
DOI: 0.1080/19491034.2015.1062194

You retain the right as author to post your Accepted Manuscripts on your departmental or personal website with the following acknowledgment: "This is an Accepted Manuscript of an article published in *Nucleus* online [June 22, 2015], available online:

<http://www.tandfonline.com/doi/full/10.1080/19491034.2015.1062194>

To be used as a section in your dissertation

This permission is for all electronic editions.

For the posting of the full article it must be in a secure, password-protected intranet site only.

An embargo period of twelve months applies for the Accepted Manuscript to be posted to an institutional or subject repository.

We will be pleased to grant you permission free of charge on the condition that:

This permission is for non-exclusive English world rights. This permission does not cover any third party copyrighted work which may appear in the material requested.

Full acknowledgment must be included showing article title, author, and full Journal title, reprinted by permission Taylor & Francis LLC, (<http://www.tandfonline.com>).

Thank you very much for your interest in Taylor & Francis publications. Should you have any questions or require further assistance, please feel free to contact me directly.

Sincerely,

Mary Ann Muller
Permissions Coordinator
Telephone: 215.606.4334
E-mail: maryann.muller@taylorandfrancis.com

530 Walnut Street, Suite 850, Philadelphia, PA 19106 • Phone: 215-625-8900 • Fax: 215-207-0050
Web: www.tandfonline.com



Permissions

T & F Reference Number: P051515-05

5/15/2015

Dale Corkery
PhD Candidate
Dept. Biochemistry and Molecular Biology
Dalhousie University
dale.corkery@dal.ca

Dear Mr. Corkery,

We are in receipt of your request to reproduce your Open Access article

Dale P. Corkery, Cécile Le Page, Liliane Meunier, Diane Provencher,
Anne-Marie Mes-Masson & Graham Dellaire (2015)
PRP4K is a HER2-regulated modifier of taxane sensitivity
Cell Cycle 14 (7): 1059-1069.

in your thesis

This permission is all for print and electronic editions.

We will be pleased to grant you permission free of charge on the condition that:

This permission is for non-exclusive English world rights. This permission does not cover any third party copyrighted work which may appear in the material requested.

Full acknowledgment must be included showing article title, author, and full Journal title, reprinted by permission of Taylor & Francis LLC (<http://www.tandfonline.com>).

Thank you very much for your interest in Taylor & Francis publications. Should you have any questions or require further assistance, please feel free to contact me directly.

Sincerely,

Mary Ann Muller
Permissions Coordinator
Telephone: 215.606.4334
E-mail: maryann.muller@taylorandfrancis.com



**JOHN WILEY AND SONS LICENSE
TERMS AND CONDITIONS**

May 21, 2015

This Agreement between Dale P Corkery ("You") and John Wiley and Sons ("John Wiley and Sons") consists of your license details and the terms and conditions provided by John Wiley and Sons and Copyright Clearance Center.

License Number	3633671002562
License date	May 21, 2015
Licensed Content Publisher	John Wiley and Sons
Licensed Content Publication	British Journal of Haematology
Licensed Content Title	Leukaemia xenotransplantation in zebrafish – chemotherapy response assay in vivo
Licensed Content Author	Dale P. Corkery,Graham Dellaire,Jason N. Berman
Licensed Content Date	Apr 22, 2011
Pages	4
Type of use	Dissertation/Thesis
Requestor type	Author of this Wiley article
Format	Print and electronic
Portion	Full article
Will you be translating?	No
Title of your thesis / dissertation	PRP4K is a novel HER2-regulated modifier of anoikis and taxane resistance
Expected completion date	Aug 2015
Expected size (number of pages)	250
Requestor Location	Dale P Corkery 960 Barrington St. Apt. 405 Halifax, NS B3H2P7 Canada Attn: Dale P Corkery
Billing Type	Invoice
Billing Address	Dale P Corkery 960 Barrington St. Apt. 405 Halifax, NS B3H2P7 Canada Attn: Dale P Corkery
Total	0.00 CAD

[Terms and Conditions](#)**TERMS AND CONDITIONS**

This copyrighted material is owned by or exclusively licensed to John Wiley & Sons, Inc. or one of its group companies (each a "Wiley Company") or handled on behalf of a society with which a Wiley Company has exclusive publishing rights in relation to a particular work (collectively "WILEY"). By clicking accept in connection with completing this licensing transaction, you agree that the following terms and conditions apply to this transaction (along with the billing and payment terms and conditions established by the Copyright Clearance Center Inc., ("CCC's Billing and Payment terms and conditions"), at the time that you opened your Rightslink account (these are available at any time at <http://myaccount.copyright.com>).

Terms and Conditions

- The materials you have requested permission to reproduce or reuse (the "Wiley Materials") are protected by copyright.
- You are hereby granted a personal, non-exclusive, non-sub licensable (on a stand-alone basis), non-transferable, worldwide, limited license to reproduce the Wiley Materials for the purpose specified in the licensing process. This license is for a one-time use only and limited to any maximum distribution number specified in the license. The first instance of republication or reuse granted by this licence must be completed within two years of the date of the grant of this licence (although copies prepared before the end date may be distributed thereafter). The Wiley Materials shall not be used in any other manner or for any other purpose, beyond what is granted in the license. Permission is granted subject to an appropriate acknowledgement given to the author, title of the material/book/journal and the publisher. You shall also duplicate the copyright notice that appears in the Wiley publication in your use of the Wiley Material. Permission is also granted on the understanding that nowhere in the text is a previously published source acknowledged for all or part of this Wiley Material. Any third party content is expressly excluded from this permission.
- With respect to the Wiley Materials, all rights are reserved. Except as expressly granted by the terms of the license, no part of the Wiley Materials may be copied, modified, adapted (except for minor reformatting required by the new Publication), translated, reproduced, transferred or distributed, in any form or by any means, and no derivative works may be made based on the Wiley Materials without the prior permission of the respective copyright owner. You may not alter, remove or suppress in any manner any copyright, trademark or other notices displayed by the Wiley Materials. You may not license, rent, sell, loan, lease, pledge, offer as security, transfer or assign the Wiley Materials on a stand-alone basis, or any of the rights granted to you hereunder to any other person.
- The Wiley Materials and all of the intellectual property rights therein shall at all times remain the exclusive property of John Wiley & Sons Inc, the Wiley Companies, or their respective licensors, and your interest therein is only that of having possession of and the right to reproduce the Wiley Materials pursuant to Section 2 herein during the continuance of this Agreement. You agree that you own no right, title or interest in or

to the Wiley Materials or any of the intellectual property rights therein. You shall have no rights hereunder other than the license as provided for above in Section 2. No right, license or interest to any trademark, trade name, service mark or other branding ("Marks") of WILEY or its licensors is granted hereunder, and you agree that you shall not assert any such right, license or interest with respect thereto.

- NEITHER WILEY NOR ITS LICENSORS MAKES ANY WARRANTY OR REPRESENTATION OF ANY KIND TO YOU OR ANY THIRD PARTY, EXPRESS, IMPLIED OR STATUTORY, WITH RESPECT TO THE MATERIALS OR THE ACCURACY OF ANY INFORMATION CONTAINED IN THE MATERIALS, INCLUDING, WITHOUT LIMITATION, ANY IMPLIED WARRANTY OF MERCHANTABILITY, ACCURACY, SATISFACTORY QUALITY, FITNESS FOR A PARTICULAR PURPOSE, USABILITY, INTEGRATION OR NON-INFRINGEMENT AND ALL SUCH WARRANTIES ARE HEREBY EXCLUDED BY WILEY AND ITS LICENSORS AND WAIVED BY YOU
- WILEY shall have the right to terminate this Agreement immediately upon breach of this Agreement by you.
- You shall indemnify, defend and hold harmless WILEY, its Licensors and their respective directors, officers, agents and employees, from and against any actual or threatened claims, demands, causes of action or proceedings arising from any breach of this Agreement by you.
- IN NO EVENT SHALL WILEY OR ITS LICENSORS BE LIABLE TO YOU OR ANY OTHER PARTY OR ANY OTHER PERSON OR ENTITY FOR ANY SPECIAL, CONSEQUENTIAL, INCIDENTAL, INDIRECT, EXEMPLARY OR PUNITIVE DAMAGES, HOWEVER CAUSED, ARISING OUT OF OR IN CONNECTION WITH THE DOWNLOADING, PROVISIONING, VIEWING OR USE OF THE MATERIALS REGARDLESS OF THE FORM OF ACTION, WHETHER FOR BREACH OF CONTRACT, BREACH OF WARRANTY, TORT, NEGLIGENCE, INFRINGEMENT OR OTHERWISE (INCLUDING, WITHOUT LIMITATION, DAMAGES BASED ON LOSS OF PROFITS, DATA, FILES, USE, BUSINESS OPPORTUNITY OR CLAIMS OF THIRD PARTIES), AND WHETHER OR NOT THE PARTY HAS BEEN ADVISED OF THE POSSIBILITY OF SUCH DAMAGES. THIS LIMITATION SHALL APPLY NOTWITHSTANDING ANY FAILURE OF ESSENTIAL PURPOSE OF ANY LIMITED REMEDY PROVIDED HEREIN.
- Should any provision of this Agreement be held by a court of competent jurisdiction to be illegal, invalid, or unenforceable, that provision shall be deemed amended to achieve as nearly as possible the same economic effect as the original provision, and the legality, validity and enforceability of the remaining provisions of this Agreement shall not be affected or impaired thereby.
- The failure of either party to enforce any term or condition of this Agreement shall not constitute a waiver of either party's right to enforce each and every term and condition of this Agreement. No breach under this agreement shall be deemed waived or excused by either party unless such waiver or consent is in writing signed by the party granting such waiver or consent. The waiver by or consent of a party to a breach of

any provision of this Agreement shall not operate or be construed as a waiver of or consent to any other or subsequent breach by such other party.

- This Agreement may not be assigned (including by operation of law or otherwise) by you without WILEY's prior written consent.
- Any fee required for this permission shall be non-refundable after thirty (30) days from receipt by the CCC.
- These terms and conditions together with CCC's Billing and Payment terms and conditions (which are incorporated herein) form the entire agreement between you and WILEY concerning this licensing transaction and (in the absence of fraud) supersedes all prior agreements and representations of the parties, oral or written. This Agreement may not be amended except in writing signed by both parties. This Agreement shall be binding upon and inure to the benefit of the parties' successors, legal representatives, and authorized assigns.
- In the event of any conflict between your obligations established by these terms and conditions and those established by CCC's Billing and Payment terms and conditions, these terms and conditions shall prevail.
- WILEY expressly reserves all rights not specifically granted in the combination of (i) the license details provided by you and accepted in the course of this licensing transaction, (ii) these terms and conditions and (iii) CCC's Billing and Payment terms and conditions.
- This Agreement will be void if the Type of Use, Format, Circulation, or Requestor Type was misrepresented during the licensing process.
- This Agreement shall be governed by and construed in accordance with the laws of the State of New York, USA, without regards to such state's conflict of law rules. Any legal action, suit or proceeding arising out of or relating to these Terms and Conditions or the breach thereof shall be instituted in a court of competent jurisdiction in New York County in the State of New York in the United States of America and each party hereby consents and submits to the personal jurisdiction of such court, waives any objection to venue in such court and consents to service of process by registered or certified mail, return receipt requested, at the last known address of such party.

WILEY OPEN ACCESS TERMS AND CONDITIONS

Wiley Publishes Open Access Articles in fully Open Access Journals and in Subscription journals offering Online Open. Although most of the fully Open Access journals publish open access articles under the terms of the Creative Commons Attribution (CC BY) License only, the subscription journals and a few of the Open Access Journals offer a choice of Creative Commons Licenses: Creative Commons Attribution (CC-BY) license [Creative Commons Attribution Non-Commercial \(CC-BY-NC\) license](#) and [Creative Commons Attribution Non-Commercial-NoDerivs \(CC-BY-NC-ND\) License](#). The license type is clearly identified on the article.

Copyright in any research article in a journal published as Open Access under a Creative Commons License is retained by the author(s). Authors grant Wiley a license to publish the article and identify itself as the original publisher. Authors also grant any third party the right to use the article freely as long as its integrity is maintained and its original authors, citation details and publisher are identified as follows: [Title of Article/Author/Journal Title and Volume/Issue. Copyright (c) [year] [copyright owner as specified in the Journal]. Links to the final article on Wiley's website are encouraged where applicable.

The Creative Commons Attribution License

The [Creative Commons Attribution License \(CC-BY\)](#) allows users to copy, distribute and transmit an article, adapt the article and make commercial use of the article. The CC-BY license permits commercial and non-commercial re-use of an open access article, as long as the author is properly attributed.

The Creative Commons Attribution License does not affect the moral rights of authors, including without limitation the right not to have their work subjected to derogatory treatment. It also does not affect any other rights held by authors or third parties in the article, including without limitation the rights of privacy and publicity. Use of the article must not assert or imply, whether implicitly or explicitly, any connection with, endorsement or sponsorship of such use by the author, publisher or any other party associated with the article.

For any reuse or distribution, users must include the copyright notice and make clear to others that the article is made available under a Creative Commons Attribution license, linking to the relevant Creative Commons web page.

To the fullest extent permitted by applicable law, the article is made available as is and without representation or warranties of any kind whether express, implied, statutory or otherwise and including, without limitation, warranties of title, merchantability, fitness for a particular purpose, non-infringement, absence of defects, accuracy, or the presence or absence of errors.

Creative Commons Attribution Non-Commercial License

The [Creative Commons Attribution Non-Commercial \(CC-BY-NC\) License](#) permits use, distribution and reproduction in any medium, provided the original work is properly cited and is not used for commercial purposes.(see below)

Creative Commons Attribution-Non-Commercial-NoDerivs License

The [Creative Commons Attribution Non-Commercial-NoDerivs License](#) (CC-BY-NC-ND) permits use, distribution and reproduction in any medium, provided the original work is properly cited, is not used for commercial purposes and no modifications or adaptations are made. (see below)

Use by non-commercial users

For non-commercial and non-promotional purposes, individual users may access, download, copy, display and redistribute to colleagues Wiley Open Access articles, as well as adapt, translate, text- and data-mine the content subject to the following conditions:

- The authors' moral rights are not compromised. These rights include the right of "paternity" (also known as "attribution" - the right for the author to be identified as such) and "integrity" (the right for the author not to have the work altered in such a way that the author's reputation or integrity may be impugned).
- Where content in the article is identified as belonging to a third party, it is the obligation of the user to ensure that any reuse complies with the copyright policies of the owner of that content.
- If article content is copied, downloaded or otherwise reused for non-commercial research and education purposes, a link to the appropriate bibliographic citation (authors, journal, article title, volume, issue, page numbers, DOI and the link to the definitive published version on **Wiley Online Library**) should be maintained. Copyright notices and disclaimers must not be deleted.
- Any translations, for which a prior translation agreement with Wiley has not been agreed, must prominently display the statement: "This is an unofficial translation of an article that appeared in a Wiley publication. The publisher has not endorsed this translation."

Use by commercial "for-profit" organisations

Use of Wiley Open Access articles for commercial, promotional, or marketing purposes requires further explicit permission from Wiley and will be subject to a fee. Commercial purposes include:

- Copying or downloading of articles, or linking to such articles for further redistribution, sale or licensing;
- Copying, downloading or posting by a site or service that incorporates advertising with such content;
- The inclusion or incorporation of article content in other works or services (other than normal quotations with an appropriate citation) that is then available for sale or licensing, for a fee (for example, a compilation produced for marketing purposes, inclusion in a sales pack)
- Use of article content (other than normal quotations with appropriate citation) by for-profit organisations for promotional purposes
- Linking to article content in e-mails redistributed for promotional, marketing or educational purposes;
- Use for the purposes of monetary reward by means of sale, resale, licence, loan, transfer or other form of commercial exploitation such as marketing products
- Print reprints of Wiley Open Access articles can be purchased from:
corporatesales@wiley.com

Further details can be found on Wiley Online Library

<https://s100.copyright.com/App/PrintableLicenseFrame.jsp?publisherID=140&publisherName=Wiley&publication=BJH&publicationID=27925&rightID=1&type...> 6/7

<http://olabout.wiley.com/WileyCDA/Section/id-410895.html>

Other Terms and Conditions:

v1.9

Questions? customercare@copyright.com or +1-855-239-3415 (toll free in the US) or +1-978-646-2777.

Gratis licenses (referencing \$0 in the Total field) are free. Please retain this printable license for your reference. No payment is required.

Appendix B ImageJ Macro

The following is the cell quantification macro used to count fluorescent cancer cells within images of dissociated zebrafish material. Individual fluorescent images are opened in imageJ and the macro applied.

```
run("Images to Stack", "name=Stack title=[] use");
run("8-bit");
//run("Brightness/Contrast...");
setMinAndMax(50, 200);
run("Apply LUT", "stack");
run("Close");
setAutoThreshold("Default dark");
//run("Threshold...");
setAutoThreshold("Default dark");
setOption("BlackBackground", true);
run("Convert to Mask", "method=Default background=Default black");
run("Close");
run("Analyze Particles...", "display summarize stack");
```

Appendix C Cell Lines Used

Cell Line	Organism	Disease	Characteristics
SK-BR-3	Human	Breast Adenocarcinoma	HER2 (+), ER (-), PR (-)
MCF-7	Human	Breast Adenocarcinoma	HER2 (-), ER (+), PR (+)
MDA-MB-231	Human	Breast Adenocarcinoma	HER2 (-), ER (-), PR (-)
IGROV-1	Human	Ovarian Adenocarcinoma	
SKOV-3	Human	Ovarian Adenocarcinoma	
HeLa	Human	Cervical Adenocarcinoma	
TOV1369	Human	High-Grade Serous Ovarian Cancer	Cells isolated from solid tumour at time of diagnosis
OV1369(R2)	Human	High-Grade Serous Ovarian Cancer	Cells isolated from ascites post-relapse from paclitaxel treatment
K562	Human	Chronic Myelogenous Leukemia	Express BCR-ABL fusion gene
NB-4	Human	Acute Promyelocytic Leukemia	Express PML-RAR α fusion gene
ID8	Mouse	Epithelial Ovarian Cancer	Transplanted in mice as an orthotopic, syngeneic model of EOC